5-2-2022

Water Use Patterns of a Riparian Forest in a Humid Subtropical Catchment in the Southeastern United States

Jeffrey Riley

Water Use Patterns of a Riparian Forest in a Humid Subtropical Catchment in the Southeastern

United States

by

Jeffrey Riley

Under the Direction of Luke Pangle, Ph.D

A Dissertation Submitted in Partial Fulfillment of the Requirements for the Degree of

Doctor of Philosophy

in the College of Arts and Sciences

Georgia State University

2022

ABSTRACT

The role of groundwater in sustaining plant transpiration has been studied for nearly a century. However, the body of literature investigating plant uptake of groundwater has largely been focused on arid and semiarid climates, with few examples from more humid locations. In this dissertation, I attempt to contribute a rigorous evaluation of groundwater transpiration (T_G) from a humid riparian forest to fill in this knowledge gap. In chapter two, I explored the groundwater use by a riparian forest using techniques that exploit diurnal water table fluctuations from groundwater wells. Specifically, I investigated the spaciotemporal variability of T_G using nine groundwater wells in a small headwater catchment in the Piedmont of Georgia. Results indicated a relatively high degree of variability, 3.30 ± 1.05 mm d^{-1} but lacking a consistent spatial pattern. Furthermore, groundwater derived transpiration was approximately 22 % of the average baseflow discharge over the growing season; indicating that even in humid regions plant transpiration can be a substantial component of the seasonal water budget. In chapter three, I incorporated an independent estimate of canopy transpiration (E_C) to better constrain the estimates of T_G from chapter two. This was motivated by wanting to partition the total water used by the riparian forest into groundwater and soil water sources. However, the results were not as anticipated. For the 2019 growing season T_G was 455 mm, approximately twice as much as E_C (241mm). This instead highlighted a methodological issue that had not been previously addressed. The formulae for estimating T_G lacks a defined area of influence; however, in the present study I estimated this area of influence would have be 2 – 10 times larger than the delineated riparian zone for the fluxes to balance. In chapter four I explored the response of a riparian forest to a rapid onset flash drought. Results indicated that there was not watershed wide response of the forest canopy to the drought. However, at individual trees water use patterns did

suggest a drought response, one that was dominated by an increase in reverse sap flow

suggesting hydraulic redistribution was occurring to compensate for the excessively dry soils.

Water Use Patterns of a Riparian Forest in a Humid Subtropical Catchment in the Southeastern

United States

by

Jeffrey Riley

Committee Chair: Luke Pangle

Committee: Dajun Dai

Jeremy Diem

Brian Meyer

Brent Aulenbach

Electronic Version Approved:

Office of Graduate Services

College of Arts and Sciences

Georgia State University

May 2022

DEDICATION

This dissertation is dedicated to my family, friends, colleagues, mentors, and everyone else who has supported me along the way and has been there to listen to me ramble about water, trees, dirt, and rocks.

ACKNOWLEDGEMENTS

The work presented in this dissertation would not have been possible without the help of so many people. On the academic side, I must thank my advisor Dr. Pangle for taking me on mid-way through my studies and being flexible and helping to chart a path of mutual interest that is this dissertation. Dr. Pangle provided loads of sap flux equipment to get me started working in a new (to me) and very exciting area of ecohydrology. I am also grateful for the field assistance of Dr. Pangle and lab mates who helped hand auger wells and install sap flux sensors. Furthermore, Dr. Pangle's tireless edits of the dissertation chapters herein are noted and greatly appreciated. I would also like to thank my committee members whose feedback on my proposal and dissertation made me think about problems from different angles rather than purely hydrology. I am grateful for the support provided by the Department of Geosciences. Lastly, a special thanks to Dr. Katie Price for initially bringing me into the GSU Geosciences Department and getting me started on this journey.

To my family, thanks for always being there, being supportive, and understanding when I was staring at computer screens or in the field rather than spending time with you all. Thanks to my wife, Brie, for wrangling a baby, then toddler, and allowing me to get work done in spurts, and in general, just being a great partner. Much love! Thanks to Flora Riley, (that toddler that is now a kindergartner!) for being a cool and creative kid, that is happy to go stomping through creeks and wetlands and offers up her own cool ideas about the natural world. Love ya nugget!

Finally, I must thank all my colleagues at the U.S. Geological Survey who were flexible with field schedules, gracious with personal time to help with field work, happy to chat and bounce ideas, and just overall supportive. I also acknowledge my supervisors over this time, Mindi Dalton and Dan Calhoun, both of whom were very supportive of my academic endeavors

and were very accommodating with my work schedule to attend classed and complete field

work.

TABLE OF CONTENTS

LIST OF TABLES

LIST OF FIGURES

1   INTRODUCTION

1.1   Motivation

Water is the one substance that connects all living creatures on earth. There are no known living organisms that can survive without water (although some don't necessarily consume liquid water) and humans can only survive about 3 days without water. This suggests robust water management should eclipse, or at least be equal to, all other concerns of a well-functioning civil society. Yet, that does not seem to be the case. Recent (ca. 2020 – present) droughts over the Western U.S. have resulted in the largest reservoirs (Lakes Mead and Powell) in the country reaching their lowest levels since initial filling. This has the potential to reduce potable water supplies to large cities and impact power generation from hydroelectric dams. But this is only an issue in the more arid Western United States, right?

In the humid Southeastern United States drought is a relatively common occurrence (USFS, 2017) albeit often of shorter duration when compared to the western U.S. (Seager et al., 2009). While the likelihood of an event on the scale of what is presently occurring in the West is low, a coalescing of drought and increasing demand could quickly place more humid regions in dire situations as well. This could be especially true if we see continued drought conditions force certain parts of the agricultural sector to move from the Central Valley of California and the Midwestern U.S. to the Southeast U.S. where growing conditions are favorable, and water is more readily available. Furthermore, as drought continues to fuel wildfires in the West, the Southeast could also see an increase in industrial forests. Both these activities could further intensify water demand and lead to catastrophic consequences for ecosystems caught in the battle between municipal and agricultural water users if water availability (i.e., water budgets) is not accurately constrained.

This dissertation is no attempt to solve all our issues related to water protection or equitable water allocation. Rather, the goal of this dissertation was to shed light on one component of the water budget that has historically been overlooked in humid regions, that is the role of trees and forests (i.e., transpiration) on **groundwater budgets** (equation 1.1).

$$\frac{dS}{dt}(t) = R_I(t) + R_{SW}(t) + GW_{In}(t) - Q_{GW}(t) - G_{out}(t) - CR(t) - T_G(t) \qquad \text{equation 1.1}$$

Where $\frac{dS}{dt}$ is the change is water storage in the aquifer, R_I is the rechange from precipitation infiltration, R_{SW} is the rechange from surface water sources, GW_{In} is the groundwater flowing into the aquifer from adjacent (underlying) aquifers, Q_{GW} is the water discharged from the aquifer to streams, G_{out} is the water flowing out of the aquifer in the subsurface either across a basin divide or vertically to a deeper aquifer, CR is water moving from the aquifer to the unsaturated soil due to capillary rise, T_G is the direct uptake of groundwater by vegetation, and (t) indicates each term is time dependent. Importantly, the last term in equation 1.1 (T_G) is rarely considered and is often assumed negligible. However, past work has highlighted the connection between plants and various water budget components. For example, at the catchment scale, the effects of forest harvest on annual streamflow have been investigated for over a century (Bosch and Hewlett, 1982). The most common metric assessed in these studies is annual water yield and there are many important details that are lost when aggregating to the annual scale. Water availability is often most critical during the growing season, when tree growth and transpiration is the greatest and when drought is most likely to occur and result in negative impacts. Vigorous tree growth in the growing season can lead to depletion of soil moisture, and where accessible, direct uptake of water from the surficial aquifer. This can in turn reduce stream baseflow, which is also sustained by the surficial aquifer between rain events. This may seem like a minor issue but given the potential for increased demand on the Southeastern U.S. for agricultural and

forestry products, along with the rapid population growth, now is the time to lay the groundwork to diligently account for **ALL** components of the water budget. This will help guide science based environmental statutes and facilitate a data driven approach to equitable water allocation and environmental protection.

1.2   Contributions

I identified two areas that were hindering our ability to account for this seasonally important flux of water. They both relate to methodological issues, specifically, the lack of a well constrained approach to quantify the loss of water from surficial aquifers via transpiration. Several hydrometric methods have been proposed that rely on the diurnal oscillation of water table levels (or elevation). Most of the methods are based on, or modifications of, White (1932) which was the first publication to rigorously investigate the phenomenon and formalize a method to estimate plant water use from the diurnal water table fluctuation (DWTF). Other researchers have offered slight changes and updates to the methods, but most still retain the fundamental components initially laid out by White (1932). I had two main concerns with the current body of literature: 1. Most studies have been conducted in arid, semi-arid, and Mediterranean climates and the landscapes have generally been flat with little topographic variability. This leaves a huge gap regarding application of these techniques in different settings. Are DWTF methods appropriate in more topographically complex landscapes? Are the drivers the same? Are the interpretations the same? 2. In addition to the lack of application in humid and topographically complex landscapes there are only a few studies that quantify the variability of the estimated flux across a study site. Thus, it is unknown how well as single monitoring location may capture the "average flux" across an area of interest or stated in a different way, how many monitoring locations are needed over a given area to accurately estimate the flux of transpired groundwater?

These basic pieces of information are needed to accurately quantify this important, but underappreciated water budget component.

The research in this dissertation is focused on a small catchment in the Piedmont physiographic province of GA. This catchment may be viewed as a model for other Piedmont watersheds. However, I expect these results will also have some general applicability to other humid regions. The following sections of this dissertation are broken into three chapters that each assess a different knowledge gap.

The second chapter of this dissertation has been submitted for publication in *Water Resources Research* and is currently in review. The aim of the is chapter to better understand the spatial and temporal variation of plant uptake of groundwater. This key piece of information is needed if water table fluctuation methods are to be applied with any sort of consistency to understand the actual magnitude of the groundwater flux. Our current understanding is that trees use groundwater when it is close to the surface and that generally occurs in riparian zones. However, details are lacking on the specifics, or what thresholds may exist for when and where groundwater is used by trees. Even in arid regions where this flux has been extensively characterized, rarely has the lateral spatial dynamics been assessed. Thus, the goal of ch.2 was to explore the spatial variation and extent of groundwater uptake and the conditions under which it occurred. Filling a critical knowledge gap in catchment hydrology of humid regions.

Chapter three is formatted for and is intended to be submitted to the journal *Ecohydrology*. In this chapter I dig deeper into the findings of chapter two and compare the estimated groundwater flux with an independent estimate of canopy transpiration (E_C). This was motivated initially by the desire to estimate how much of the total canopy transpiration was derived from the surficial aquifer. Based on the findings from chapter two, along with a critical

analysis of the literature related to groundwater transpiration and canopy transpiration from other southeastern study sites, there was some concern that the T_G estimation approach may result in overestimation of actual water use. Therefore, the goal was to examine plot and whole riparian zone scale ratios of T_G:E_C, with an expected outcome to be some fraction less than one. However, this was not the case. The fraction was consistently greater than one. While not the intended outcome, this is very useful information and charts a path for future research into the methods used to estimate the quantity of groundwater that is transpired by vegetation. This will hopefully jumpstart a research theme to better understand where and under what conditions water table fluctuations approaches are applicable.

The final investigation of the dissertation is presented in chapter 4. The chapter is formatted for submission to the journal *Agricultural and Forest Meteorology*. This chapter was born out of the serendipitous occurrence of a rapid onset drought event. This provided an opportunity to investigate the ecohydrologic response of trees (meaning, changes in water uptake patterns, changes in timing, magnitude, and direction of water flowing through the tree and changing sources of water uptake). Rapid onset droughts have been gaining recognition in recent years as being a subset type of drought, labeled "flash drought". Research on this topic has been very popular over the last decade, however, most studies of impact have been focused on agricultural regions and a detailed look at how natural forests respond has not been undertaken. Therefore, this chapter does just that. The final chapter (five) summarizes the findings from the study chapters and highlights the contribution of each to the disciplines of catchment and ecohydrology. Last, I present some thoughts for future studies that could address some of the remaining uncertainties that were encountered during the course of this dissertation.

2   GROUNDWATER TRANSPIRATION DYNAMICS OF A HEADWATER RIPARIAN ZONE IN A HUMID-SUBTROPICAL CATCHMENT IN THE SOUTHEASTERN U.S.

2.1   Abstract

In environments with shallow water-tables, vegetation may use groundwater to support transpiration (T_G). This process has been carefully studied in some arid climates, but rarely in humid climates—even those with severe droughts and seasonal water deficits. As such, the role of T_G in humid-catchment hydrology is poorly constrained. We analyzed water-table fluctuations from nine wells along three transects in a second order forested catchment to estimate T_G at plot and whole-riparian-zone scales. Average T_G estimated around all well locations ranged from 1.06 – 4.95 mm d^{-1} and did not change systematically as a function of distance from stream channel or with plot-scale tree basal area. Counter to some previous studies, we found that T_G was greater when the water table depth was deeper. Furthermore, the pattern of T_G with water table depth was not monotonic at all locations. The ratio of T_G to potential evapotranspiration tended to increase over the growing season, reflecting the progressive decrease in soil-moisture storage and a greater reliance by vegetation on groundwater. Due to the lack of spatial structure in T_G we explored the number of monitoring wells needed to consistently estimate average T_G within the 95% confidence bounds of the true mean. Based on this analysis, five or more wells were needed to consistently fall within the 95% confidence interval of the grand mean. While this is based on the observed variability at a single site, it provides information for others considering this approach in similar upland forested catchments in humid regions.

2.2   Introduction

In low-order watersheds with perennial streams, the flow of water in the channel during inter-storm periods is sustained by discharge from an unconfined, riparian aquifer. When the water table is sufficiently close to their roots, plants may extract from the riparian aquifer some portion of the total water volume they transpire (T_G). These flows may prove to be significant components of the overall water balance of riparian aquifers and catchments, and groundwater utilization by riparian plants may disproportionately influence daily to seasonal streamflow generation. Although our qualitative understanding of this phenomenon is long-standing, our quantitative understanding of groundwater utilization by riparian plants remains limited. This is especially true in more humid environments.

Transpiration of groundwater occurs when plant roots are immersed in the surficial aquifer or capillary fringe. Across Earth's biomes, approximately 75% of roots exist within 50 centimeters from the land surface, while approximately 95% of roots exist within a depth of 150 centimeters (Schenk and Jackson, 2002). In arid environments it is not uncommon for plant roots to extract groundwater at even greater depths (e.g., McLendon et al., 2008). Interpolation schemes suggest that, on average, the depth to the water table is less than two meters over more than 10% of continental areas (Fan et al., 2013). Considered together, this suggests that T_G may be a significant component of aquifer and catchment mass balances for a sizable portion of the Earth's continents.

The depth to water table is temporally dynamic, however, which induces temporal variation in the occurrence and magnitude of T_G, even in environments where the average water-table depth is relatively shallow. The magnitude of T_G may decline as the water-table depth below land surface increases, due to a smaller portion of the root biomass having access to the

aquifer. For example, Rosenberry and Winter (1997) observed that rates of T_G from a wetland Bulrush community declined as water-table depth below land surface increased and practically ceased when the water-table depth exceeded 1.2 – 1.4 meters. In a Eucalyptus tree plantation in the Argentinian Pampas region, Engel et al. (2005) showed that total transpiration (T) declined from, on average, approximately three to two millimeters per day as the water-table depth increased from two to three meters below ground. This decline in T likely reflects a similar decline in T_G since the authors demonstrate that the trees rely almost entirely on groundwater during this late phase of their summer season. Cooper et al. (2006) reported a 68% reduction in T_G within a riparian corridor in the San Luis Valley of Colorado, USA in response to a long-term increase in the depth to water table from, on average, 0.92 to 2.5 meters. The same qualitative relationship between T_G (as well as total T) and water-table depth has been documented across a broad range of ecosystem types (Sanderson and Cooper, 2008; Shah et al., 2007; Steinwand et al., 2006; Thompson et al., 2011, Yue et al., 2016). Hence, a persistent challenge in quantifying time-integrated magnitudes of T_G for distributed clusters of vegetation is the accurate measurement or modeling of water-table dynamics within those zones.

The second fundamental challenge is knowing where within a watershed T_G is likely to occur and how the areal extent changes over time. Knowledge of plant rooting depths and water-table elevation help constrain the geographic area where T_G may occur. In fact, knowledge about the presence of known phreatophytic species has been utilized to constrain the mapped discharge zones in regional groundwater models (Batelaan et al., 2003). In upland environments with hilly to mountainous topography, the basin area where the water-table surface may exist at less than 2-m depth is temporally variable, but generally comprises some near-stream corridor. Based on observed diurnal fluctuations in streamflow, and a coarse interpolation technique, Bond et al.

(2002) estimated that the forested area responsible for causing the diurnal oscillation in the stream hydrograph ranged from 0.3 to less than 0.1 ha. This study was conducted in a steeply incised watershed draining approximately 100 ha in the western Cascade Mountains of Oregon, USA where the lateral extent of the riparian zone is on the order of only a few meters. Quantifying T_G across the entire riparian-plant community requires monitoring—or modeling—of the lateral extent from the stream channel where the water-table intersects the plant root zone. Even within this corridor there can be tremendous variability in T_G due to local variations in groundwater depth, species composition, canopy exposure of nearby plants, and the hydraulic properties of the soil and saprolite (e.g., Butler et al., 2007; Sanderson and Cooper, 2008; Satchithanantham et al., 2017). As such, extrapolating estimates of T_G across entire riparian-zones within upland catchments with diverse topography and plant assemblages remains a considerable challenge that has been rarely attempted (e.g., Goodrich et al., 2000; Mac Nish et al., 2000; Scott et al., 2000, Scott et al. 2008). Many studies have simply assumed that point-scale measurements are representative of larger areas of interest—an assumption that can yield uncertain extrapolations.

The body of research that examines T_G disproportionately reflects studies in arid/semi-arid climates. The process is rightfully perceived as critical in those regions for understanding groundwater budgets, the potential interactions between groundwater utilization and plant species assemblages, and ancillary impacts such as soil salinization and exotic-invasive species intrusion (e.g., Cooper et al., 2006; Goodrich et al., 2000; Naumburg et al., 2005; Nosetto et al., 2005; Nosetto et al., 2007; Scott et al., 2000; Smith et al., 1998). Yet, groundwater utilization by plants appears to be ubiquitous across hydroclimatic zones, as evidenced by commonly observed diurnal oscillations in well and stream hydrographs (Ciruzzi & Loheide, 2021; Czikowsky and

Fitzjarrald, 2004; Fan et al., 2014; Gribovszki et al., 2010; Lundquist and Cayan, 2002). Much of the southeastern United States is considered a humid sub-tropical climate—most of that region receiving greater than one meter of precipitation per year—yet even in this humid region potential evapotranspiration (PET) often is approximately equal to precipitation across years, and significant water deficits often occur during summer and early autumn (Aulenbach and Peters, 2018). Groundwater utilization would be a competitive advantage for plants during water-stressed times and may comprise a more significant portion of the catchment water balance than previously assumed. Enhanced understanding of T_G is needed to inform policies influencing riparian-zone management even in humid environments, where, to date, insufficient knowledge is available to justify consideration of this process in the development of environmental statutes.

The primary objective of our study is to quantify riparian zone T_G for a second-order headwater catchment in the humid subtropical climate of the Piedmont province of Georgia, USA. Little work has been done applying water table fluctuation methods in humid and topographically complex landscapes, and it is unknown if insights from more arid and topographically simple landscapes are transferable. Specifically, we estimated T_G from nine riparian monitoring wells that spanned a rather narrow gradient of topography and water table depths and evaluated the spatial and temporal dynamics of T_G across the catchment's riparian zone and examined the plausibility for extrapolating whole-riparian-zone T_G from individual, and groups of wells. Lastly, we investigated how many monitoring locations were necessary to estimate T_G within 5% of the true mean (based on all nine wells). We hypothesized that estimates of T_G would decrease as the water table depth increased. Therefore, we expected using an average or median T_G from each landscape position would represent the best approach for quantifying riparian zone wide T_G.

2.3   Materials and Methods

2.3.1   *Study Site*

This study was conducted at the Panola Mountain Research Watershed (PMRW) in the Piedmont physiographic province of Georgia, which is located approximately 25-km southeast of Atlanta, GA USA (Figure 2.1). The study watershed drains 41 ha, comprised of approximately 30 ha of hillslopes, 8 ha of valley bottom, and 3 ha of exposed bedrock. This study is focused on an approximately 3-ha portion of the riparian zone. Soils in the riparian zone are generally sandy-loam to loam textured and are classified as Cartecay and Chewacla series (Natural Resources Conservation Service, 2017). Based on the proportion of sand and fine (silt and clay) particle size fractions, the aquifer sediment texture was classified as sandy-loam to loamy sand.

The riparian forest is composed of at least 11 tree species, but basal area around the study wells is dominated by 6: the broadleaf deciduous species *Liriodendron tulipifera; Quercus alba; Quercus nigra; Nyssa sylvatica*; *Liquidambar styraciflua*; and the needle-leaved evergreen *Pinus taeda*. The understory is dominated by *Carpinus Caroliniana* and lesser amounts of shrub and grass cover. The climate is classified as humid temperate/subtropical. Rainfall at PMRW averages 1240-mm per year and is spread approximately evenly over the year (Aulenbach and Peters, 2018). Average-annual temperature is 15.2 C with average monthly temperature lowest in January (5.5 C) and highest in July (25.2 C).

2.3.2   *Study Design and Data Collection*

The study design consisted of nine wells arranged in three transects across the riparian zone that were located to replicate landscape position on each transect (Figure 2.1). Landscape

positions were classified as near stream (~ 3 – 8 m from the main channel), middle riparian zone (*hereafter* mid-riparian, ~ 35 – 52 m from the main channel), and hillslope-riparian zone transition (*hereafter* hillslope*, ~ 65 – 90 m from the main channel). Wells were constructed of
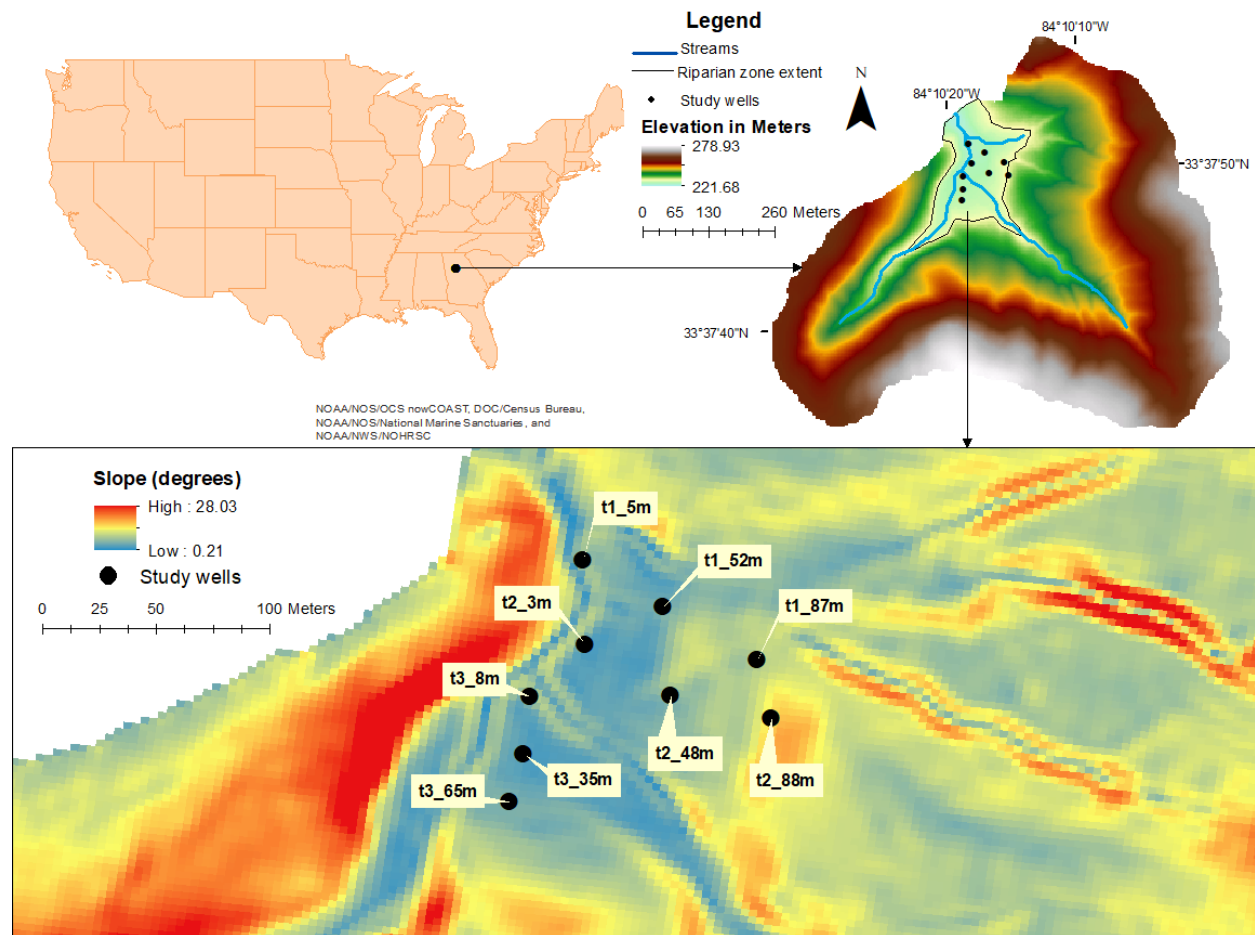
Figure 2.1 Study area map. Lower panel displays the surface slope over the riparian zone.

PVC of either 3.175 cm or 5.08 cm diameter and were screened across the water table. Each well was instrumented with an absolute pressure sensor (onset HOBO U20L-04, stated typical error ± 0.4 cm) and logged at a 5-minute interval. Monitoring began in April 2017 for three existing wells (t3_8m, t3_35m, and t3_65m) and in May 2018 for the remaining wells (Table 2.1). An additional sensor was placed in a dry well 1-m below land surface and used for barometric

Table 2.1 Description of landscape features surrounding wells, typical water-table depths and magnitude of fluctuation, and total days of data included in the analysis for each well.

Well ID	Transect	Landscape position	Basal area cm²/plot[a]	Mean water-table depth (m)[b]	DWTF magnitude (cm)[c]	Days included per year[d]
t1_5m	1	near stream	1996	-0.75	4.5	NA, 108, 141
t1_52m	1	mid-riparian	1470	-0.13	4.5	NA, 106, 140
t1_87m	1	hillslope	8142	-2.14	5	NA, 125, 140
t2_3m	2	near stream	3408	-0.81	4.5	NA, 126, 139
t2_48m	2	mid-riparian	331	-0.34	6	NA, 123, 141
t2_88m	2	hillslope	3610	-2.63	3.5	NA, 127, 138
t3_8m	3	near stream	6679	-0.82	4	130, 135, 141
t3_35m	3	mid-riparian	6245	-0.92	6.5	132, 135, 140
t3_65m	3	hillslope	2488	-1.89	5.5	131, 134, 141

[a] plots were 100 m² centered on each well and basal area of trees ≥ 5cm DBH
[b] mean water table depth over entire study period growing seasons
[c] typical maximum diel water-table fluctuation (DWTF) magnitudes observed during the growing season
[d] days in 2017, 2018, 2019, respectively. "NA" indicates data were not collected in 2017.

compensation. Manual water-table depth measurements were taken approximately monthly to convert pressure measurements into depth below land surface using Hoboware Pro software (Onset Corporation, 2019).

A meteorological station exists in a clearing just outside the watershed and collected air temperature, precipitation, and relative humidity. A soil moisture monitoring site with sensors at 15 cm, 40 cm, and 70 cm below the surface was installed in a toe slope position across the stream from the studied riparian zone (for details on equipment used and raw data, see Riley, 2021). We converted the volumetric water content to depth equivalent storage assuming a 1-m soil depth (Aulenbach and Peters, 2018). We conducted vegetation surveys in 100 m² plots centered on each well. We identified and measured diameter at breast height (DBH, ~ 1.3 m

above ground) of all woody stemmed vegetation ≥ 5 cm DBH to determine basal area of trees surrounding each well.

2.3.3   Estimating Groundwater Transpiration (T$_G$)

A detailed comparison of different techniques for estimating T$_G$ was presented by Fahle and Dietrich (2014). These authors compared results from several methods to T$_G$ estimated from their weighing lysimeter. They found that the complexity of the method had no bearing on its accuracy and that the method of Gribovski et al. (2008) had the highest correlation with measured T$_G$. This, along with our desire for sub-daily estimates of T$_G$ led us to use the empirical approach of Gribovski et al. (2008). This approach requires only high frequency groundwater level data and an estimate of aquifer specific yield (S$_Y$). This method relies on recession periods. We therefore discarded data from days when cumulative precipitation was ≥ 3 mm and data from the following day to exclude periods that may have transient water tables and substantial vadose zone moisture redistribution (Shah et al., 2007). The 3-mm threshold is somewhat arbitrary and was used to prevent excluding days unnecessarily when no water-table response is likely to occur. This threshold is in the range of forest-canopy storage estimated from data in Cappellato and Peters (1995). The method for estimating T$_G$ is based on a mass-balance equation for the water storage within an idealized volume around the well, as follows:

$$\frac{dS}{dt} = S_y \frac{dh}{dt} = Q_{net} - T_G \qquad \text{eq.2.1}$$

$$T_G = S_Y * \left(r - \frac{dh}{dt} \right) \qquad \text{eq.2.2}$$

The term $\frac{dS}{dt}$ is the change is storage over time [L/T], S_Y is the specific yield of the aquifer

[L^3/L^3], $\frac{dh}{dt}$ is the change in hydraulic head over time[L/T], r is the time dependent recharge rate

estimated from the daily maximum and minimum rates of water level change, $Q_{net} = r*S_Y$ and

represents the net inflow or outflow from the well [L/T], and T_G is the transpired water derived

from the aquifer. The method is demonstrated graphically in Figure 2.2.
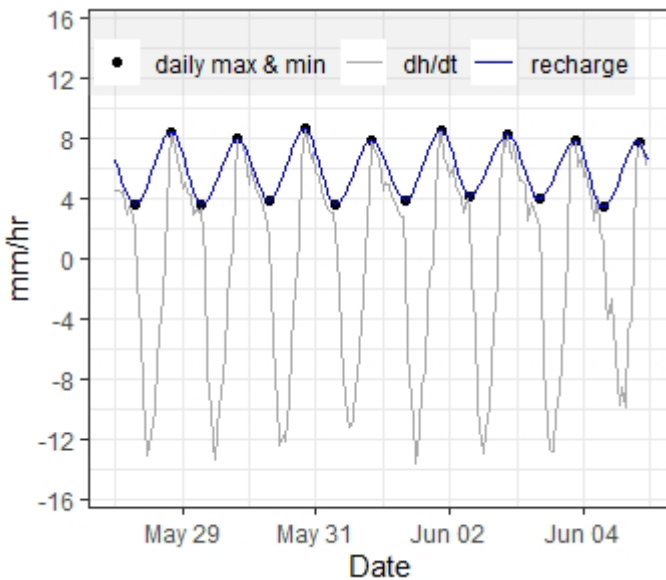
Figure 2.2 Graphical representation of the Gribovski et al. (2008) empirical approach for estimating T_G. The light curve (dh/dt) is subtracted from the dark curve (estimated recharge) and the resulting difference is multiplied by specific yield to give T_G. The daily min and max were used for estimating instantaneous recharge as described in the methods.

The dark curve represents the estimated recharge [L/T] to the well (Q_{net}/S_y) which is determined

empirically by selecting the daily minimum (average of pre-dawn hours when ET and r are

lowest) and maximum $\left(\frac{dh}{dt}\right)$ and by fitting a spline function to interpolate hourly values. The

light curve represents the hourly change $\left(\frac{dh}{dt}\right)$ in groundwater level [L/T]. We made two

deviations from the empirical method described in Gribovski et al. (2008). First, we used data

from 2 AM – 6 AM local time for estimating the minimum dh/dt, as we found this time period

was more appropriate for our study site. Second, we only aligned the min dh/dt with min WTD—

since it was an average and didn't have a precise temporal location—but used the actual

temporal location where the maximum dh/dt occurred rather than aligning it with the time of

max WTD. Because this method requires taking the difference in groundwater level when there

is very little change, it is important to smooth the time series to reduce errors associated with

small fluctuations inherent with pressure transducers (Gribovszki et al., 2008; Loheide, 2008).

We used a moving-window median with a window size of 55 minutes. This window was

examined graphically against the raw data and against windows of 15 and 35 minutes. The 55-

minute window size offered the best smoothing without altering the temporal position of min and

max values. Groundwater transpiration was only estimated during the growing season (April 15

– October 30) when diel water table fluctuations were present.

2.3.4   *Estimating Specific Yield (S$_Y$)*

To estimate specific yield we conducted slug tests, also known as the "auger hole

method" (Van Beers, 1983; Gribovski, 2018; Van der Molen et al., 2007; U.S. Bureau of

Reclamation, 1984) at each well to estimate K$_{sat}$ and used the empirical relations of Van Beers

(1983) to estimate S$_Y$. Gribovski (2018) found the auger hole method to be the most accurate of

five different S$_Y$ estimation techniques when compared to in-situ methods using vertically nested

soil moisture content sensors and water table fluctuations. The study of Gribovski (2018) was

conducted in a forested catchment with similar soil texture to the current study area. Since

parameters derived from slug test methods reflect a relatively small volume of the aquifer

(Swartz and Zhang, 2003), we took the median S$_Y$ estimated from all wells to use in the final

water table fluctuation analysis (table 2.2).

Table 2.2 Specific yield estimated from individual wells and summary stats.

Well ID	$S_{Y\text{-}augerhole}$[a]
t1_5m	0.02
t1_52m	0.04
t1_87m	0.06
t2_3m	0.06
t2_48m	0.08
t2_88m	0.14
t3_8m	0.08
t3_35m	0.06
t3_65m	0.08
Median	0.06
MAD[b]	0.02

[a] S_Y estimates based on empirical relation of Van Beers (1983) between K_{sat} and S_Y presented in van der Molen (2007). K_{sat} was estimated using 2 – 6 replicate auger hole slug tests

[b] MAD refers to the median absolute deviation

Because several of the wells in our study had consistently shallow WTD it was important to consider the effect of WTD on S_Y (Crosbie et al., 2005; Duke, 1972; Loheide et al., 2005; Nachabe et al., 2002; Shah et al., 2007; Shah & Ross, 2009). We used the approach of Crosbie et al. (2005), which the authors termed, apparent specific yield (S_{ya}):

$$S_{ya} = S_{yu} - \frac{S_{yu}}{\left[1 + \left(\alpha\left(\frac{z_i - z_f}{2}\right)\right)^n\right]^{1-\frac{1}{n}}} \qquad \text{eq.2.3}$$

where S_{yu}, is the ultimate specific yield which reflects the classic definition; z_i and z_f are the initial and final depths to water, respectively; and α and n are empirical van Genuchten soil parameters. We used the ROSETTA *Light* functions within Hydrus 1D software (Schaap et al., 2001; Simunek et al., 2013) to estimate parameters for the van Genuchten-Mualem soil-hydraulic

model based on soil texture. One deviation from Crosbie et al. (2005) is that we used the S_Y estimated from the above approach rather than the traditional method ($\theta_s - \theta_r$). This constrained the upper bounds of S_Y to a more reasonable value. Given the relatively short drainage time, it is unlikely that aquifer sediments would ever reach S_{yu}.

2.3.5   *Potential Evapotranspiration*

We estimated daily potential evapotranspiration (PET) using the Priestly-Taylor (P-T) formula (Allen et al., 1998; Priestley & Taylor, 1972) to compare with estimates of T_G. We selected P-T because it had been shown to provide reasonable estimates of ET over southeastern U.S. forests (Lu et al., 2005; Rao et al., 2011). We also included a correction for daily vapor pressure deficit and used an albedo of 0.16, which represents a weighted average based on the percentage of different land-covers (Aulenbach and Peters, 2018). All input data were from the meteorological station just outside the watershed, except solar radiation, which was obtained from satellite derived estimates of hourly solar radiation (SolarAnywhere, 2019). These data were based on average conditions over a 1-km^2 grid and the watershed was in parts of four grid cells. We spatially weighted the solar radiation data based on the proportion of the watershed in each cell.

2.4   Results

2.4.1   *Meteorological and Water-Table Characteristics*

Growing season rainfall during 2017 and 2018 was greater than the long-term average (1985-2015), while the total rainfall during 2019 was near average (Table 2.3). However, rainfall in June and September of 2019 was 5.59 cm and 8.14 cm below average, respectively. Average soil moisture storage across all three growing seasons showed little variability (Table 2.3). Similar, to precipitation, average soil moisture during September 2019 was the lowest observed

over the monitoring period (12.2 cm). The soil moisture decline in June 2019 was less substantial (15.1 cm of soil-water storage), likely due to moisture storage remaining from dormant season recharge. PET during the growing season was near average for all years. Among the three years, PET exceeded precipitation by 9 – 32 cm, indicating the apparent need for plants to utilize groundwater.

Table 2.3 Growing season (April – October) totals of rainfall, PET, and soil moisture storage (SM). All variables are expressed in centimeters. The mean value of rainfall is based on a record from 1985-2015; for PET it is 1998-2018, and for SM it is 2017-2019.

	2017	*2018*	*2019*	*Mean*
Rainfall	90.1	83.1	70.4	71.5
PET	99	97	102	102
SM	28	28	25	27

The water table depth was variable across the different landscape positions (Figure 2.3). Within each position, the mean was slightly lower in 2018 than 2019, with the hillslope and mid riparian locations differing by 9 and 15 cm, respectively (table 2.4). In contrast, the near stream landscape position was similar both years (Figure 2.3, table 2.4).

Across all well locations, diel water table fluctuations (DWTF) became apparent in the first or second week of April each year and continued until late October. DWTF were visually apparent when water-table depths ranged from a few centimeters to three meters below land surface (mbls). The only exception was at *t3_65m* where the water-table falls below the rooting zone at approximately 2.1 mbls, as evidenced by the cessation of DWTF. Maximum daily water-table elevations occurred most frequently from 08:00 - 09:00 followed by a decline to minimum elevations, most often reached between 17:00 – 18:00. Maximum daily fluctuations ranged from 3.0 – 6.5 cm across wells (table 2.1).
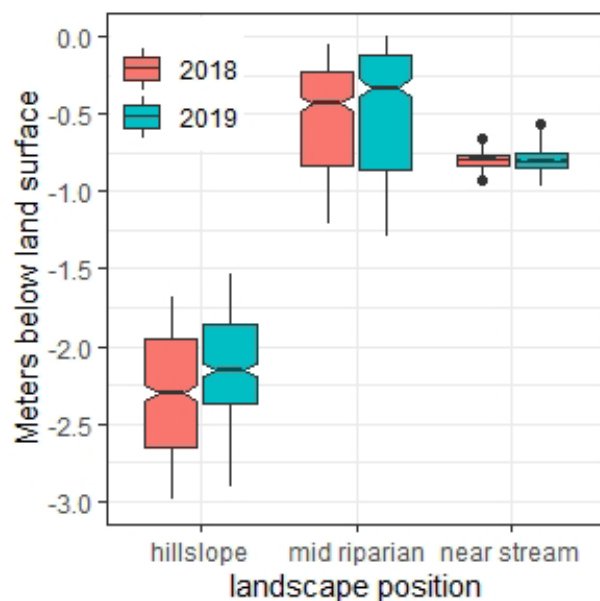
Figure 2.3 Boxplots of water table depth grouped by year and landscape position. The box represents the interquartile range (IQR), vertical lines extend to +/- 1.5 times the IQR. Dots represent data points that are beyond 1.5 times IQR. Note, data from 2017 was exclude because only one well transect was instrumented then.

Table 2.4 Welch two-sample t-test (α = 0.05) of difference in mean water table depth at a given landscape position between years.

	Difference in means (m)	Lower 95 % CI	Upper 95 % CI	p-value
Near stream	0.004	-0.004	0.013	0.321
Mid riparian	-0.085	-0.138	-0.032	0.002
Hillslope	-0.146	-0.197	-0.095	0.000

Rainfall prevalence affected the number of days which could be assessed (Table 2.1) because the method relies on periods without precipitation. The average number of sequential days with no appreciable precipitation was 8, with a median of 5 days. The longest sequence of suitable days was 47, which occurred from August 28, 2019 to October 14, 2019. On a monthly basis, the fewest days included in a given month were 8 in April 2018 and the most was 30 days in September 2019. There was an average of 19 days each month suitable for estimating T_G.

2.4.2 Differences in T_G by Landscape Position and Year

A high-level assessment was conducted to explore generalities in the spatial and temporal behavior of T_G. Variation in T_G among locations did not display a consistent spatial pattern either laterally across the riparian zone (hillslope to stream) or longitudinally (up/down valley).
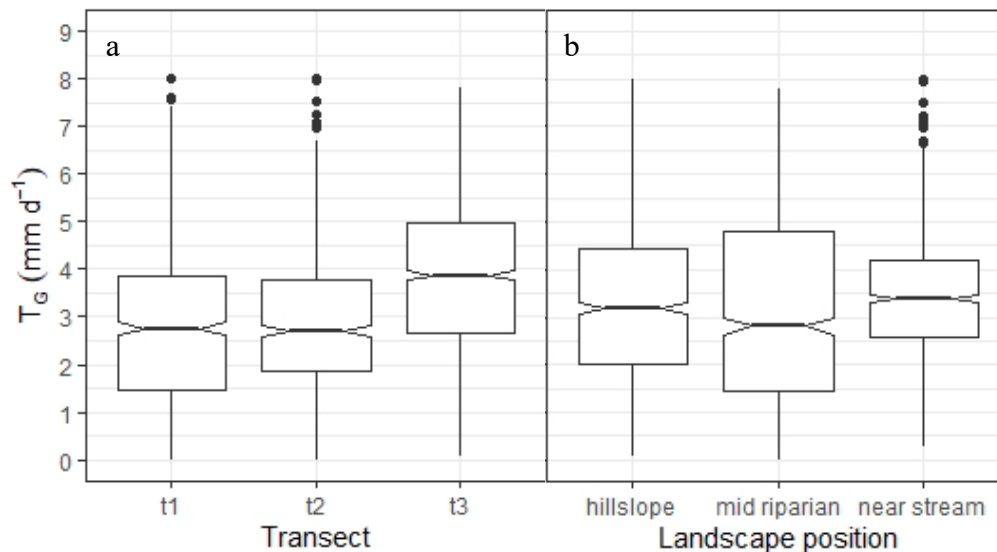
Figure 2.4 Boxplot of daily T_G over all wells at each transect (a), and landscape position (b). The box represents the interquartile range (IQR), vertical lines extend to +/- 1.5 times the IQR. Dots represent data points that are beyond 1.5 times IQR.

Transect 3 generally had the highest median T_G of 3.87 mm d^{-1} (Figure 2.4a). Transects 1 and 2 had similar median T_G of 2.78 mm d^{-1} and 2.74 mm d^{-1}, respectively. When comparing across landscape positions no systematic patterns were apparent in T_G (Figure 2.4b). Groundwater transpiration (T_G) from the mid-riparian zone wells demonstrated greater variability and was lower (2.83 mm d^{-1}) than the near-stream (3.39 mm d^{-1}) or hillslope wells (3.21 mm d^{-1}). Based on a Tukey-Kramer HSD test (table 2.5), the middle riparian zone was different (at $\alpha = 0.05$) than the other two positions, albeit not of great magnitude (~0.5 mm d^{-1}).

Table 2.5 Results of Tukey-Kramer Honestly Significant Difference tests.
Testing for difference in the mean T$_G$ (mm/day) between years and landscape positions (α =
0.05).

Comparison		Difference in means	Lower 95% CI	Upper 95% CI	p-value
2019-near stream	2018-near stream	0.594	0.267	0.921	0.0000
2019-hillslope	2018-hillslope	0.862	0.537	1.187	0.0000
2019-mid riparian	2018-mid riparian	0.053	-0.276	0.381	0.9975
2018-mid riparian	2018-hillslope	0.087	-0.248	0.422	0.9768
2018-near stream	2018-hillslope	0.463	0.129	0.797	0.0011
2018-near stream	2018-mid riparian	0.376	0.037	0.715	0.0196
2019-mid riparian	2019-hillslope	-0.722	-1.041	-0.404	0.0000
2019-near stream	2019-hillslope	0.195	-0.123	0.514	0.4986
2019-near stream	2019-mid riparian	0.918	0.601	1.234	0.0000

Temporal patterns were relatively consistent, but some differences did exist (figure 2.5).

Note, only a single transect (t3) was instrumented in 2017; therefore, only 2018 and 2019 - when

all wells were instrumented - were included in the temporal comparisons. Across all monitoring

locations, T$_G$ in 2019 was greater than 2018 (*t-test*, mean difference 0.51 mm ± 0.15 mm [95%

CI], p< 0.001, Figure 2.5a). When broken down further to assess landscape positions by year,

overall differences in years were attributable to differences at the hillslope and near stream

positions, as there was very little difference between years at the mid-riparian landscape

positions (table2.5, Figure 2.5b). While there were several occurrences where differences in

means were substantiated by p-values below the alpha = 0.05 and confidence intervals not

containing zero, they were generally of low magnitude and not suggestive of substantial spatial

patterns in T_G magnitude.
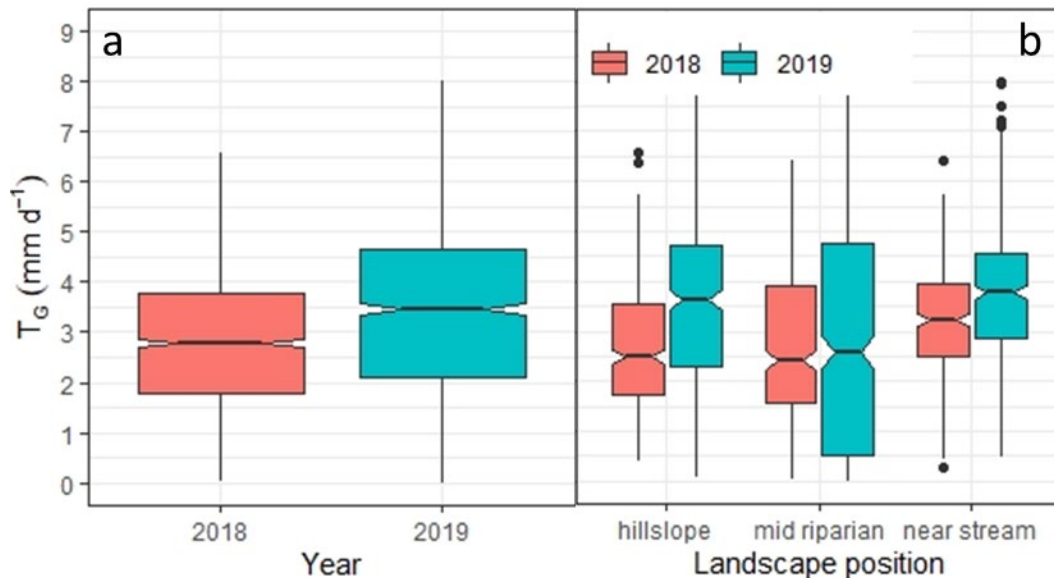
Figure 2.5 Boxplots showing the distribution of T_G across years (a), and across years by landscape position (b). The box represents the interquartile range (IQR), vertical lines extend to +/- 1.5 times the IQR. Dots represent data points that are beyond 1.5 times IQR

2.4.3 Daily T_G Estimates and Patterns

To compare T_G around individual wells we calculated the monthly median T_G for each

month in each year. The greatest monthly median was 6.4 mm d^{-1} and occurred in August of

2019 around well t3_35m (Figure 2.6). Of the top 10 highest monthly medians, 8 occurred

around well t3_35m and ranged from 5.4 – 6.4 mm d^{-1}. T_G around this well was consistently

either the highest or second highest throughout most of the study. The second greatest T_G of 3.92

– 5.56 mm d^{-1} occurred around well t3_65m, except in September and October of 2018 and

2019, when the water-table would periodically fall below the rooting zone and DWTFs would

cease. The lowest mean monthly T_G occurred around well t1_52m and t2_88m. Interestingly,

these wells represent the shallowest and deepest water table locations in the study. T_G around

these wells ranged from almost zero to 2.6 mm d^{-1}. This seemingly contradictory occurrence of

the lowest T_G occurring at both the deepest and shallowest areas is addressed in the following discussion. T_G around other wells tended to have monthly median T_G from 2.5 – 5.5 mm d^{-1}. When examining only night-time (20:00 – 06:00), T_G ranged from 0 – 1.0 mm across all wells and months which represented 2 – 48% of the daily T_G.

The extended period of near zero T_G estimated from well t1_52m, and to a lesser degree t2_48m, reflect frequently saturated conditions at the land surface during the early growing season. The more general temporal pattern that is apparent across all wells reflects the role of plant phenology and seasonal changes in meteorological forcings on daily T_G (Figure 2.6).
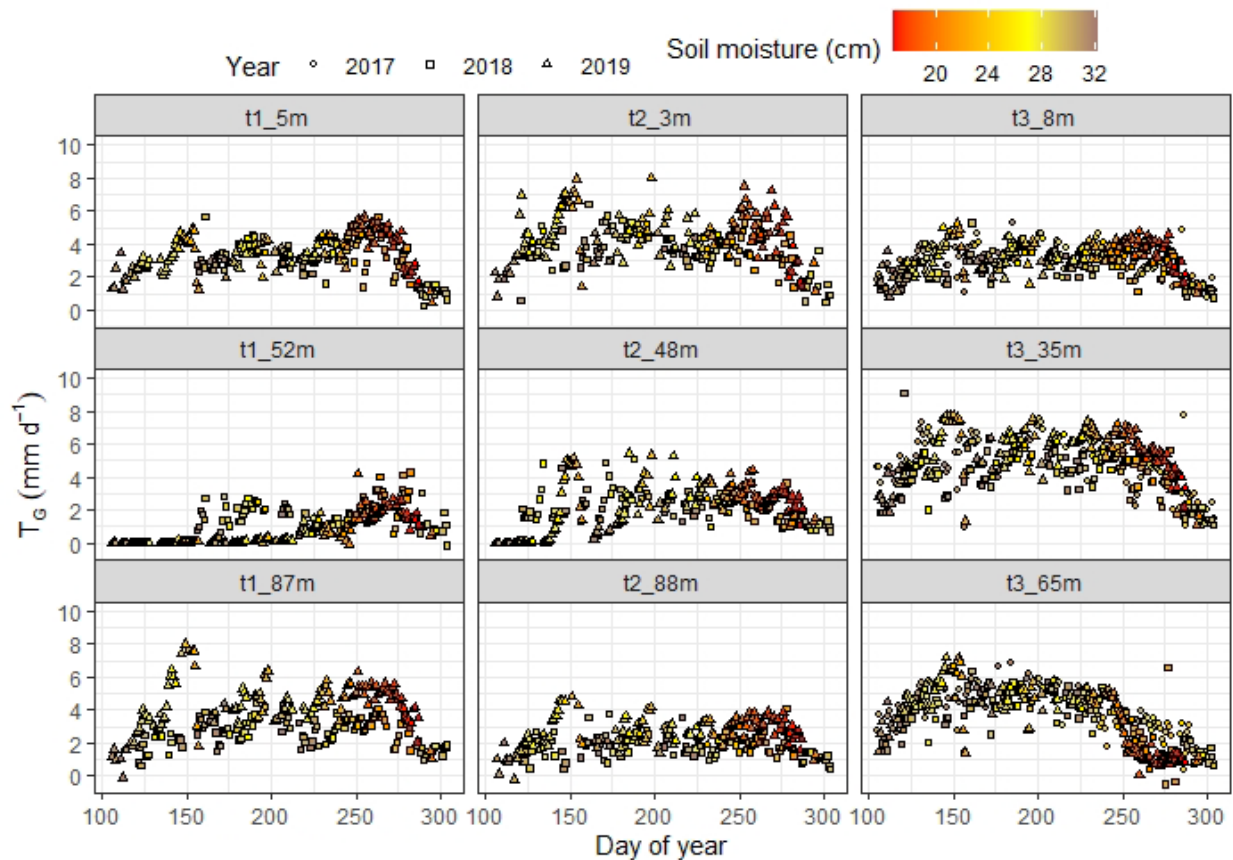
Figure 2.6 Daily T$_G$ time series for the study period. Panels are arranged with columns representing transects (1 – 3, from left to right) and rows representing landscape position (near stream to hillslope, top to bottom)

In April, trees are leafing out and moisture storage in the soil is generally high, resulting in relatively low T_G. As the season progresses trees reach maximum leaf area and air temperature

and solar radiation increase leading to increased T_G and decreased vadose zone storage. By late

September/early October, solar radiation is decreasing thereby reducing T_G. However, even

though T_G is decreasing, during this period storage has often reached the lowest point for the

year, and a greater fraction of PET may be sourced from the groundwater (Figure 2.7).

During late 2019, when there was a severe to extreme drought, a more frequent occurrence of
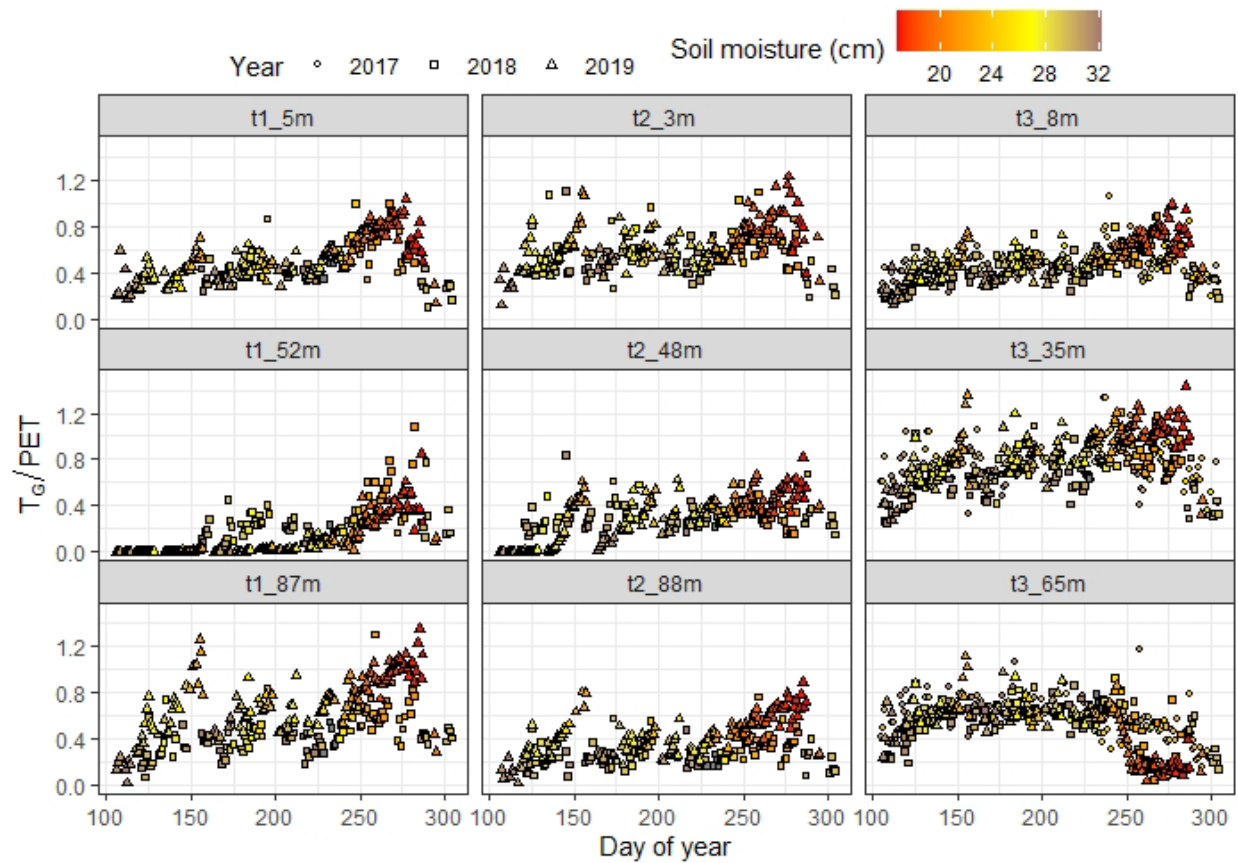
Figure 2.7 Daily Ratio of T_G: PET. Note, ratios are based only on daylight hours (7:00 AM – 7:00PM) when comparison between the two methods is most relevant. Symbol shape indicates study year and color represents soil moisture storage.

higher T_G/PET results. This suggests that groundwater is a substantial source of moisture for

riparian vegetation during this period around most of the monitored wells (Figure 2.7). One

hillslope location (well t3_65m) was the exception, as the water table dropped below the rooting

zone around the well during this period. Figure 2.7 also indicates a covariation with soil

moisture. That is, as the soils become drier there is a greater reliance on groundwater to meet

transpiration demands and therefore, a general increase in the ratio. The above patterns are also

evident at most wells during a shorter and less intense dry spell (around day 150 in 2019) that

occurred in the peak of the growing season (Figure 2.7).

We also observed a relatively consistent pattern with WTD and T_G (Figure 2.8). T_G
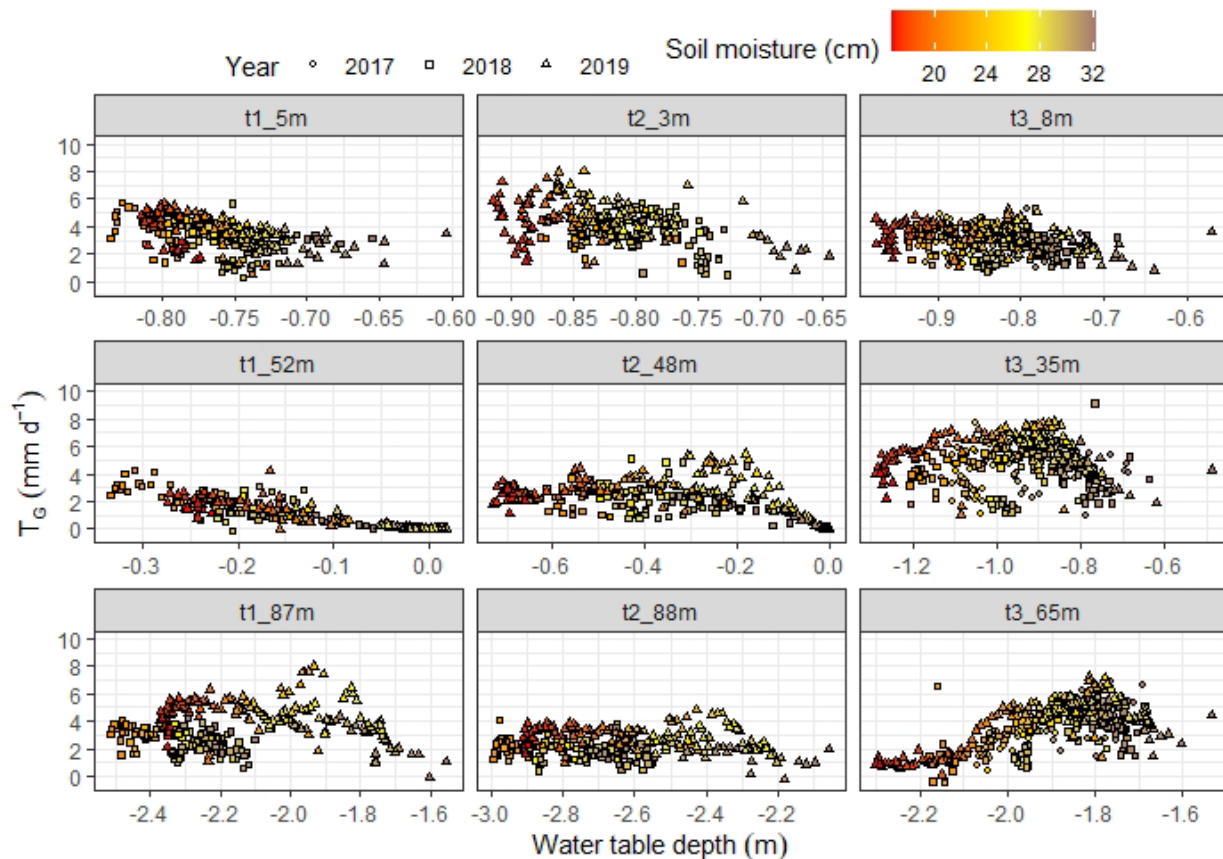
Figure 2.8 Daily T_G as a function of mean daily water-table depth and soil moisture. Points are symbolized by year and colored by soil moisture storage. Note, x-axes are not equal and represent the range of observed water-table depths over the study at each well.

generally decreased as water-table depth decreased (i.e., elevated closer to land surface). This

pattern also emerged at the hillslope position on transects 1 and 3, though notably, the qualitative

relationship between T_G and WTD varied among years and with soil moisture storage at these

locations. In 2017-2018, T_G around well t3_65m was unique in that it appeared to monotonically

increase as WTD decreased—contrasting the general trend observed across other locations. The

relationship between T_G and water table depth can also be viewed by taking into account the

PET, or the energy available to drive T_G (Figure 2.9). When viewed in this manner the variability
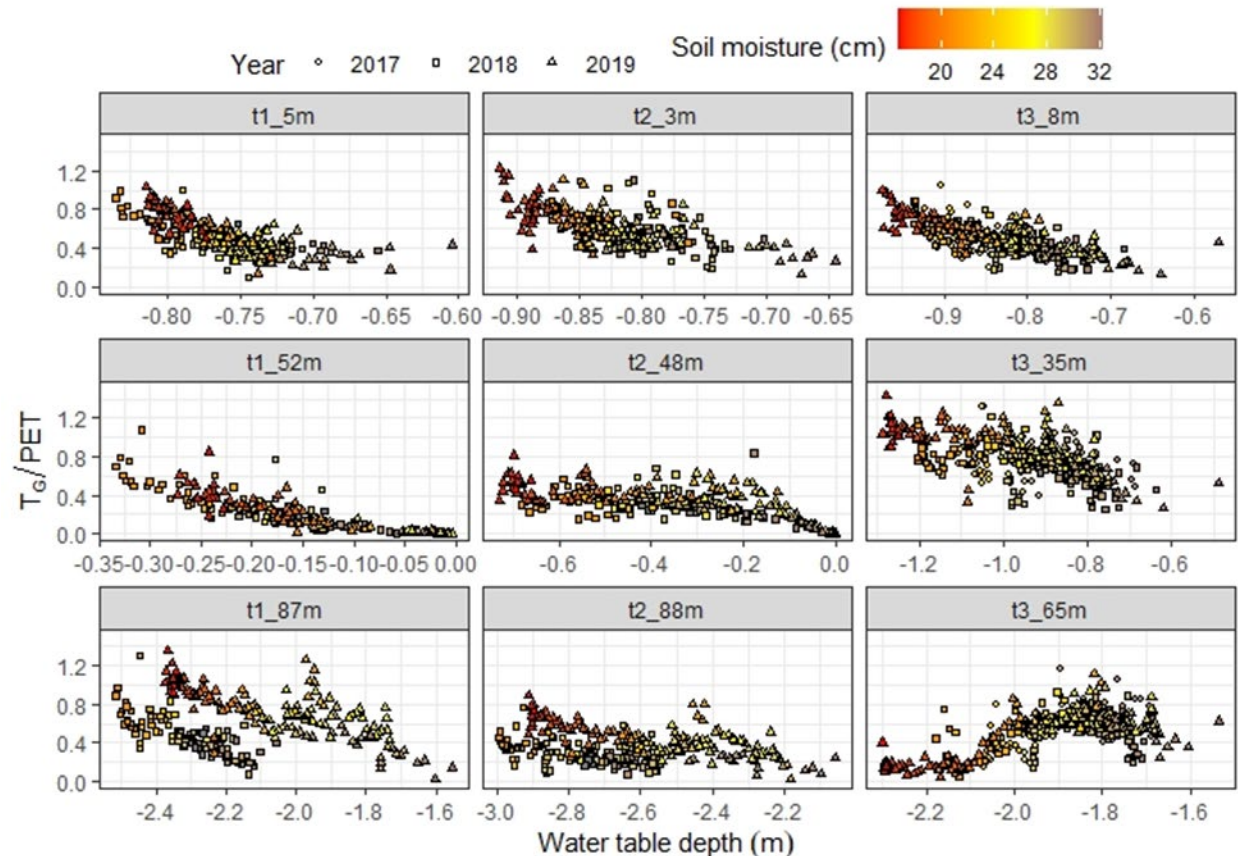
Figure 2.9 Daily TG/PET as a function of mean daily water-table depth and soil moisture. Points are symbolized by year and colored by soil moisture storage. Note, x-axes are not equal and represent the range of observed water-table depths over the study period.

decreased across locations and the response of T_G to water-table depth appears more monotonic

at most wells. As pointed out in Figure 2.6, the two different groups of T_G for a given WTD

around t1_87m become even more clear and a similar, albeit less distinct, pattern emerged at

t2_88m. Taken together, figures 2.8 & 2.9 suggest the driver of these differences is likely soil

moisture. These two distinct "groups" of T_G magnitude for a given water table depth that

occurred at the two wells with deepest WTD further suggest a decoupling of vadose zone and

saturated zone dynamics. That is, where a change in one (increase or decrease) doesn't

necessarily occur in concert with the other, and this did not occur in areas with shallower WTD.

Based on figures 2.6 – 2.9, there appeared to be a relationship between soil moisture and

water table depth that modified the relationship of WTD and T_G. We explored the linear

relationship and found a strong correlation between soil moisture and WTD, where wetter soils

generally correlated with shallower WTD (Figure 2.10). However, the relationships were non-

unique. In other words, while we fit a function to the entire dataset, it is evident in Figure 2.10

that individual recessions had similar slopes, but the intercept depended on the WTD prior to the

event and the magnitude of recharge to the soil and groundwater (Figure 2.10). The slopes were

also similar among wells for a given landscape positions and the overall pattern was consistent

across all monitoring locations (data not shown).

$$y = -1.77 + 0.0311\,x \quad R^2 = 0.76$$
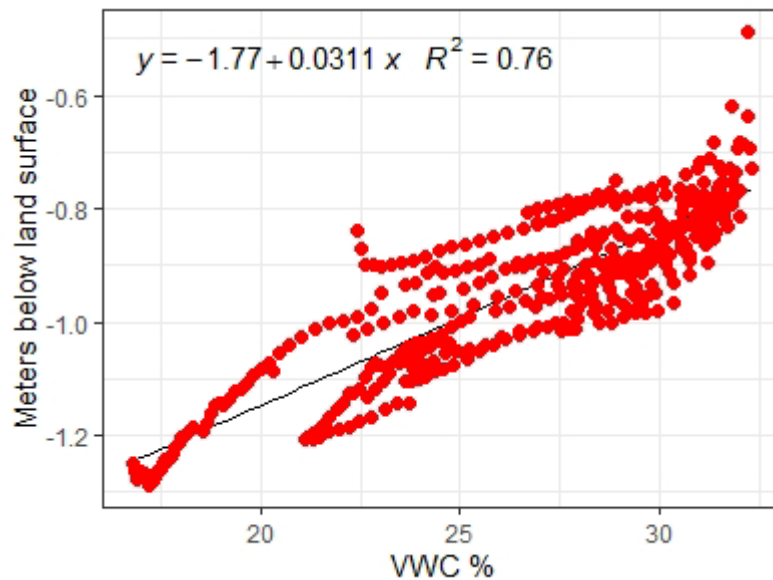
Figure 2.10 Relationship between water table depth and soil moisture. Example from plot t3_35m. This graph includes data from all days when T_G was estimated.

2.4.4 Annual T_G and PET

We examined the cumulative growing season T_G at the annual scale and compared that with PET (Figure 2.11). Across all wells and years, the median T_G was 457 mm. Total growing season PET ranged from 728 mm in 2017 to 837 mm in 2019. Note that PET for this comparison was only summed for days where T_G was estimated to allow for a direct comparison of total fluxes. Furthermore, T_G and PET were only summed for daylight hours (07:00 – 19:00). T_G followed the same temporal pattern as PET but was far more variable across all wells, likely owing to differences in WTD and vadose zone moisture storage that controlled T_G magnitude. Well t3_35m had the greatest T_G across all years, from 765 mm in 2019 to 561 mm, in 2018. The
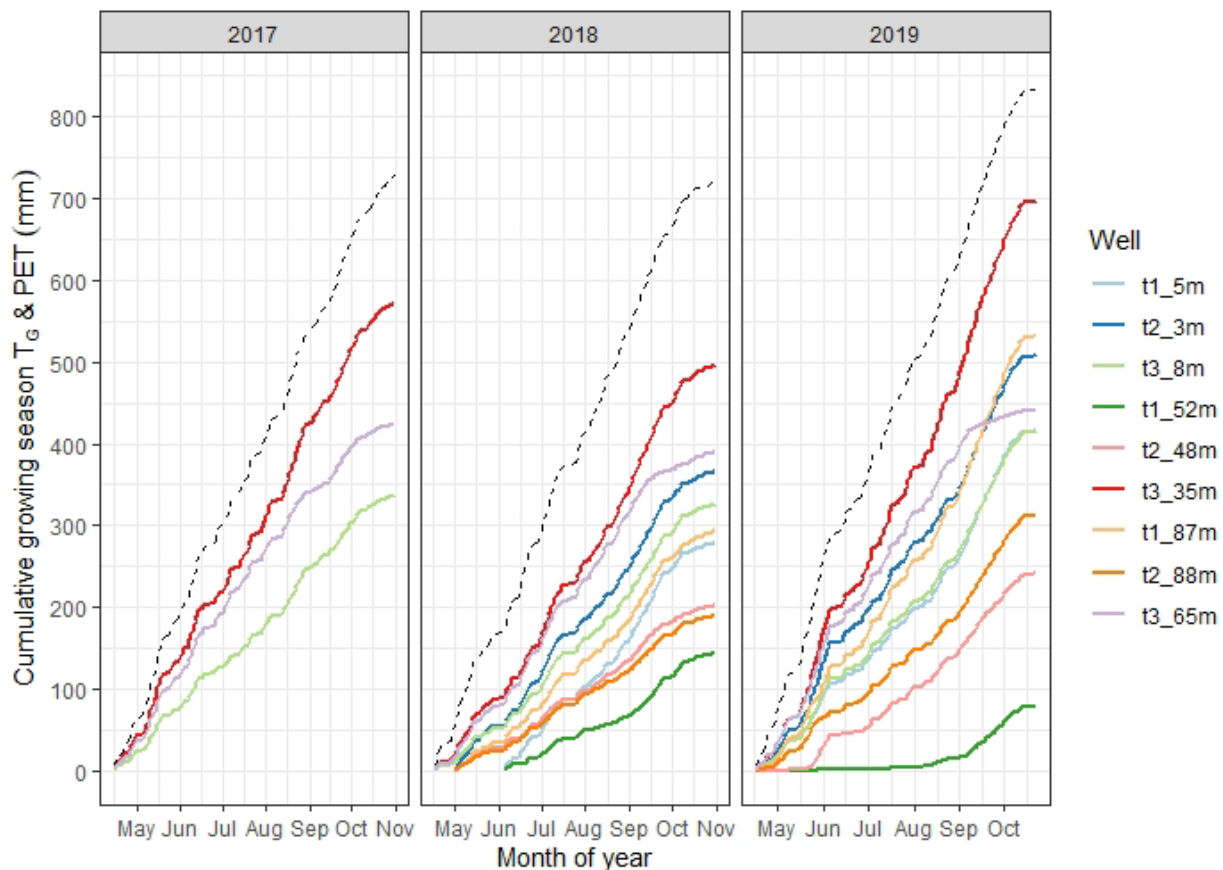
Figure 2.11 Cumulative growing season T_G for each well and year. Dashed black line is cumulative PET spanning the longest period of T_G from any well for each year. All data are only summed over daylight hours to allow direct comparison between T_G and PET.

lowest annual T_G of 100 mm was observed around well t1_52m in 2019. Interestingly, these are both middle riparian zone wells.

It is difficult to compare total T_G across all years and wells due to different starting points or missing monitoring periods at some wells in 2017 and 2018. However, when normalized to a mean daily flux for a particular year, the magnitude across wells was quite variable (0.22 – 5.6 mm d^{-1}). The median ($\pm$ MAD) T_G across all wells and years was 3.30 ± 1.05 mm d^{-1} compared to a median PET of 5.59 mm d^{-1}. This indicates that T_G could account for approximately 59 percent of the median daily PET. To explore the role of vegetation on the variation of the annual totals across well locations we examined correlations between T_G and plot level basal area. We observed a relatively poor correlation ($R^2 = 0.22$) indicating plot scale tree density was not strongly related to T_G.

Across all wells and years, T_G accounted for 9 - 83 % of PET (Figure 2.12). For the three wells that were instrumented in 2017, T_G/PET at the beginning of the growing season was highest in 2017 and similar in 2018 and 2019 (Figure 2.12). The 2017 growing season, which had the highest ratio at the start of the season, followed a region-wide severe drought in fall/winter 2016. In 2018, at all wells but t3_35m and t3_8m, T_G/PET starts near zero (indicating that PET is much greater than T_G) and rapidly increases for about one month, at which point the rate of increase stabilizes for the remainder of the season. In 2019 (Figure 2.12), around most wells, a rapid rise was observed at the beginning of the growing season then a brief decline in the ratio due to rainfall in May that replenished soil moisture. In September 2019 we see T_G/PET increase at a greater rate in response to hot and dry conditions. T3_65m was the exception to the general increase as the water table dropped below the rooting zone in September leading to a decrease in T_G and hence T_G/PET.
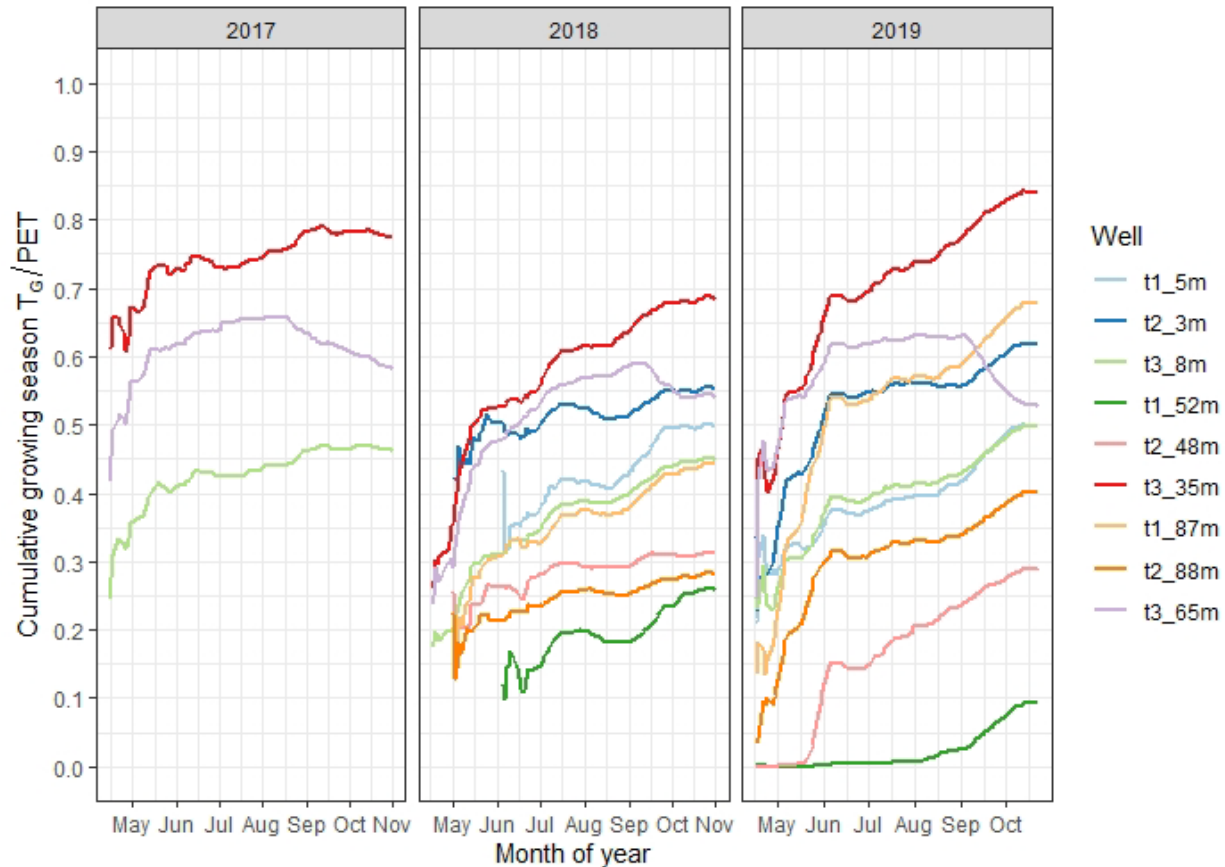
Figure 2.12 Ratio of cumulative sums of T_G and PET at each well, for each year. This plot illustrates the changing contribution of T_G to the overall PET. Data were only summed over daylight hours for direct comparison

2.4.5   Extrapolating T_G for Whole Riparian Zone Estimates

While the above results provide detailed information regarding the transpiration flux derived from groundwater at discrete points in the landscape and the variability encountered, we ultimately sought to estimate the total riparian zone T_G flux. Because our initial hypothesis, that T_G would be a function of landscape position and water table depth, was not entirely supported, or at least not consistently so (figures 2.4 & 2.5), we used the median T_G for each landscape position, since there were minor differences in T_G (Figure 2.4b, table 3) and considered each position made up equal portions of the riparian zone (i.e., each had a weight of 0.33). The median T_G was 3.15 mm d^{-1} and when applied to the entire riparian zone (3 ha) translates to a

loss of 94.5 m^3d^{-1} from the saturated zone. Aggregated over the growing season (assuming the average number of suitable days for T_G estimates in this study represents average conditions, 135 days), the total transpiration flux was 12757 m^3. This volume of water represents a rather substantial portion of the water budget in this small headwater catchment.

2.5 Discussion

2.5.1 T_G Estimates Compared to Other Studies

Our estimates of T_G are within the range of values reported from the few other studies in humid sub-tropical climates—all of which point to a strong reliance on groundwater to support transpiration. Our median T_G (3.40 ± 1.09 mm d^{-1}) is within the range estimated by Fan et al. (2014) of 0.3 - 5.8 mm d^{-1} from wells in their native and planted forest plots, and that of Nachabe et al. (2005) who observed approximately 1.7 – 6.4 mm d^{-1} using daily oscillations in soil moisture. Both referenced studies occurred in areas with sandy soils where vadose zone moisture may have provided relatively less water for transpiration compared to our site with loamy to sandy loam soils which have greater water retention. A study in the Southeastern U.S. coastal plain, focused on a 17-year-old pine plantation found mean T_G 3.01 mm d^{-1} (Domec et al., 2012).

Compared to sites in less humid regions, our median T_G was lower but comparable to T_G estimated around individual wells. Butler et al. (2007) observed an average of 4.2 mm d^{-1} in August from a riparian zone comprised of Cottonwood, Mulberry and Willow and Gribovski et al. (2008) observed, on average, 7.8 mm d^{-1} from a riparian zone dominated by Alder. Shilling (2007) observed peak T_G rates of 5.02 – 6.32 mm d^{-1} from a well in forest cover in Iowa, USA. Notably, only a few of the above studies considered more than one well in total or in each vegetation type for estimating T_G.

2.5.2 Effects of Vegetation on T_G

Variability in T_G has been observed by others across disparate vegetation types or species (e.g., Fan et al., 2014; Jia et al., 2021; Schilling, 2007; White, 1932; Yue et al., 2016). For example, Satchithanantham et al. (2017) compared a stream-side zone of grasses with an adjacent reach dominated by box elder and found the grasses used approximately 50% less groundwater than the tree reach. Fan et al. (2014) compared T_G between exotic pine, native banksia, and grasses in a sub-tropical barrier island setting and found that the mean T_G was greatest in the exotic pine stand (2.9 mm d^{-1}), followed by native banksia (1.6 mm d^{-1}), and that grasses in the study area did not use groundwater over their study period. We think our lack of correlation between T_G and tree basal area could be due, at least in part, to the relatively stronger effect of WTD on T_G. Past studies that demonstrated an influential role of vegetation type or characteristics on DWTFs and T_G may have been successful in making the connection between vegetation and T_G because only a few species were present, or focused on, or that differences in plant form (grass vs. trees) provided stark differences in relative saturated zone water uptake for a given WTD (Fan et al., 2014; Satchithanantham et al. 2017; Yue et al., 2016; Jia et al., 2021). In our case, we had a relatively diverse, mixed riparian forest with a large range of age classes and canopy positions. This could make drawing clear associations between vegetation and T_G more difficult than in a plantation type setting (e.g., Engel et al., 2005; Fan et al., 2014) or where a dominant woody phreatophyte was present (e.g., Butler et al., 2007).

2.5.3 Relationship Between T_G and Water Table Depth

We hypothesized that T_G would decrease as water-table depth increased, based on the conceptual model that T_G should be positively related to the fraction of plants root systems that are immersed in the aquifer or capillary fringe. This conceptual model has empirical support

from a range of field studies (Engel et al., 2005; Fan et al., 2014; Schilling, 2007; Yue et al., 2016) and leads to the secondary assertion that T_G by trees should decline at increasingly far distances from the stream channel because the depth to the water table also generally increases at those distances (e.g., Figure 2.3). Our results are mostly to the contrary. At only 1 of 9 well locations did we clearly see the anticipated relationship between WTD and T_G (Figure 2.8). Trees adjacent to the channel exhibited greater T_G as water-table depth increased. The same relationship emerged at one mid-slope position, although at the other 4 locations the dependency of T_G on WTD was not apparent (Figure 2.8). Aggregating the site-specific data from Figure 2.8 by landscape position reveals no apparent relationship between T_G and WTD at mid-slope and hillslope positions. Further, there were negligible differences in the average rate of T_G across all landscape positions (Figures 4 and 5). Like many Piedmont watersheds, the PMRW exhibits significant geomorphic and pedologic variability over spatial scales of tens of meters— variability that is compounded by intensive erosion resulting from historical agricultural and other land use practices. Rather than trending monotonically across the elevation gradient, total T_G, and the dependency of T_G on WTD, appear to be largely site specific within the valley bottom of this Piedmont watershed.

Absent any estimate of whole-riparian-zone transpiration, the ratio T_G:PET is at least a proxy for the fraction of tree-water use that originates from riparian aquifers, rather than the vadose zone. This normalized variable was more clearly dependent on WTD across all landscape positions (Figure 2.9) than was T_G, although contrary to our expectation T_G:PET increased as water-table depth increased. Only one well location was an exception (t3_65, Figure 2.9), which appears to represent the sole location where the water table dropped entirely out of range of local tree roots (Figure 2.9). Our results appear to support an alternative conceptual model whereby

the fraction of potential transpiration emanating from groundwater is actually positively related to water-table depth—at least up to a threshold depth corresponding to the maximum rooting depth. This, somewhat counter-intuitive, dependency is clearly mediated by vadose-zone moisture content (Figure 2.10). When vadose-zone moisture is abundant, its relative contribution to T is enhanced while that of T_G is diminished. Since WTD increases as vadose-zone moisture declines, there emerges simultaneously a positive relationship between T_G:PET and WTD.

Considering our results and those from previous studies we have cited, we identify three key factors that may determine the relationship between T_G (or T_G:PET), WTD, and landscape position at any watershed. The first is methodological. Specific yield is known to decrease as the water-table becomes closer to the land surface. Quantitative methods exist to approximate this relationship (Crosbie et al., 2005; Duke, 1972; Loheide et al., 2005; Nachabe, 2002). In some studies, though, these methods have not been employed (e.g. Satchithanantham et al., 2017; Sueki et al., 2015) and in those cases it is reasonable to suspect that estimates of T_G may be artificially high at those times when the water table is near the surface. This could result in an artificial, inverse relationship between WTD and T_G. The second key factor is soil texture (Butler et al., 2007; Loheide et al., 2005; Shah & Ross, 2009). In very coarse, sandy soils, the vadose-zone may drain very rapidly following precipitation events. The water table may rise in response to this recharge, while the plant-available water in the vadose zone quickly becomes limited. In such a case, the ratio of T_G:PET (or total T) may be comparable, or greater, when the WTD is shallow rather than deep. The third key factor is the comparative depths of water table and roots. The latter are documented across biome types (Schenk & Jackson, 2002, 2005), although the former requires at least some field observation, expert knowledge, or model simulation at

specific sites. Collectively, local knowledge about these three factors will best inform

hypotheses about the relationship between T_G (or T_G:PET) and WTD across diverse watersheds.

2.5.4   Interannual T_G Dynamics

The average T_G differed across years (Figure 2.5) and likely reflects several different

driving mechanisms. First, precipitation was greater and more frequent in 2018 leading to greater

water storage in the vadose zone, thus necessitating less groundwater uptake. Second, along with

greater rainfall came greater cloud cover and higher humidity, leading to lower PET. In Contrast,

2019 was hot and dry with long periods of little rainfall resulting in periods of increased T_G.

Considering differences in cumulative T_G, t3_35m and t1_87m were on the high end and t1_52m

and t2_48m on the low end, with others falling in between. This again highlights the variability

we observed and the lack of consistent patterns with landscape position. T_G fluxes estimated

from well t3_35m and t1_87m in 2019 were 67 – 83% of PET. As we previously pointed out in

the results, the area around the wells with the deepest (t2_88m) and shallowest water table depths

(t1_52m) had consistently low T_G and reflect two different situations and processes. The area

around well t1_52m had an extremely low flux that was largely due to frequent saturation around

the well that led to depth compensated S_Y approaching zero and was not necessarily an indication

that plants in the area were transpiring at a greatly reduced rate. Although, extended saturation

could have caused localized reductions in transpiration due to anoxic conditions in the suburface

(Kozlowski, 1984). Following Shah et al. (2007), when the water-table is at or near the surface,

all water is derived from the saturated zone, and the vadose zone is merely a conduit. Therefore,

T_G likely equals actual evapotranspiration in the vicinity of this well. Under these situations,

when the capillary fringe reaches the surface, the concept of specific yield is not applicable

(Loheide et al., 2005). Therefore, when using the present method that requires S_Y, it is not

possible to estimate a "true" T_G flux under these conditions and another method to estimate AET must be used. The area around t1_52m was the only location where this was a persistent issue. While it occurred around well t2_48m it was far less frequent. The low T_G that occurred at the deepest well in the study likely resulted from relatively little root biomass in contact with the aquifer as the water table dropped deeper below the surface. From simulation results present by Shah et al (2007), the extinction depth, where groundwater no longer contributes to ET, is around 3.30m for a sandy loam texture. This suggests that the area around t2_88m was approaching the limiting depth where T_G would be expected to occur.

2.5.5   Considerations for T_G Extrapolation in Heterogeneous Landscapes

Our estimate of total riparian zone T_G represented a rather significant portion of the water budget in this small headwater catchment. To put this in perspective, stream baseflow at the outlet of the 41-ha catchment during the growing season was on average 0.70 mm d^{-1} (Aulenbach & Peters, 2018). Scaled to the duration of an entire growing season, baseflow is on average, 57,400 m^3. This indicates that T_G could represents a storage reduction equal to approximately 22 % of baseflow during an average growing season.

Aulenbach and Peters (2018) used a water-budget approach and estimated that average watershed storage decreased by 0.97 mm d^{-1}. Comparatively, our average daily T_G estimate- which also represents a loss from storage – of 3.15 mm d^{-1}, is substantially higher than this prior estimate. However, it likely represents the higher end of the range of transpiration flux and is only applicable in the 3-ha riparian zone due to the readily accessible aquifer. Most of the watershed area is comprised of hillslopes that likely experience water stress (AET<PET) for a portion of most growing seasons. On a volumetric basis, the riparian zone may account for 26 % of the total 398 m^{3}d^{-1} (96 m^{3}d^{-1}) of average daily storage loss, which is disproportionally large

compared to its area (~ 7% of the watershed area). This suggests riparian zone T_G could be a substantial, but overlooked, component of the water budget in other humid watersheds as well.

We observed great variability in T_G across our study site and an overall lack of systematic variation across landscape positions. These observations suggest that the arithmetic average, or median, of T_G measured across sites will be a more apt predictor of whole-riparian-zone T_G than would an average based on any spatial interpolation scheme. To provide a practical assessment of the variability we observed, we calculated the mean T_G for all possible combinations of wells, to determine how many wells would be needed to reduce the error to an acceptable level, which we defined as falling within the 95% confidence bounds of the true mean. We defined the "true mean" in this case as the mean T_G estimated from all nine wells. Figure 2.13 demonstrates that to consistently reduce the error rate to within the 95% confidence bounds, one would need to use
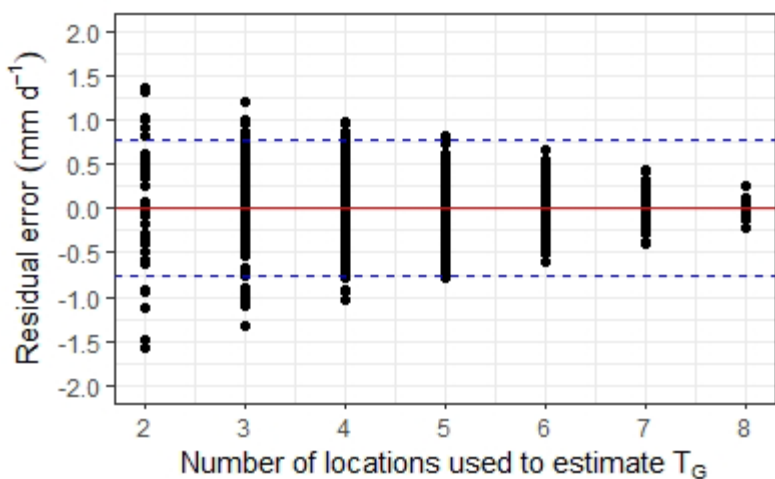
Figure 2.13 Number of wells needed to consistently estimate average T_G within the 95% confidence bounds of the true mean. The dashed blue lines indicate the 95 % confidence bounds around the mean

at least five monitoring locations. Of course, this assumes that similar variability exists among other locations with similar forests and topographic conditions and the wells would be distributed across the area of interest. Given the dearth of information in similar environments, it

provides some guidance on considering and addressing possible variability that may be present in similar settings elsewhere.

2.6   Conclusions

We investigated the applicability of a water table fluctuation approach in a humid and topographically diverse catchment, a setting where these methods have not been widely applied. We also explored the variability of T_G to understand if general patterns observed in other areas were applicable to our settings. Our results highlighted that even in a humid well- watered catchment, seasonally, T_G can be a substantial component of the water budget. We also observed patterns of T_G with WTD that ran counter to much of the existing literature; where T_G increased as the WTD increased, and in some locations, the pattern was not monotonic. We showed that this nonintuitive pattern was induced by soil moisture. When soil moisture was high, trees used less groundwater, only when soil moisture became limited did they increase groundwater uptake. Our results also suggest that past studies that have use a single or a few wells or were conducted in less topographically or vegetatively diverse locations, may not be widely transferable to more complex settings. To provide some guidance to others who may work in similar settings, we evaluated the number of monitoring locations necessary to reduce the error to within the 95 % confidence bounds of the average T_G over a similar area. Even still, there is much more work needed to further understand what can be generalized regarding T_G and what may be regional or site-specific idiosyncrasies.

While trees in our site are not true phreatophytes they may be considered facultative phreatophytes, or generalists, that will extract saturated zone moisture when necessary. This process is likely quite common in most humid regions but, presumably, since it has only limited impact on human use, it has received little attention. As we see increasing variability in water

resources coupled with increased demand, more accurate accounting of all aspects of the water

budget becomes critical even in humid well-watered environments.

3 COMPARING RIPARIAN ZONE TRANSPIRATION FROM SAP FLOW MEASUREMENTS AND GROUNDWATER DERIVED TRANSPIRATION FROM WATER TABLE FLUCTUATIONS IN A MIXED EVERGREEN-DECIDUOUS FOREST IN A HUMID-SUBTROPICAL CLIMATE

3.1 Abstract

Transpiration is a substantial component of catchment water budgets in forested environments. Yet, it is rarely determined in isolation (i.e., usually lumped as evapotranspiration) as it is a difficult flux to adequately measure. In riparian forests, where water tables are relatively shallow, water table fluctuation approaches may be used to estimate the quantity of transpiration derived from the surficial aquifer (T_G). This can provide an independent estimate of transpiration that will likely be biased low due to some transpiration also being derived from the unsaturated soils. However, a key issue that remains is water table fluctuation approaches have rarely been constrained against independent estimates of canopy transpiration (E_C). This is especially true in humid upland catchments. The aim of this study was to compare E_C from scaled sap flux measurements to T_G estimated from a diel water table fluctuations in a humid upland catchment. We estimated a growing season E_C of 241 mm and T_G of 451 mm, almost twice the total canopy transpiration. This seemingly erroneous result led us to intensively scrutinize the data and processing steps. However, after considering possible issues we considered the critical parameter that is not present in any formula to estimate T_G - land area. Therefore, there is an implicit assumption that the monitoring well used for the estimate of T_G incorporates the desired area of vegetation. Based on the relationship between tree height and rooting extent we estimate that the area of forest that could be contributing to the water table fluctuations may be ~ 2.5-times greater

than just the riparian zone we were considering, making comparisons with E_C uncertain. Given the relative accessibility of water table fluctuation approaches, and the unique and important information they contain, we think this is a fruitful avenue for further exploration, and we provide some ideas we think could help elucidate the true area of vegetation.

3.2   Introduction

The role of forests in modulating hydrologic fluxes has long been an interest to hydrologists; both from a basic standpoint of understanding the processes and pathways in which govern the flow of water, but also on a more applied level, concerning the quantity of water delivered from forested headwaters for downstream users. This is especially relevant since most watersheds that are used for water supply are sourced in headwater areas that are generally dominated by forested land cover (Alexander et al., 2007). Forest may alter water budgets through precipitation interception and transpiration. At global scale, Schlesinger and Jesechko (2014) report that 51 – 70 % of evapotranspiration (ET) on land can be attributed to transpiration (T). Similar proportions of T in total ET have been measured within individual catchments using various methodologies (e.g., Wilson et al., 2001; Domec et al., 2011). Even though transpiration is a key water budget component it is rarely quantified in isolation and is usually lumped as ET or approximated using potential evapotranspiration (PET), and sometimes estimated as the water budget residual (e.g., Wilson et al., 2001; Aulenbach and Peters, 2018).

Transpiration fluxes vary across a watershed due to multiple factors, including variable access to soil moisture and groundwater. Trees with sufficient root depth may directly extract water from the capillary fringe above, or directly within, unconfined riparian aquifers (e.g. Dawson, 1996; Barbeta & Penueles, 2017). During the growing season, it is possible that groundwater extraction by trees represents a substantial loss of water from riparian aquifers that

would have otherwise been discharged to streams. In humid regions, direct groundwater uptake

by trees is usually restricted to riparian zones or other landforms with shallow water tables (e.g.,

Bosch et al., 2014). Access to groundwater can sustain plant water use during drought periods,

whereas vegetation in other parts of a watershed, such as on hillslopes and ridges, may

experience water limiting conditions (Hawthorne & Miniat, 2018; Mitchell et al., 2012; Tromp-

van Meerveld & McDonnell, 2006). Discerning the transpiration component of total ET is a

technical challenge; deciphering what portion of T is derived from groundwater only adds to the

difficulty. As such, investigations of the catchment water balance that partition E and T have

rarely taken the next step of quantifying T_G, although a few exceptions exist (e.g., Domec et al.,

2012; Engel et al., 2005; Miller et al., 2010).

One approach that has been used to quantify water drawn from the saturated zone is the

analysis of diurnal water-table fluctuations (DWTF). This approach (Eq. 3.1) was first presented

by White (1932) and has been modified, or the basis for development of similar methods by

many researchers (*for a comparison of methods see* Fahle and Dietrich, 2014). The calculation

was presented by White (1932) as follows:

$$ET = S_Y(24r \pm s) \qquad\qquad\qquad \text{eq.3.1}$$

where ET is the rate of evapotranspiration of water drawn from the aquifer or capillary

fringe [L/T]; S_Y is the specific yield of the aquifer [L^3/L^3]; r is net recharge, defined as the rate of

increase of water-table elevation [L/T] from midnight to 4 AM; and s is the change in water-table

elevation over a fixed 24-hour interval [L/T]. DWTF analysis have been used in many different

environments to quantify the groundwater component of ET (Buter et al., 2007, McLaughlin and

Cohen, 2012, Riley 2022, ch.2). In some environments the estimates may reflect a combination

of evaporation and transpiration. This will largely depend on the climate, sediment texture, and

water-table depth (Loheide et al., 2005; Shah et al., 2007). However, in humid forested

catchments, the E component is likely exceedingly small due to the low energy and more humid

conditions below the canopy (e.g., von Arx et al., 2012) coupled with the low rate of vapor

transport in moist soils. The application of DWTF methods have been most widely applied in

semiarid to arid environments, likely reflecting the critical importance of groundwater in these

climates. Relatively few studies have been conducted in humid regions, and of those most have

focused on monoculture forest plantations in lowland landscapes (e.g., Domec et al., 2011; Fan

et al., 2014). An interesting finding from many studies, across regions, is that T_G is

approximately equal to, or exceeds, PET (Domec et al., 2011; Gribovski et al., 2008; Martinet et

al.,2009; Nachabe et al., 2005; Sachinathetham et al., 2017; Soylu et al. 2012). In contrast,

studies in the Southeastern U.S. have demonstrated that actual, total ET rarely equals PET during

the growing season and is often substantially lower (Aulenbach and Peters, 2018; Oishi et al.,

2010; Wilson et al., 2001). Clearly T_G cannot be greater than total T or ET. In the former studies

either groundwater is the primary—possibly singular—source of water for vegetation or the

seemingly high magnitudes of T_G may result from methodological artifacts such as poorly

constrained aquifer-hydraulic properties (i.e., S_Y) or PET estimates.   Additional research is

needed to resolve these uncertainties about the magnitude of T_G and its relative importance in the

catchment water balance.

     Our prior work at this site (Riley, 2022, ch2) applied an adaptation of equation 3.1

presented originally by Gribovski et al. (2008), which was identified as a superior approach by

the empirical work of Fahle and Dietrich (2014). Our average estimates of growing season T_G

ranged from 1.14 to 4.83 mm day^{-1} across nine monitoring wells spanning near-stream to incipient hillslope landscape positions. These estimates are within the range of values reported from past studies (Butler et al., 2007; Domec et al., 2012; Fan et al., 2014; Gribovszki et al., 2008; Schilling, 2007). The relative magnitudes of growing season T_G, expressed as T_G:PET, ranged from 9 to 83 % across two years, and were also within the range of previous reports (Fan et al., 2014; Loheide, 2008). However, other studies conducted in forests of the southeastern United States estimated whole-canopy transpiration (derived from all water sources) to be 30 - 40% of PET (Wilson et al., 2001; Wullschleger & Hanson, 2006). Our results combined with pre-existing studies of whole-canopy transpiration exemplify the apparent contradiction we discussed above: either T_G is a surprisingly large component of total T and ET, or our approach to estimating T_G involves latent biases that have not been fully comprehended.

Our literature review reveals relatively few past studies that have quantified in isolation the transpiration component of whole-forest ET. It further reveals a greater scarcity of works that have specifically quantified T while also resolving that amount of T that is derived specifically from groundwater within shallow aquifer rather than the vadose zone. Results from the few studies that have point to counterintuitively high magnitudes of T_G. To address these uncertainties, we conducted a field study with two main objectives. First, we attempted to estimate whole-canopy transpiration from a riparian forest by upscaling tree-level transpiration measurements to the plot, then whole riparian-zone scale. Second, we compared these estimates of E_C to estimates of T_G (based on well hydrograph analysis) to quantify the fraction of total canopy transpiration that is sourced from groundwater. As will be shown, outcomes from achieving these two objectives motivated a third objective focused on understanding reasons for incongruency between our, and previously reported, estimates of T_G versus E_C.

3.3   Materials and Methods

3.3.1   *Site description*

This study was conducted at the Panola Mountain Research Watershed (PMRW) in the Piedmont region of Georgia, USA, which is located ~ 48 km southeast of Atlanta, GA within the Panola Mountain State Conservation Park (Figure 3.1). The study watershed is 41 ha with a low-relief riparian zone of approximately 3 ha. The climate is humid subtropical (*Cfa*) based on the Köppen classification system. Rainfall at PMRW averages 1240 mm y^{-1} and is spread evenly over the year (Aulenbach and Peters, 2018). Average temperature is 15.2 C with average-monthly temperature generally lowest in January (5.5 C) and warmest in July (25.2 C). Soils are sandy-loam to loamy textured with bedrock or saprolite approximately 1 – 5-m below the
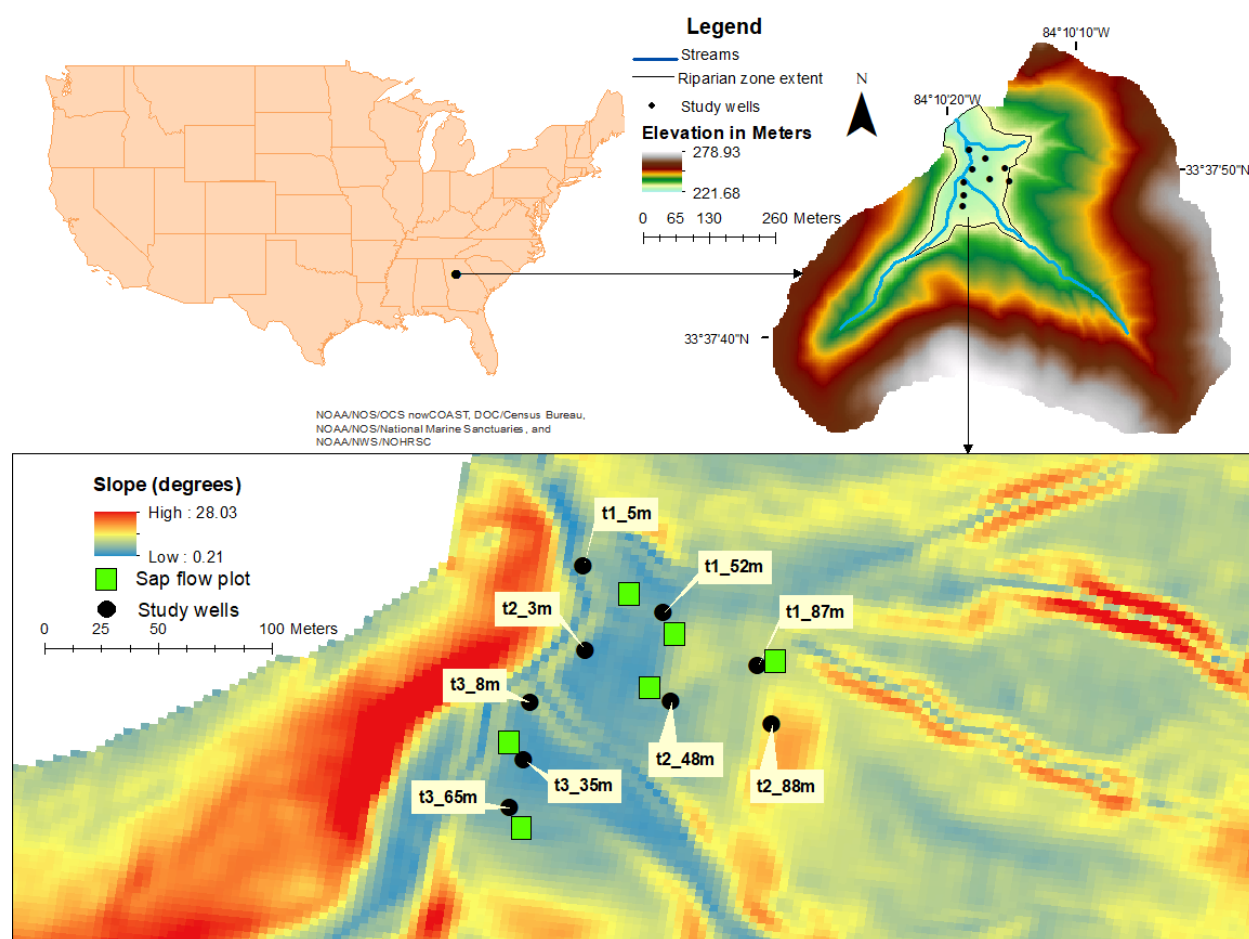
Figure 3.1 Study site location and monitoring layout.

surface. The riparian forest is composed of at least 13 tree species, but basal area is dominated by 5: *Quercus alba, Liriodendron tulipifera, Nyssa sylvatica, Liquidambar styraciflua* and *Acer rubrum*. The understory is dominated by *Carpinus caroliniana* and lesser amounts of shrubs and herbaceous cover. While the tree species are generally well distributed across the riparian zone there is a greater amount of oak/hickory at the hillslope position and loblolly pines were exclusively in this landscape position.

3.3.2   *Meteorological data*

Meteorological data were collected in a clearing just outside of the watershed. Parameters included air temperature, precipitation, and relative humidity. We also used these data to estimate potential evapotranspiration (PET) using the Priestly-Taylor (P-T) formula (Allen et al., 1998; Priestley & Taylor, 1972). We selected P-T based on other studies that demonstrated reasonable estimates of ET over southeastern U.S. forests (Aulenbach and Peters, 2018; Lu et al., 2005; Rao et al., 2011). All data for PET calculations were from the meteorological station except solar radiation, which was from satellite derived estimates of hourly solar radiation (SolarAnywhere, 2019). These data were based on average conditions over a 1 km^2 grid and the watershed was in parts of four grid cells. We spatially weighted the solar radiation data based on the proportion of the watershed in each cell. Soil moisture was also monitored in a toe slope position across the stream from the studied riparian zone. Sensors were installed at 15 cm, 40 cm, and 70 cm below the surface. Volumetric water content was converted to depth equivalent storage assuming a 1 m soil depth (Aulenbach and Peters, 2018).

3.3.3   *Monitoring wells*

We installed shallow wells to monitor water table fluctuations at nine locations along three transects within the riparian zone (Figure 3.1). Three wells were located within 8 m of the

stream in what we defined as the "near-stream zone". Second and third groups of wells (n=3 per group) were installed at distances of 35-52 m and 65-88 m from the stream. We defined those locations as the "middle-riparian zone" and "hillslope-riparian transition" zones, respectively. Hereafter, we will refer to those positions as low, mid, and up, respectively. Each well was instrumented with a pressure transducer (Hobo U20, total pressure sensor). We also installed an additional dry well for the barometric pressure sensor. The dry well was within the water table and prevents large swings in temperature, which can result in relatively large errors when adjusting total pressure sensors for atmospheric pressure (Mclaughlin and Cohen, 2011)

3.3.4   Estimating sap-flux density and transpiration at whole-tree to stand-level

We used heat-pulse velocity (HPV) probes (Implexx Sap Flow Sensor, Implexx Sense, Melbourne, Australia and East 30 Sensors, Pullman, WA) to quantify sap-flux density within tree stems and scaling techniques to extrapolate whole-tree and stand-level transpiration. The HPV sensors have three needles; the middle needle is an inline heater that delivers the heat-pulse, and the outer two needles contain thermistors located at 5mm, 17.5mm, and 30mm depths. The multiple thermistors allow an assessment of the radial variability of sap flow in the outer portion of the conductive tissue, which is critical in species with thick sapwood. To inform our species selection (Table 1), we surveyed all trees > 5-cm diameter at breast height (DBH, ~ 1.3m above ground) in a 100 m^2 plot centered on each well. We selected species that, collectively, comprised > 80 % of basal area. We installed HPV sensors in select trees around six of the wells (Figure 3.1). At each location, 3 – 4 trees (19 total) were instrumented with a single HPV sensor on the north or south side of the tree. Another sensor was designated as a "rover" that was to be moved between trees at a location to better characterize the azimuthal variability of sap-flux density within the stem. However, after two sensors were destroyed during removal, we halted that

practice. We selected only canopy dominant and sub-dominant trees with no obviously

anomalous stem or canopy growth. We attempted to select individuals representing the range of

DBH observed in our survey, within the constraints of available cable length and data loggers.

All sensors were covered with a layer of reflective insulation and adhesive plastic wrap to reduce

temperature variation at the sensor.

Table 3.1 Quantity and diameter of trees instrumented with heat pulse velocity sensors. *Species code is the first 2 letters of the scientific binomial. In subsequent analyses, QUINI and QUAL were combined and presented as QUsp or ring.*

Number of trees[1]	Species	Species code	Mean DBH (cm) ± 1 SD	Common name
1	*Quercus nigra*	QUNI	67.5	water oak
4	*Nyssa sylvatica*	NYSY	31 ± 3.7	Black tupelo
3	*Liquidambar styraciflua*	LIST	39.7 ± 19.6	sweetgum
4	*Quercus alba*	QUAL	41.6 ± 14.3	White oak
3	*Pinus taeda*	PITA	48.3 ± 4.5	Loblolly pine
4	*Liriodendron tulipifera*	LITU	44.7 ± 6.9	Yellow poplar

[1.]Several sensor failures resulted in only partial records for 2 NYSY and 2 QUAL. Thus, reducing the number of total trees to 15.

3.3.5   *Processing heat-pulse velocity data*

We followed the Dual Method Approach described in Forster (2019, 2020) for converting

the raw temperature data into sap flux density. Briefly, this approach generally follows the slow

rate of flow (heat-ratio) method described by Marshall (1958) and modified by Barrett (1995) but

also combines the t-max method of Cohen (1981) if/when sap velocities are high. This approach

takes advantage of the optimal range of sap velocities of each method. Before calculating the sap

velocity, the heat pulse velocity was corrected for wounding due to probe installation following

Burgess et al. (2001). Sapwood properties (moisture content and density) were estimated from 5 mm diameter increment cores taken just below the sensor after removal. Further, we took an additional core approximately 90 degrees from the first to estimate an average sapwood depth. We identified the sapwood-heartwood boundary by a change in wood color.

3.3.6   *Estimating Radial Profiles of Sap Flux*

The heat pulses were measured by thermistors located at three discrete locations along the length of the probe. A scheme was required to scale these measurements across the entire radial depth of the sapwood, then circumferentially across the entire sapwood area. For all trees except the ring-porous oaks, sapwood depth extended beyond the length of the sensor. Therefore, it was important to estimate the flow rate over the unmeasured portion of the sapwood (e.g., Ford et al. 2004). To estimate sap flux density (J_S) across the entire sapwood area, we used an approach similar to Forrester (2015). This method assumes zero flux at the sapwood heartwood boundary and fits a second order polynomial to the measured data and the zero point as a function of depth from cambium. One large *List* was poorly fit by a 2nd order polynomial and was instead fit using a linear model with a natural log transformation on sapwood depth. Model fitting was conducted using R (R-core team, 2017) and the dplyr package (Wikham et al. 2019). All trees were interpolated using a increment size of 1.25 cm between the inner most thermistor position and the heartwood boundary. The 1.25 cm width represents the approximate spacing of measurement mid-points on the sensors. Sap flux density radial profiles were fit to the hourly aggregated data (data were collected at 10 min intervals) so that flux across the entire sapwood was estimated at each time point. This was important due to the shape of the polynomial changing from day to night. Fit was generally very good during the peak hours (10AM – 6 PM) but tended to decrease at most trees when sap flux was low (i.e., overnight).

We experienced several data gaps and/or sensor failure at all 4 oak trees (i.e., QUAL, QUNI), 1 *List* and 3 *Nysy*. We filled these gaps using multi-variable linear regression with meteorological variables (Domec et al, 2011; Ford et al., 2005). At a few trees this required filling large gaps at the end of the record. We modeled daily sapflow (Q) against combinations of daily mean solar radiation, daily mean air temperature, daily mean relative humidity, and daily mean soil moisture. The meteorological variables that provided the best fit varied by tree. We used k-fold cross validation to assess the model accuracy and observed that the models captured between 52 and 91 percent of the variation in Q (See supplemental material in Appendix 1 for details).

3.3.7   *Scaling Sap-Flux to the Whole Tree, Plot, and Riparian Zone*

To estimate whole tree water-use, the measured and modeled J_S were multiplied by the area of each sapwood band (annuli) and integrated to hourly and daily totals. Whole tree water use in ring porous oaks (i.e. *Quercus alba* and *Q. nigra*) was handled by applying the mean J_S for the thermistors that were in conductive tissue to the entire sapwood area, similar to Oishi et al. (2008). When scaling to the plot and riparian zone, we first used allometric equations to relate DBH to sapwood area (e.g., Vertessy, 1998). Sapwood area was calculated as the area of an annulus as follows:

$$S_A = \pi \left(\left(\frac{DBH}{2} \right)^2 - \left(\frac{DBH}{2} - S_d \right)^2 \right) \qquad\qquad \text{Eq. 3.2}$$

Where DBH is the stem diameter at 1.3 m above ground level (excluding bark thickness) [L] and S_d [L] is the average sapwood depth from two increment cores. We developed equations at the site for *LITU*, *NYSY*, LIST*,* and *QUAL* (table 2). We only had estimates from monitored species, although a broader range of species existed across the riparian zone. Therefore, we also fit composite equations based on xylem type for plot level scaling (Wullschleger et al., 2001;

Oishi et al., 2008). We measured DBH and collected increment cores from a total of 35 riparian

zone trees to estimate sapwood depth and calculate S_A (table 4). From this, we fit power

functions to the observed relationships between DBH and S_A to estimate the proportion of each

stem that was sapwood and to facilitate scaling of the sap flow estimates.

Table 3.2 Coefficients from allometric equations for estimating sapwood area from DBH. The number of trees of each species is indicated in column n, a and b are empirical parameters (form of equation is $S_A = a \times DBH^b$), and R^2 is the coefficient of determination.

Species code	n	a	b	R^2
LIST	5	1.067	1.8772	0.98
LITU	9	0.2154	2.2102	0.93
NYSY	6	0.6007	2.0486	0.97
QUAL	6	0.2297	1.9484	0.96
Ring porous	7	0.1034	2.1838	0.92
Diffuse porous	25	0.6500	1.9568	0.85

For scaling sap flow to the plot and stand level, we followed methods presented by

Cermak et al. (2004). Briefly, we evaluated the correlation between sapwood area and daily sap

flow for each species on each day using linear regression analysis. Cermak et al. (2004) pointed

out that this will likely be a non-linear function. However, since we focused our monitor on

larger canopy trees, and not a wide range of sizes, a linear fit was appropriate. We also used the

approach of inserting "dummy trees" where we believe sap flow would be negligible. To do this,

we selected the smallest tree of each species in the plot surveys to represent negligible sap flow.

Each one of these trees was an understory individual that likely transpired much less than the

canopy dominant trees we monitored. This had the effect of anchoring the scaling curve (Cermak

et al., 2014). Like the composite allometric equations, we used all trees of a given xylem

structure to develop a daily Q – SA relation that was applied to non-monitored species of a given

xylem type. This is similar to the approach of Wullschleger et al., (2001), who averaged the mean daily sap flux density (*Js*) for all trees based on xylem structure to estimate total sap flow from those non-monitored species. We scaled our whole tree estimates to the plot scale-100 m^2 immediately surrounding the groundwater wells- and the 3-hectare riparian zone, to approximate canopy transpiration (E$_C$) on an areal basis that could then be compared to PET and transpiration derived from water-table fluctuations (T$_G$). Ford et al. (2007) demonstrated that the most influential step in scaling water use from trees to stands was accurately estimating the stand density and sapwood area. To better characterize the whole riparian zone and facilitate more accurate scaling across the 3-ha riparian zone, we surveyed an additional 27 plots (*hereafter*, extensive plots) that covered a total area of 5400 m^2. These plot surveys assessed DBH of all trees >= 10 cm. We used the allometric equations in table 2 for estimating riparian zone S$_A$. To calculate canopy transpiration (E$_C$), we used the following equation:

$$E_c = \sum_{i=1}^{n} \frac{\beta_{1(k)} SA_{(i,k)} + \beta_{0(k)}}{A} \qquad \text{Eq. 3.3}$$

Where E$_c$ is the total daily canopy transpiration [L], n refers to the total number of individual (*i*) trees, $\beta_{1(k)}$ is the slope of the relationship between daily Q [L^3/T] and SA [L^2] for species *k* and SA$_{(I,k)}$ [L^2] is the total sapwood area of individual *i* of species *k*, $\beta_{0(k)}$ is the intercept of the daily relation between total Q and SA for species *k*, and A [L^2] is the ground area over which SA was determined (either 100m^2 for intensive plots or 5400 m^2 for the extensive footprint * 1.6 to scale to the entire 3 ha riparian zone).

3.3.8 Estimating T_G

To estimate the transpiration from groundwater (T_G) we evaluated the diurnal water table fluctuations. Specifically, we used the empirical method of Gribovski et al. (2008) with modifications presented by Riley (2022, ch.2). This approach requires only high frequency groundwater level data and an estimate of aquifer specific yield (S_Y). To estimate aquifer specific yield, we used the auger-hole method (Van Beers, 1983; Gribovski, 2018; Van der Molen et al., 2007; U.S. Bureau of Reclamation, 1984)), This approach uses a slug test to estimate saturated hydraulic conductivity and then employed the empirical relationship of van Beers (1983) to estimate S_Y. Gribovski (2018) found this approach to be the most accurate among the five methods tested. For further details on data processing *see* (Riley, 2022, ch2). The method for estimating T_G is based on a mass-balance equation for the water storage within an idealized volume around the well casing, as follows:

$$\frac{dS}{dt} = S_Y \frac{dh}{dt} = Q_{net} - T_G \qquad \text{eq.3.4}$$

$$T_G = S_Y * \left(r - \frac{dh}{dt} \right) \qquad \text{eq.3.5}$$

The term $\frac{dS}{dt}$ is the change is storage over time [L/T], S_Y is the specific yield of the aquifer [L^3/L^3], $\frac{dh}{dt}$ is the change in hydraulic head over time[L/T], r is the time dependent recharge rate estimated from the daily maximum and minimum rates of water level change, $Q_{net}=$ $r*S_Y$ and represents the net inflow or outflow from the well [L/T], and T_G is the transpired water derived from the aquifer [L/T]. We also applied a depth correction to S_Y following Crosbie et al. (2005) to account for reduced drainage when water table depths were near the surface (Riley, 2022, ch2).

3.4. Results

3.4.1 Temporal Variation of Climatic and Hydrological Variables

The watershed received 750 mm of precipitation between November 1, 2018 and April 1, 2019, yielding above-average groundwater and soil-water storage at the onset of the growing season (Figure 3.2). Between April 1 and October 23 (i.e., the growing season), precipitation totaled 703 mm, which is close to average for the watershed (715 mm, 1985 – 2015). However, during June and September precipitation was far below average, leading to large decreases in soil moisture (Figure 3.2). PET over the growing season was 1018 mm which is equal to the long-term average (1998 – 2018). However, while growing season precipitation and PET were close to average, PET exceeded precipitation by 307 mm. Soil moisture storage was high at the start of the season averaging 31 cm for April and May, then rapidly decreased in June. Frequent precipitation in July and early August intermittently recharged soil moisture but was followed by a long period with no precipitation and substantial declines in soil moisture reaching a minimum of 17 cm (Figure 3.2). The water-table over the growing season followed the general pattern of soil moisture but was more subtle and tended to remain stable when not responding to rainfall with a slow rate of decline until the soil moisture was depleted then began to decline more rapidly (Figure 3.2d). Across the growing season and all monitoring wells, the water-table ranged from ponded at the surface to 2.92 m below land surface (mbls).
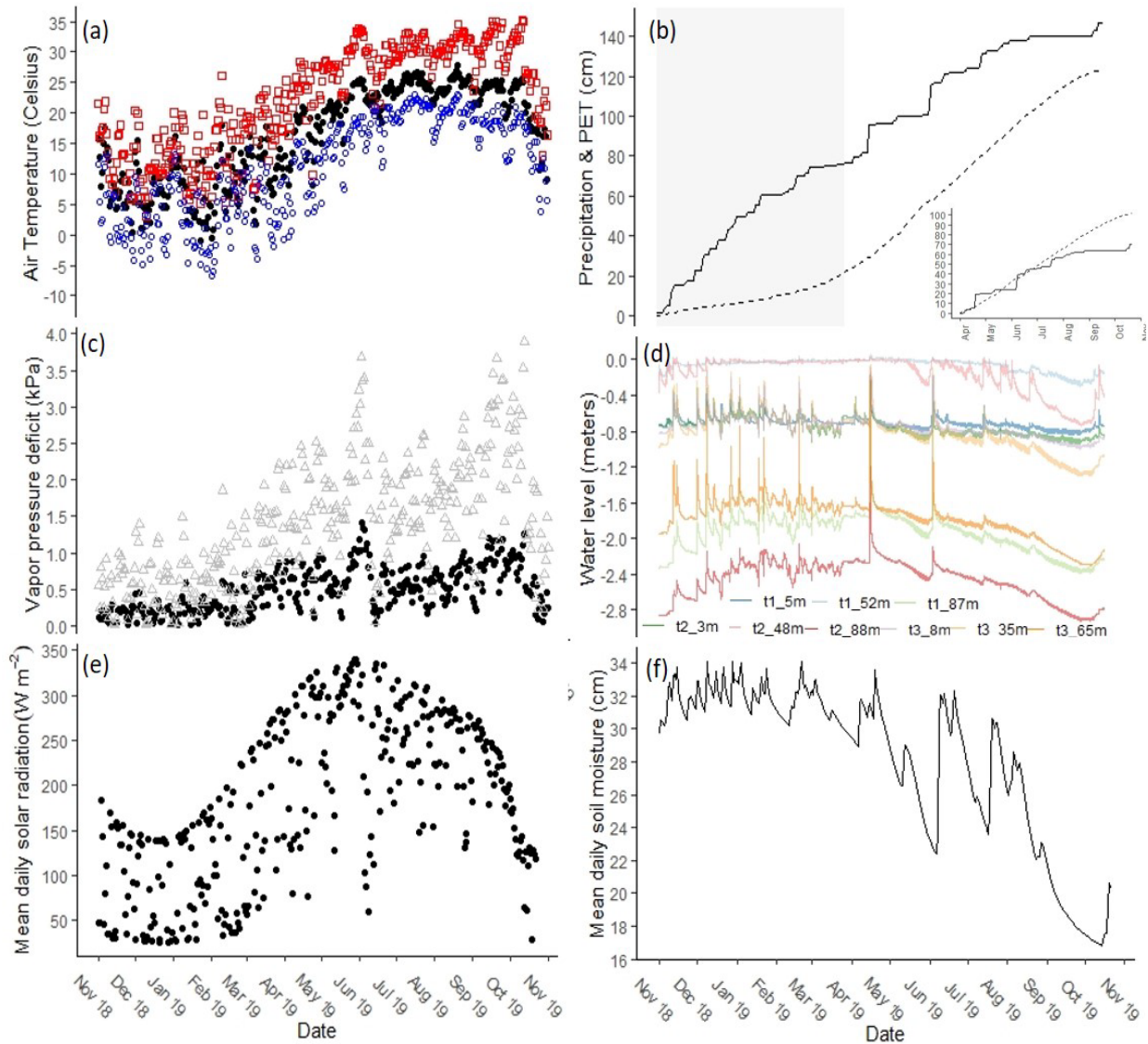
Figure 3.2 Timeseries of meteorological conditions and water table depth. a) air temperature, solid symbols are daily mean, red squares the maximum, and open blue dots the minimum; b) cumulative precipitation (solid line) and PET (dashed line), grey shading indicates dormant season prior to focal period, c) solid dots are mean daily vapor pressure deficit and open triangles are the daily max vapor pressure deficit; d) Water table depth relative to land surface at the nine monitoring wells, e) mean daily solar radiation, d), inset figure between b and d displays cumulative PET and P over just the growing season; and f) mean daily soil moisture storage.

3.4.2   Forest Characteristics at Study Plots

At our nine 100 m^2 monitoring plots (*hereafter*, intensive plots), we measured a total of

71 trees representing eleven different species (table 3.3). Across all plots the most abundant tree

was the understory species, CACA (21 stems), followed by LIST (10) and NYSY (9). In terms of

basal area (B_A), LITU accounted for 23% of the total followed by QUAL (18%), and PITA

(14%). Considering only the conductive tissue, or sapwood, LITU also accounted for the greatest

percentage of the total S_A (24%), followed by NYSY (16%) and PITA (14%). The extensive

plots were surveyed to better characterize the entire riparian zone for broader extrapolation and

Table 3.3 Estimates of forest characteristics by species. Extensive plots were used for broader characterization and intensive plots were where monitoring equipment was located.

species code[1]	$n_{extensive}$	$n_{intensive}$	$BA_{extensive}$ cm^2m^{-2}	$BA_{intensive}$ cm^2m^{-2}	$SA_{extensive}$ cm^2m^{-2}	$SA_{intensive}$ cm^2m^{-2}
qual	**32**	**6**	**7.92**	**6.53**	**1.90**	**1.57**
litu	**36**	**6**	**7.37**	**8.35**	**4.45**	**5.46**
nysy	**43**	**9**	**5.20**	**3.93**	**4.72**	**3.55**
list	**24**	**10**	**2.99**	**2.99**	**2.59**	**2.87**
acru	28	8	2.91	2.29	2.06	1.65
quru	3	0	1.09	0.00	0.30	0.00
caca	27	21	1.06	2.29	0.77	1.69
pita	**3**	**2**	**0.97**	**4.84**	**0.79**	**3.34**
qumi	3	0	0.87	0.00	0.23	0.00
quni	**5**	**1**	**0.81**	**3.94**	**0.21**	**1.52**
cato	4	0	0.47	0.00	0.12	0.00
osvi	3	0	0.20	0.00	0.14	0.00
prse	1	2	0.09	0.51	0.02	0.37
fram	0	2	0.00	1.06	0.00	0.76
cofl	0	2	0.00	0.19	0.00	0.14
total	212	71	31.96	36.93	18.30	22.92

[1]Species code denotes the first two letters of scientific binomial: ACRU, Acer rubrum; CACA, Carpinus caroliniana; COFL, Cornus florida; FRAM, Fraxinus americana; CATO, Carya tomentosa; LIST, Liquidambar styraciflua; LITU, Liriodendron tulipifera; NYSY, Nyssa sylvatica; OSVI, Ostrya virginiana; PITA, Pinus taeda; PRSE, Prunus serotina, QUAL, Quercus alba; QUNI, Q. nigra; QURU, Q. rubus; QUMI, Q.michauxii. Rows with bold text correspond to the monitored species.

had similar composition and species distribution to the intensive plots (table 3.3). Basal area was

dominated by QUAL (25%), LITU (23%), and NYSY (16%), whereas S_A was dominated by

NYSY (26%), LITU (25%), and LIST (14%). The one notable difference was the general lack of

PITA across the broader assessment area. Basal area ranged from 3.31 - 81.42 $cm^2\,m^{-2}$ and S_A

ranged from 2.30 - 45.85 cm^2 m^{-2} across the 100 m^2 plots (table 3.4). Plots that were dominated

by QUAL or QUNI (ring porous species), such as t2_88m, tended to have high B$_A$ to S$_A$ ratios.

Following the landscape positions defined for the well locations (table 3.4), in the extensive

plots, mid position had the greatest basal area dominated almost evenly by NYSY and QUAL.

Basal area at the hillslope and near-stream positions were nearly identical with both dominated

by LITU. Similarly, S$_A$ was greatest at the mid position and was strongly dominated by NYSY.

The hillslope and near-stream positions had similar S$_A$ that were both dominated by LITU.

Table 3.4 Forest characteristics and fluxes for each 100-m^2 intensive plot.
Fluxes are totals from April 1 – October 23

Plot ID	Landscape position	BA cm^{2}m^2	SA cm^{2}m^2	E$_C$ (mm)	T$_G$ (mm)
t1-5m	Near stream	19.96	15.88	37	493
t1-52m	Mid-riparian	14.70	13.01	35	100
t1-87m	Hillslope	81.42	45.85	117	580
t2-3m	Near stream	34.08	24.62	101	625
t2-48m	Mid-riparian	3.31	2.30	12	324
t2-88m	Hillslope	36.10	9.48	35	351
t3-8m	Near stream	66.79	42.76	159	461
t3-35m	Mid-riparian	62.45	26.25	77	765
t3-65m	Hillslope	24.88	19.43	33	522
Landscape weighted median	NA	NA	NA	NA	455

3.4.3 Daily Tree Water-Use

Mean daily tree water use was remarkably similar across species, and among individuals

of a single species (Figure 3.3). *Pinus taeda* (PITA), oaks (QUAL & QUNI), and LITU had their

maximum daily water use in late April, with 24, 22, and 17 liters per day, respectively.

Sweetgum peaked in June at 22 liters per day following a hot dry period, and NYSY had two

peak periods, one in late May, at 9 liters per day, and then at the beginning of a hot dry period in

early September when the max rate reached 11 liters per day. Over the entire period, *Nyssa*

sylvatica had the lowest average rate of sap flow across the growing season (Figure 3.3). Ring

porous oaks had the next lowest sap flow, driven largely by their low sapwood area, as their sap
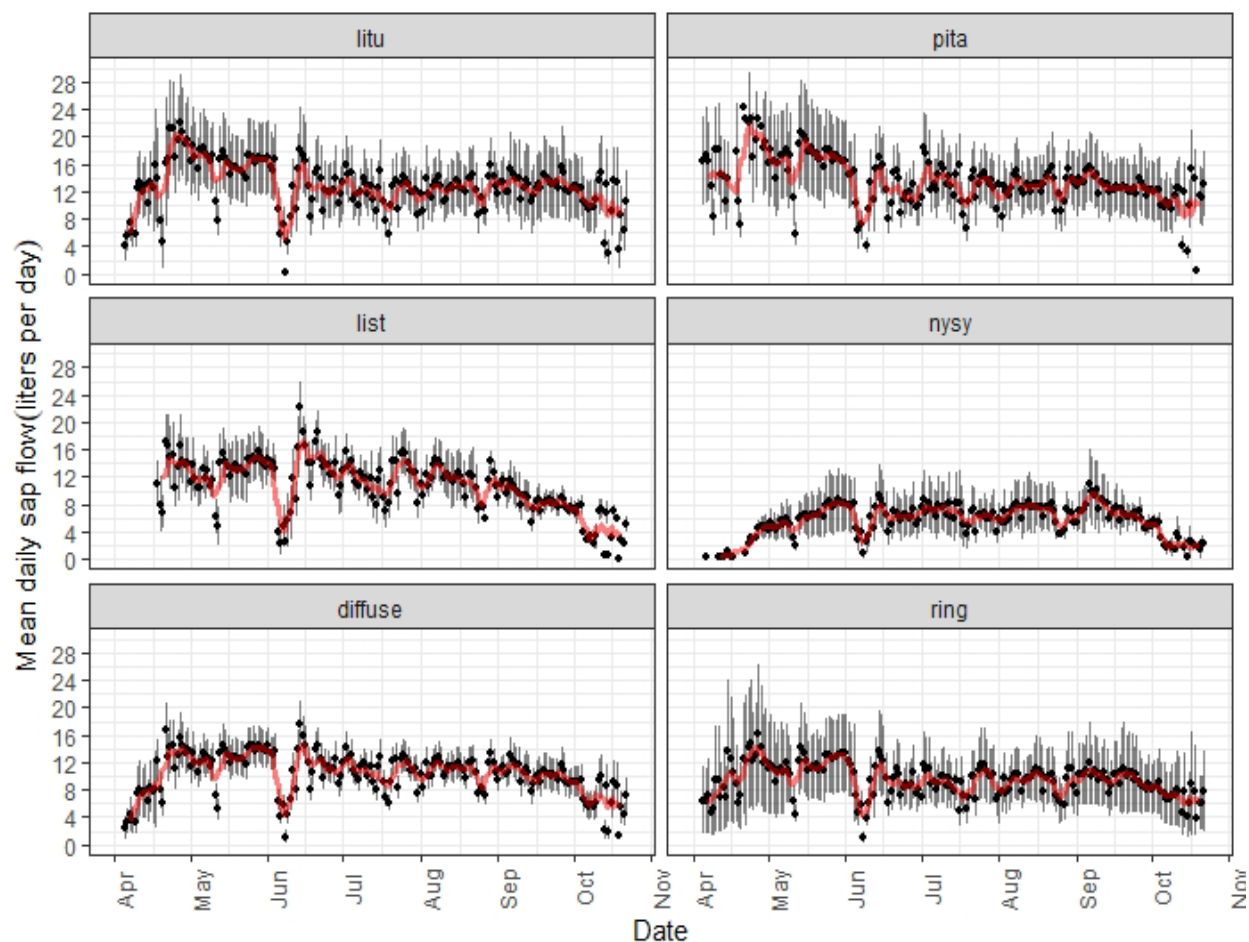
Figure 3.3 Mean daily sap flow by species. Error bars represent ± 1 SE about the mean. The panel labeled "diffuse" is the average across all the monitored trees with diffuse porous type xylem and the panel labeled "ring" is all monitored species with ring porous xylem (i.e., QUAL & QUNI). The red line represents the 5-day moving average. Some of the data included in these plots represent gap filled estimates which are described in text S1 in Appendix 1.

flux density (J_S) was often greater than the other monitored species (Figure 3.S2). The pattern of

sap flow over time varied by species, with NYSY demonstrating the most gradual ramp up

reflecting the slow observed leaf out. Other species tended to maintain consistent sapflow until

around mid-September when flow started to decrease, likely responding to the decreased energy

conditions, and possibly exacerbated by low soil moisture.

3.4.4 *Daily T_G across wells*

T_G was variable across all plots and was likely driven by differences in water-table depth,

soil moisture, and characteristics of local vegetation. The patterns across most locations showed

responses to short-term changes in meteorological forcings, (in-line with the patterns seen in the

sap flow) and soil moisture on top of an overall pattern of increasing T_G across the growing

season, until mid-September, when T_G declined sharply. The hillslope plot on transect-3 was the

exception to this pattern, as the water-table dropped below the root zone at this location and the

decline occurred earlier (Figure 3.4, left panels). The overall increasing trend is even more

evident when examining T_G: PET (Figure 3.4 bottom row). Across all plots, from August to

October, T_G: PET approximately doubles, indicating a greater proportion of the transpiration is

being sourced from the saturated zone. Even when the absolute magnitude of T_G begins to

decline (Figure 3.4 top row) the ratio continues to increase. This increased reliance on

groundwater is supported by the steep decline in soil moisture over this period (Figure 3.2f).

Monitoring plots in the mid-riparian area had some of the largest variability within a given

landscape position. A discontinuous bog feature in this part of the riparian zone led to soil

saturation over various periods, which is evident in Figure 3.4 (middle panel) where T_G didn't

ramp up at transect-1 until mid-July, approximately 3 months later than other plots, when surface

saturation receded.
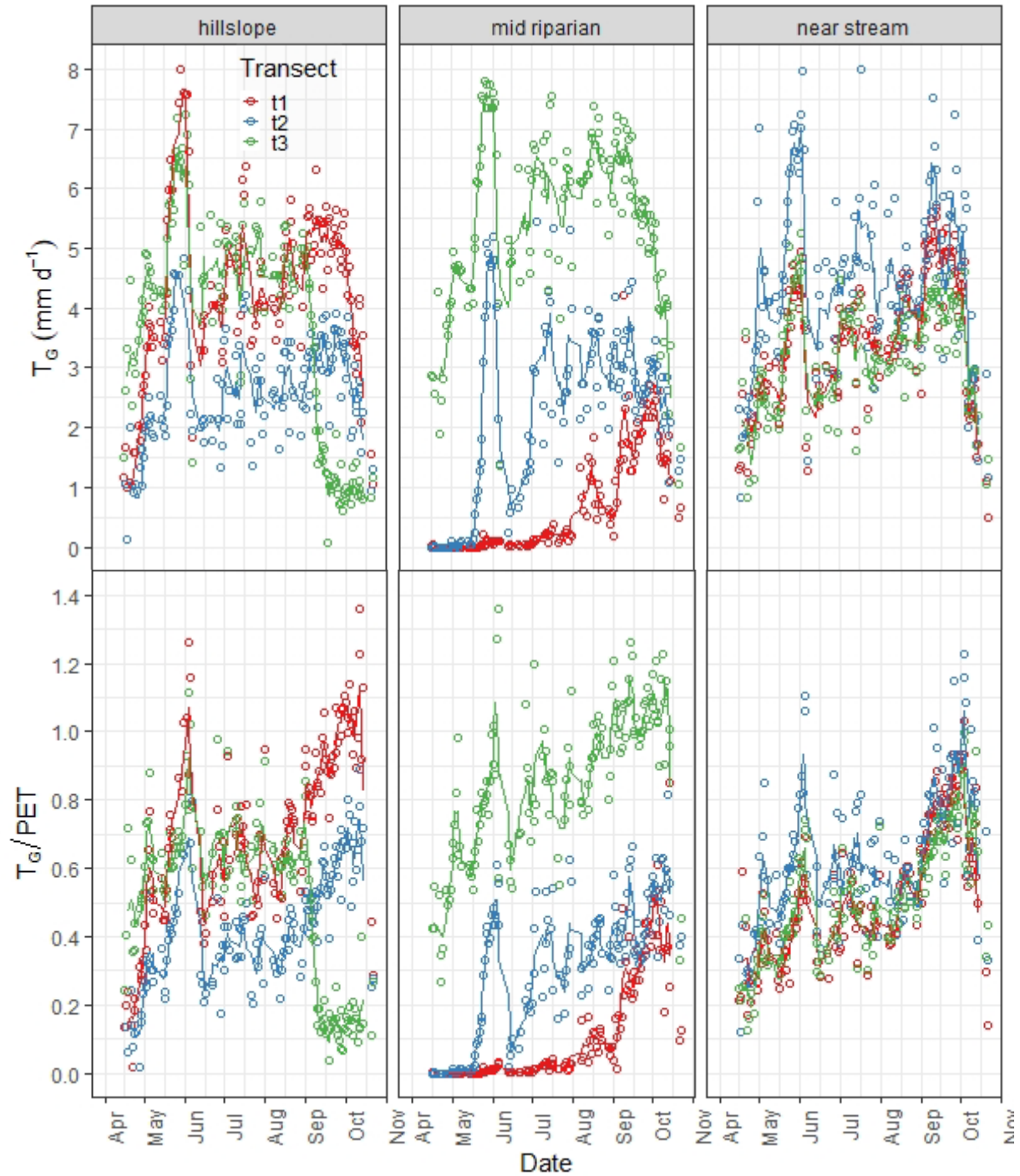
Figure 3.4 Timeseries of T_G and T_G/PET grouped by landscape position. Dots are the daily data, and the lines represent 5-day moving averages.

3.4.5   *Seasonal Canopy Transpiration and Groundwater Uptake*

At the intensive plots, scaled sap flow estimates of E_C were highly variable and were largely

driven by differences in S_A (table 4, Figure 3.5). However, species level sap flux also affected

plot level E_C. This effect can be seen by comparing plots t1_87m and t3_8m (Figure 3.5).
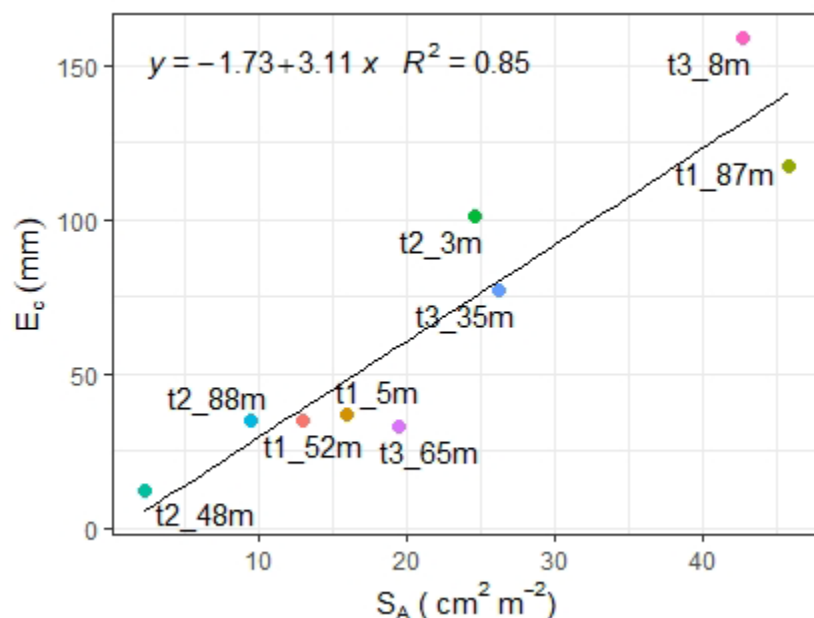
Figure 3.5 Relationship between plot scale canopy transpiration (E_C) and sapwood area (S_A).

The former has higher S_A but lower total transpiration. Plot t1_87m had several large pine trees

that contributed most of the sapwood area but had lower sap flux (J_s) than QUAL and LITU

(Figure 3.S2), that were dominant at t3_8m. At the plot scale, total T_G was quite variable and did

not show a consistent relationship with S_A ($R^2 = 0.26$, graph not shown) as was observed in E_C

(table 4, Figure 3.5). Furthermore, there was little correlation between T_G and E_C at a given plot

($R^2 = 0.20$).

When scaled to the entire riparian zone extent, using sapwood area estimates from the extensive

plots, growing season E_C was 241 mm (1.2 mm d^{-1}). LITU contributed the most to total E_C

(30%), followed by non-monitored trees in the diffuse category, of which S_A was dominated by

red maple (23%), NYSY (18%), ring porous species, of which 75% were QUAL or QUNI

(14%), LIST (12%), and last was PITA at only 3%. This largely reflects the proportion of

sapwood area represented by each species or xylem category in the extensive survey (table2).

Following prior work at the site that demonstrated some systematic patterns in T_G by landscape

position, we took the median T_G at each landscape position, equally weighted each position, and

summed the results, which equaled 455 mm (2.3 mm d^{-1}). This estimate of T_G across the entire

riparian zone is 89% greater than the estimate of total E_C across the same area. Figure 3.6

demonstrates this as well, where daily T_G is consistently greater than E_C, except at the very

beginning and end of the period and on days with rain, when T_G could not be estimated. These

seemingly conflicting estimates, where T_G far exceeds E_C, are addressed in the discussion.
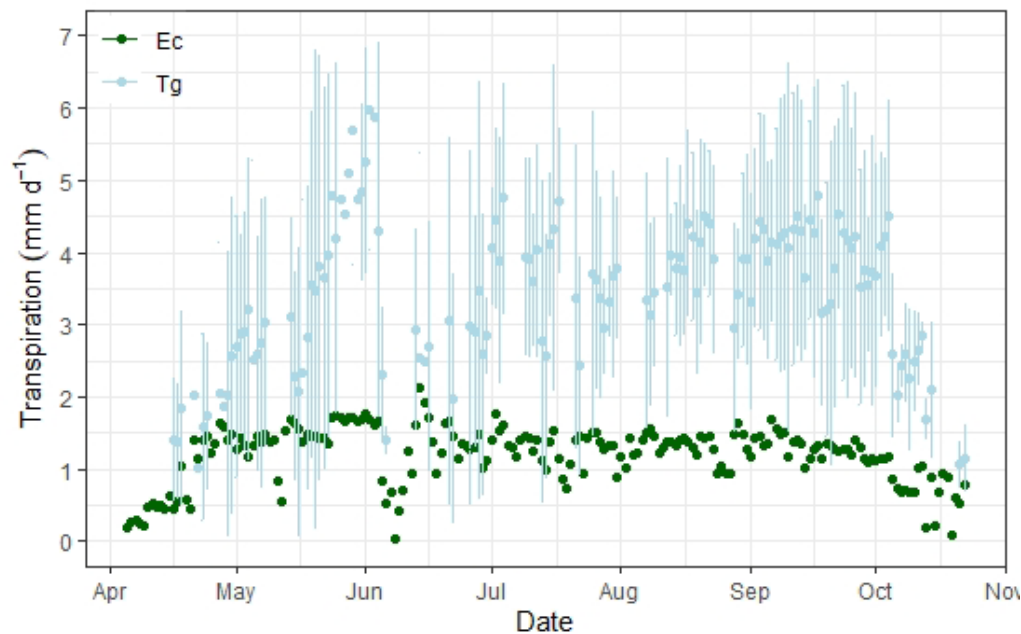
Figure 3.6 Daily estimates of total riparian zone transpiration (E$_C$) and transpiration derived from groundwater (T$_G$). T$_G$ is the median-daily rate described above and error bars represent the median absolute deviation.

3.5. Discussion

3.5.1   Comparing E_C to Past Work and Similar Sites

Compared to past work at PMRW and other sites with humid climates and broad leaf

forest, our results fall on the low end of reported E_C (Figure 3.7). Cumulative E_C from April
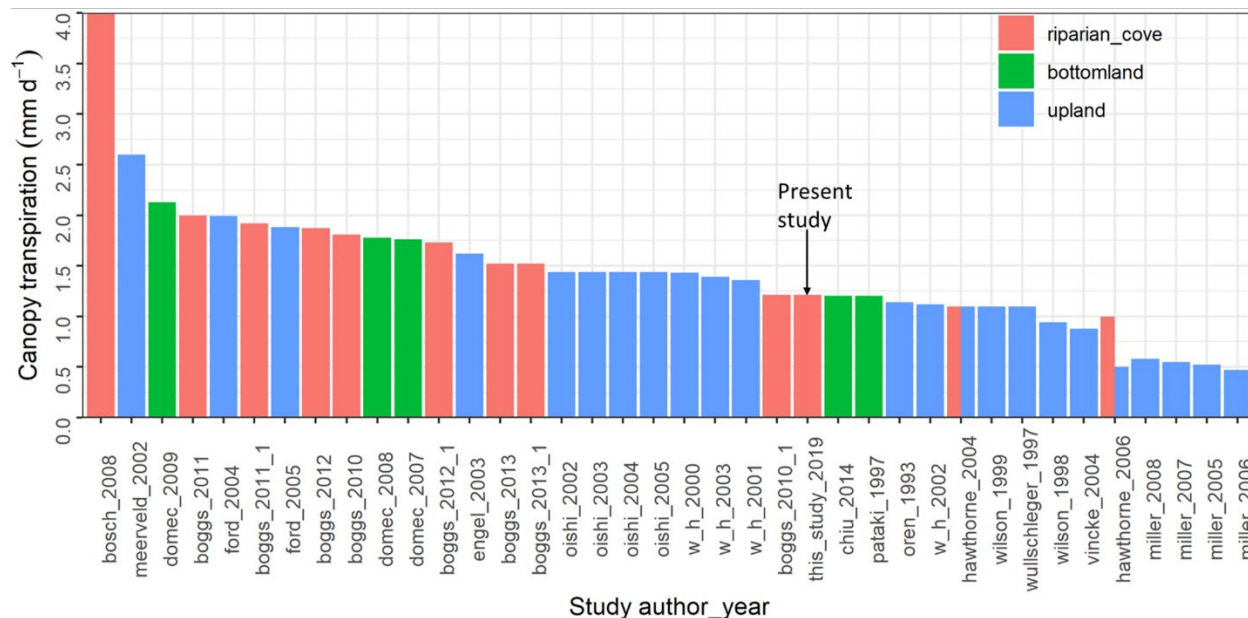
Figure 3.7 Canopy transpiration normalized to a daily rate across 17 different studies.
Colors represent general landscape position. Note, all studies except those of Domec, Engle, and
Miller are from broadleaf humid forests. These other studies were included because they have
concurrent estimates of T_G. See table S2 (Appendix A) for a cross walk of study id and citations.

through October was 241 mm across the riparian zone, or on average, 1.2 mm d^{-1}. Meerveld and

McDonnell (2006) estimated E_C to be 2.4 mm d^{-1} from May to August on a hillslope plot within

the PMRW. If we similarly constrict our averaging period to May through August, then the

average-daily rate of E_C increases to 1.3 mm d^{-1}. The difference is partially explained by

landscape position. Their study plot had a southeastern aspect that receives greater solar

insolation than our plots, which are flat or have slight northerly aspect. Their study plot was

located on a steep hillslope whereas ours were within a riparian zone with little overall relief.

The trees in their plots likely experienced less inter-canopy shading on the steep hillslope than

the trees in our plots, in addition to the topographic shading of our study plots early and late in

the period when sun angles were relatively low. The differences may also result from

methodological artifacts discussed by Meerveld and McDonnell (2006). They estimated sapwood

area, which is a critical scaling parameter for estimating canopy transpiration, using allometric

equations developed from another site and assumed J_S from the monitored hickories was

representative of all species on the hillslope. Pataki and Oren (2003) presented data showing

hickories had similar or greater J_S than oaks (depending on the species) - which were the other

dominant species on the hillslope- potentially leading to inflated transpiration estimates.

Aulenbach and Peters (2018) estimated AET for the whole PMRW as the residual term in the

catchment water balance equation. Using data sets spanning 1985 – 2015, their estimates of

average-daily ET across years ranged from 2.21 – 4.75 mm d^{-1} (Aulenbach and Peters, 2018).

Their estimates of ET are expected to be greater than our estimates of E_C, or those of Meerveld

and McDonnell (2006), because that term encompasses E_C as well as canopy-interception loss

and soil evaporation. In a similar forest within the Piedmont of North Carolina, Oishi et al.

(2008) estimated that E_C comprised, on average, 65% of total ET. Applying their average to the

ET estimates of Aulenbach and Peters (2018) suggests that average-daily E_C for the whole

PMRW could range from 1.3 to 3.1 mm d^{-1} across years—a range that nearly encompasses our

estimate of 1.2 mm d^{-1} that is specific to the riparian zone.

Compared to other studies with similar forest types, within climatically similar regions,

we also find that our E_C estimate from the riparian zone at Panola was on the low end of the

range. Boggs et al. (2015) estimated E_C to be 220 mm (~1.3 mmd^{-1}) over the growing season

(May – October) prior to forest management activity. This value increased to 350 mm the

following year after forest thinning treatments. The study of Boggs et al. (2015) is of particular

relevance as it is the only other study focused specifically on a riparian zone and has remarkably

similar forest composition with the exception of no reported NYSY. In the nearby Walker

Branch watershed, throughfall displacement experiments were conducted to investigate impacts

of reduced soil moisture on canopy transpiration (Hanson and Wullschluger, 2006). These

authors estimated annual growing season (April – October) E_C from 212 – 319 mm for the dry

site and 255 – 325 mm for the control site. In a prior study at Walker Branch, Wilson et al.

(2001) estimated growing season (April – November) E_C of 230 – 269 mm. In the Piedmont of

North Carolina, Oishi et al. (2008) estimated growing season E_C from 299 – 311 mm. The above

cited estimates of E_C are all from broadleaf deciduous forest in the Southeastern U.S. and based

on up-scaled sap flow measurements from plot-scale studies. Taken together, these studies

correspond to average-daily E_C rates of 1.1 to 1.7 mm d^{-1}. Interestingly, similar magnitudes of

E_C (~ 1.2 mm d^{-1}) were observed in humid broadleaf forests in southern Japan (Chui et al., 2016).

While this Japanese forest has a different species assemblage, it is climatically similar to our

study site. Considering the above estimates of ET and E_C from past studies at PMRW and E_C

from similar sites, our riparian zone is at the lower bounds for E_C estimates in the region.

We think our relatively low E_C may be explained by the riparian setting. In landscapes

with complex terrain, riparian zones can receive less solar insolation due to canopy shading from

adjacent hillslopes. While dry soils can limit transpiration, they are rare in riparian zone.

However, saturated conditions can have a similar impact on transpiration (Kozlowski, 1984) and

occur relatively frequent in the middle of this riparian zone. We note that the riparian zone at

PMRW includes a perennial bog dominated by NYSY (a species demonstrating the lowest

transpiration rates, Figure 3.3 & S2). The bog encompasses, though expands well beyond, our

plots t2_48m and t1_52m (figure 1), and should have a pronounced negative impact on E_C.

Because of this hydrogeomorphic feature, the aspect, and topographic position, we conclude that

our E_C estimate specifically for the riparian zone logically forms the lower boundary of E_C values derived from previous works at PMRW.

3.5.2 *Comparing T_G to Past Work with Independent Estimates of E_C*

Very few studies have compared T_G with an independent estimate of transpiration beyond calculating PET from meteorological data, although there are some exceptions that use other field techniques (e.g., Domec, et al., 2011; Engle et al. 2005; Scott et al., 2008, Vincke and Thiry, 2008; White 1932). If we consider other studies in the region, with similar forest composition, that have assessed the ratio of canopy transpiration (E_C) to PET, we find values that are consistently near or below 50%. In a forest plot at the Walker Branch Watershed in Eastern TN, E_C was 30% of PET (Wilson et al. 2001). A later study at Walker Branch focused specifically on a ridge top and upper slope position and found that E_C was 40% of PET (Wullschleger and Hanson, 2006). In a forest with comparable species composition, Oishi et al. (2010) found E_C averaged 36% of PET over four years. While none of these studies in the region were specifically focused on riparian zones, which generally have plentiful moisture compared to hillslopes and ridges, they suggest PET may not be the most robust benchmark for assessing T_G. Thus, based on studies from the region we would expect growing season E_C and therefore T_G, to be ≤ 50% of PET. Figure 4.8 presents T_G comparisons with numerous studies highlighting that estimates from this study site fit well within the range of many previous studies. However, there was considerable variation among the estimates from different wells at this site (Figure 3.4). The

median (±MAD) T_G over the growing season across all plots was 3.48 ± 1.31 mm d^{-1}, which
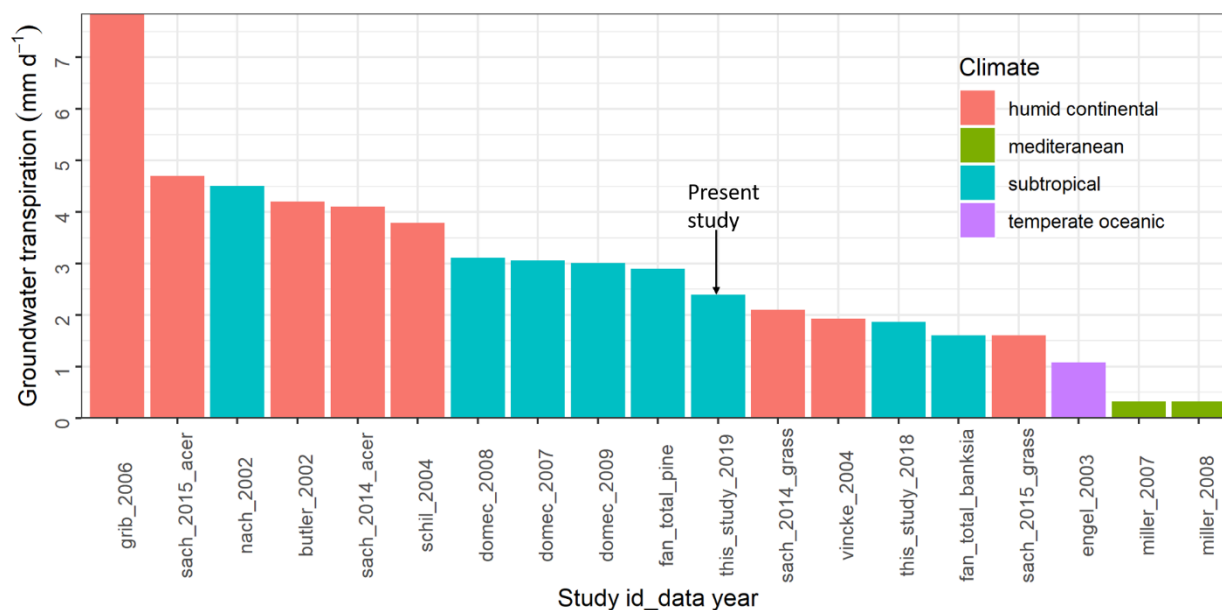
Figure 3.8 Groundwater derived transpiration from water table fluctuation methods normalized to a daily rate across 10 different studies. This comparison focused on studies in non-arid environments and generally forested landcover. The bar color represents general climate classification of the study sites. See table S2 (Appendix A) for a cross walk of study id and citations.

represents 63% of PET and 189 % of the annual E_C. T_G exceeding E_C suggested a possible

methodological issue, as T_G should not exceed E_C unless groundwater is being directly

evaporated, which is likely an exceedingly small component at our study site. A similar, albeit

less extreme, deviation was also presented by Domec et al. (2011). This study was conducted on

pine plantations in the coastal plain of the SE U.S. and showed T_G consistently overestimated ET

(E_C + soil evaporation) on an annual basis by 10 – 20 percent (Domec et al. 2011). Fan et al.

(2014), also working in a shallow water table setting, observed some days where T_G exceeded

E_C. The only study that presented logical results comparing transpiration and T_G, was that of

Engel et al. (2005). This study used similar methods as the present study and found that

transpiration was 40 – 60 % of PET and direct uptake from groundwater accounted for 67 % of

the E_C. However, this study focused on a Eucalypt species rather than pine (compared to Domec

et al 2011, and Fan et al 2014) and was in an environment with a deeper water table, indicating there may be certain scenarios (e.g., deeper water table and deeply rooted trees) where the method is more applicable, however more studies are needed to further test that assertion.

A similarity among the three previously cited studies is that they are all focused on a single tree species, and all were in flat landscapes. Trees of a single species, age class, and growing under identical environmental conditions likely have very similar water use patterns, so that T_G estimated from a single well may be representative of groundwater uptake by the whole forest. Furthermore, these types of plantation forests often allow for a relatively definitive demarcation of the vegetation influencing T_G. For example, the study of Engel et al (2005) was conducted on a eucalypt plantation surrounded by grasslands—the latter vegetation type lacking sufficiently deep roots to extract groundwater at all. The sites studied by Domec et al. (2011) were flanked by canals and ditches to improve drainage. Our plot boundaries were arbitrarily centered on each well to allow for consistent comparisons of flux estimates without any particular biological relevance. The riparian zone was defined based on topography and vegetation, but in this gently sloping part of the landscape, it too is quite fuzzy and may be more appropriately thought of as a gradient rather than a sharp boundary. Depending on antecedent wetness, the area of groundwater accessibility like expands and contracts, changing the functional extent of the riparian zone. Diverse tree species and age classes will have very different rooting extents and patterns of water-use, making generalizations about T_G using a single, or even a few well locations, highly uncertain (Riley, 2022, ch.2).

Our results indicated substantial discrepancies in E_C and T_G, and not in the manner that we expected, where T_G would have only been a fraction of E_C. Instead, we found that T_G was consistently greater than E_C. This raised serious concerns over data processing or other sources

of error, leading us to heavily scrutinize the raw data and processing steps to rule out human errors. So, what is driving the discrepancies observed in our study? One possibility is our failure to account for understory transpiration. In other broadleaf humid forests, understory transpiration has been estimated to account for 4% (Chui et al., 2016) to 16% (Wullschleger et al., 2001) of the total E_C. Based on these estimates our E_C may be underestimated by 10 – 39 mm, still far less than the 455 mm of T_G. Another factor leading to the disagreement could be related to typical errors that may manifest in opposite directions. Forster (2014) and Steppe et al (2010) presented data showing sap flow methods tend to underestimate actual sap flow based on comparison with gravimetric estimates, and Wilson et al (2001) showed underestimation of scaled sap flow through differencing above and below canopy eddy flux estimates. However, other studies have found good agreement using scaled sap flow and eddy covariance methods (Hogg et al. 1997; Oishi et al., 2008). Regarding T_G, one of the key uncertainties using diurnal water-table fluctuation approaches is the determination of aquifer specific yield and accounting for depth dependency when water-tables are close to land-surface (Loheide et al., 2005). Many studies that have estimated T_G and compared those fluxes with PET have found T_G approximately equal to, or exceeding PET (e.g., Domec et al. 2011; Gribovski et al., 2008; Martinet et al., 2009) and based on the prior discussion, studies in the region generally found E_C was less than 50% of PET. Thus, highlighting the potential for errors that may trend in opposite directions, effectively inflating the discrepancies in the two approaches used here. However, we can only speculate on this giving the contrasting findings regarding sap flow and E_C and the lack of studies investigating T_G in a similar environment.

We are not the first study to observe T_G exceeding E_C. Vincke and Thiry (2008) observed T_G was ~ 1.8 times greater than total transpiration and 3.3 times greater than overstory

transpiration alone. They speculated that the reason for inflated T_G estimates was that part of the diurnal oscillation in hydraulic head was caused by groundwater discharge to streams, or to underlying fractured bedrock, rather than by root uptake alone. We believe these factors are negligible to minor issues in our study. If we assume that the day-to-day decline in head, which averaged 5 mm d^{-1}, was primarily the result of losses other than transpiration (baseflow discharge and leakage into bedrock – although some is certainly transpiration) it is almost an order of magnitude smaller than the diurnal fluctuation range, which was 30 – 60 mm/day and primarily reflects plant water use. This suggests outflow or recharge is of low magnitude compared to the daily fluctuations which are indicative to plant water use.

3.5.3 *Reconciling the Appropriate Scales to Compare Fluxes*

A final point that we believe could potentially lead to the discrepancies in E_C and T_G is the lack of a known area of vegetation that is influencing T_G. The specific yield from equation 3.5 is defined as shown below:

$$S_Y = \frac{\Delta V}{A \Delta H} \qquad\qquad\qquad \text{equation 3.6}$$

where ΔV is the change in the volume of water stored within the pore space of the aquifer; A is the vertically-projected, two-dimensional area of the section of the aquifer being considered; ΔH is the change in hydraulic head. The change in the measured elevation of the water-table surface within the well provides ΔH, whereas the other two terms are unknown. When applied in equation 3.5 to estimate T_G from a measured well hydrograph, there is no way of knowing the true land area over which groundwater uptake by trees is contributing to the measured ΔH within the well. This is true of our application, and all other studies that have used similar formulations to estimate T_G. Rather, the user must make some variably-informed assumption about what land area, and inhabiting vegetation, is influencing the measured ΔH at

the well location. This unknown area was pointed out by Butler et al. (2007) and mentioned by Loheide (2008), however, we are unaware any studies that have attempted to quantify this area of influence. The need to do so was perhaps not so apparent in previous works where the resulting estimates of T_G were not immediately compared to estimates of E_C from the same site. We have made that comparison, and the results show unequivocally that more critical consideration of the area of influence is needed.

One of the interesting findings of this work relates to the degree of disparity depending on the aggregation scale. Studies investigating transpiration and plant water use are often conducted at the scale of induvial trees or at the scale of a plot (most of which are larger than our $100m^2$). While this scale was reasonable for estimating transpiration from a small group of trees it does not appear appropriate to compare with groundwater fluctuations over small areas. Across the nine monitoring plots, T_G was between 3 and 27 times greater that plot level E_C, and when scaled to the entire riparian zone T_G was about twice as large as E_C. The lateral extent of roots from large mature trees may expand from one to more than twice the height of the tree (Perry, 1982). While Perry (1982) did not specify the root diameter, this may reflect the fine root networks and not roots that are in proximity to the water table. However, Stone and Kalisz (1991) discussed rooting patterns of "sinker roots" coming off lateral branching roots at "some distance" from the root collar; unfortunately, detailed distances were lacking. The above suggests there are likely trees from multiple adjacent plots all affecting the daily water table response at multiple wells. Furthermore, it's likely that trees outside of the riparian zone are utilizing groundwater that are not being captured in our plots or our riparian zone extent. Butler et al. (2007) brought up the issue of scale of influence, or the zone of vegetation that is responsible for

the observed WTF and suggested that it is site dependent and likely a function of root networks and sediment texture.

To balance E_c from scaled sap flux estimates, T_G would have had to be derived from an area of approximately 5.7 ha, just under twice our current assumed area of just the 3-ha riparian zone. However, this also assumes 100 % of E_C is derived from the saturated zone and therefore should balance T_G. A more likely scenario is that the proportion of E_C derived from T_G encompasses the full range, from 100% in the bog area to 0% further up hillslopes where the water table is never accessible. If we consider that the canopy trees are 20 – 30 m tall and following Perry (1982) that lateral root spread is 1 to more than 2 times the height, then it is conceivable that trees well outside of our delineated riparian boundary could be accessing the shallow water-table or capillary fringe, potentially influencing T_G at the plots. If we assumed a 20 – 30m buffer of the forests could potentially be contributing to T_G estimates, that would result in an area of 5.8 – 6.4 ha, approximately 2 times our riparian zone area. Whilst these scenarios are hypothetical, and assume that our observations in the riparian zone hold true as we expand out, it provides some idea of the land area where vegetation may be contributing to T_G depending on the contribution of T_G to total E_C.

Our findings contrast the results observed by (Engel et al. 2005), which were more in line with our hypothesized outcome for the present study. Where T_G would be some fraction of E_C. As previously mentioned, the study area of Engel et al. (2005) was a eucalyptus plantation surrounded by shallow rooted grasslands that did not access the aquifer. This provided a clear constraint on the area of vegetation accessing groundwater. Furthermore, trees in the plantation were of a single species and structurally and chronologically homogeneous. This removes much of the variability that may be encountered in a natural forested setting. Even though we

delineated a riparian zone based on surface slope and species distribution, there is insufficient data and understanding on the rooting patterns of trees in humid forests. It seems likely that trees on lower hillslopes would have substantial roots running down slope toward the water table where moisture is consistently available. The lateral extent of such access and how it may vary by species, however, is unknown.

All future applications of water table fluctuation approaches should make it the foremost feature of their study design to try and elucidate what is the area of influence. Until we resolve that problem, applications of this methodology in humid climate zones, where water-tables are near the land surface over large areas, and where there is considerable topographic complexity with heterogeneous forests, will continue to be subject to great uncertainty and possibly systematic bias. Working out these remaining methodological idiosyncrasies, that may very well be landscape dependent, will increase our ability to close water budgets and get a clearer understanding of the role forests play in groundwater budgets even in humid regions. We see manipulative experiments as a way forward to address this uncertainty. Selectively harvesting trees at incremental distances (radii) from a given well could shed light on the influential area. Furthermore, combining these analyses with active tracer additions to pinpoint the water source being used by trees could further illuminate the spatial distribution of vegetation influencing the water table fluctuations. Previous forest harvest work has been done in this regard to assess vegetation effects on diurnal streamflow fluctuations with mixed findings (Bren, 1995, Dunford and Fletcher, 1947). Given the discrete nature of a well, versus a stream network, it seems this sort of manipulative experimentation could prove more fruitful.

3.6 Conclusions

Transpiration is a critical component of the water budget and one that is difficult to quantify. Water-table fluctuation approaches are attractive for their relative ease of use and low cost. Not only do they allow a quantification of a portion of transpiration, they allow insight in changes in storage not captured in catchment scale water balances. In this study, we estimated the total transpiration from scaled sap flow measurements and the transpiration component derived from groundwater using water-table fluctuations across a humid riparian zone and nine subplots within. We found the scale of inference exerted a profound influence over the comparability of T_G and E_C. When we evaluated the two fluxes at the plot scale, large discrepancies were present at all but one plot and T_G was much greater than E_C. Similar findings were also present at the riparian zone scale, where E_C was only about 50% of T_G. This led us to consider the omission of defined area of vegetation that contributing to the diurnal fluctuations in the T_G estimation method. If we made the assumption that all E_C was derived from groundwater (not a very good assumption but a starting point) then the area of vegetation contributing to T_G would have to be about twice as large, 5.8 ha for fluxes to balance. This suggests that the area is likely even larger, given that some of the transpired water is sourced from the vadose zone. Thus, moving forward more work is needed, especially manipulations and studies with rigorous designs to better constrain the area of influential vegetation. This will then allow for direct flux comparisons over consistent ground areas. Only then can water table fluctuations methods be reliably applied in similar upland forested catchments.

4   ECOHYDROLOGICAL RESPONSE OF A HEADWATER RIPARIAN FOREST TO A FLASH DROUGHT EVENT IN THE SOUTHEASTERN U.S.

4.1   Abstract

While forest response to drought has been extensively studied, we were unaware of any studies specifically investigating the response of forest water use to a flash drought event. Flash droughts differ from simple water deficit droughts in their rapidity of intensification and the often-associated high atmospheric moisture demand. This could potentially lead to tree response that differs from more traditional drought impacts that manifest over longer periods. In this study we investigated water use patterns of riparian trees and the evolving role of groundwater as a source of moisture over three periods that varied by antecedent soil moisture conditions. We observed that trees at only one monitoring plot showed a decrease in relative water use during the drought. Reverse sap flow greatly increased during the drought period to an average of 3 liters per day, suggesting the likely occurrence of hydraulic redistribution to the excessively dry soils. Also, over the drought period groundwater became a more dominant source of moisture for forest water use. The response to drought seemed to be mostly in the form of altered water uptake patterns as we did not observe any obvious stress response such as leaf shedding or sudden dramatic declines in canopy water storage. Had the flash drought occurred earlier in the growing season, or been of longer duration, impacts may have been far greater. This study indicated that response to flash drought was not different from many of the patterns noted in the literature. However, this is the first study to our knowledge to specifically investigate forest response to flash drought. As more studies are conducted, a better understanding of the full range of expected responses will emerge.

4.2   Introduction

Droughts have far reaching impacts that may affect both water availability for human consumption and ecological function (Chang & Bonnette, 2016). In forested landscapes drought can lead to increased fuel loads and increase the likelihood of wildfires. Downscaled climate models forecast more variable precipitation and higher temperatures in the future, which could lead to increased drought frequency (Carter et al., 2018). Forest response to drought has been characterized from semi-arid (e.g., Assal et al., 2016) to tropical climates (e.g., Anderson et al., 2010) and across spatial scales ranging from whole catchments to the individual tree level (e.g., Denham et al., 2021; Y. Zhang et al., 2021). Broad scales assessments of forest response to drought are often undertaken using remote sensing approaches and indices that are effective at detecting changes in spectral characteristics (absorbance and reflectance of specific wavelengths) of tree canopies that can indicate changes in chlorophyll or water content (Gao, 1996; Marusig et al., 2020; Tucker, 1979). For example, Swartz et al (2019) used the enhanced vegetation index (EVI) and the normalized difference water index (NDWI) to document drought impacts in the Tobonuco Forest in Puerto Rico. They demonstrated that drought response varied not only by landscape position but also by whether a forest was old growth or second growth. They further showed that for the single year drought they evaluated, recovery following the drought was quite rapid. Oishi et al., (2010) estimated stand level water use for 4 consecutive years (one being a drought year) in a Southeastern U.S. deciduous forest. They showed that at the stand scale, drought effects were minimal. The primary mechanism was offsetting decreased water use of drought sensitive species by drought insensitive species, that maintained, or slightly increased water use during the drought. The study of Oishi et al (2010) used sap flow methods and a scaling approach to estimate stand level water use. Wullschleger & Hanson (2006) used similar

methods but observed contrasting results. These authors observed a decrease in canopy transpiration when soils moisture was experimentally reduced via throughfall capture and rerouting. This experiment was conducted on a ridge top where moisture sources beyond shallow soil were less likely to occur due to limited upslope area from where subsurface moisture could be redistributed. This could have driven the stronger negative response compared to Oishi et al. (2010) which was conducted in a bottomland forest.

Studies at the tree level have identified contrasting mechanism of drought response (e.g., McDowell et al., 2008). These mechanisms are based on the stomatal response to decreasing soil water potentials and are referred to as anisohydric, when the leaf water potential is lowered, and isohydric when the leaf water potential is maintained. While these concepts may be described as two different strategies they are best considered as two ends of a spectrum where species may fall anywhere in between (e.g., Denham et al., 2021). In the Southeastern U.S. Piedmont, many hardwood species found in riparian zones are toward the isohydric side of the spectrum (e.g., *Liriodendron tulipifera* and *Liquidambar Styraciflua*) whereas more of the hillslope or ridgetop species are often toward anisohydric (e.g., *Quercus prinus*, *Carya, sp*.). The practical significance of these characterizations relates to how trees use water (and uptake carbon) during periods of water deficits. Therefore, if using sap flow methods, for example, a decrease in water use would be expected during drought conditions in isohydric species but not necessarily in anisohydric species. Although, this is a gross generalization and actual water use will depend on the soil water potential, which will be driven by the intensity and duration of drought conditions.

Historically, drought has been described as a slow-moving disaster (e.g., Hayes et al. 2011; Showstack, R., 1999). While the progression of drought can be prolonged, the onset can occur quite abruptly (Chen et al., 2019; Lisonbee et al., 2021; Mo & Lettenmaier, 2015, 2016;

Otkin et al., 2017; Park Williams et al., 2017). In recent years, there has been increased

recognition of rapid onset droughts, often termed "flash droughts". Much of the focus has been

on trying to better understand and define the characteristics that lead to the onset of flash

droughts (see Lisonbee et al., 2021; Otkin et al., 2018; Yuan et al., 2019). Otkin et al. (2018)

argued that flash drought should refer to the rapidity, or rate of drought onset, as opposed to a

short duration drought. However, duration is also important (see Orth et al., 2020), which led

Cristian et al. (2019) to use a threshold of at least 6 pentads (30 days) as the minimum duration.

This was primarily to account for drought impacts, which will be minimal to non-existent for

events that occur over 1 to a few pentads, which was the suggested duration by Mo and

Lettenmaier (2016). A primary concern of flash drought is the lack of early warning; thus, land

managers are caught off guard and must be reactive rather than proactive.

Flash drought still lacks a single definition, although many criteria have been proposed

(see Osman et al., 2021). One of the simplest approaches has tied flash drought onset to the rate

in which categories of the U.S. drought monitor change. For example, Chen et al. (2019)

considered a flash drought to occur when a degradation of two or more categories occurred in a

four-week period. This is a simple diagnostic measure to evaluate, and it accounts for the rapid

intensification but also considers a time period which could result in substantive impacts. The

rapid onset of flash droughts are usually characterized by an initial period(s) of below normal

precipitation. However, it is not only the lack precipitation but also an intensification of

atmospheric evaporative demand that can rapidly deplete soil moisture (Chen et al., 2019; Mo &

Lettenmaier, 2016; Otkin et al., 2017; Wang et al., 2019). This can setup a feedback loop, where

there is relatively less evaporation leading to less local cloud formation, therefore greater

incoming radiation with a larger proportion going to sensible heating that further increases

atmospheric demand and drying (Otkin, 2018). This leaves plants having to cope with decreasing soil moisture, but also greater atmospheric demand, which alone (i.e., without excessively dry soils) can invoke a similar stomatal response (*see* Novick, et al., 2016). Additionally, flash droughts do not necessarily operate in isolation, and may occur alongside, or preceding another drought classification, such hydrological or ecological drought (Otkin et al., 2018). The key point that warrants treating flash drought as a unique climatic event, is the stark contrast to the notion that droughts are "slow moving disasters".

The major focus of flash drought research has centered on agricultural regions and impacts (Christian et al., 2019; Ford & Labosier, 2017; Otkin et al., 2016; Wang et al., 2019). Flash droughts in these environments have been demonstrated to be as damaging and costly as more traditional longer-term droughts (Otkin et al., 2013, 2017; Wang et al., 2019). While impacts to forests have not been intensively investigated, a couple broad-scale remote sensing studies over China suggested forests were more resilient to flash droughts than grasslands and croplands (Guo et al., 2019; M. Zhang et al., 2020). Compared to most agricultural crops, rooting depth and extent are far greater in mature trees, providing access to a broader pool of moisture (Jackson et al., 1996; Schenk & Jackson, 2005). Access to larger areas of moisture may prevent most trees from experiencing moisture stress from short-lived droughts. However, to our knowledge, there has not been detailed field assessments of the ecohydrological response of forested catchments to flash droughts. While the literature on forest response to drought is vast, we found little in the way of drought characterization to provide context for the event(s) being studied. Therefore, it is unknown if flash drought impacts on forest ecohydrology have been explicitly explored but may not have been reported on with consistent terminology.

The goal of this study is to specifically evaluate detailed responses of tree sap flow and water-table fluctuations in response to a rapid onset flash drought event. The novelty of the study results from our ability to monitor these response variables specifically in response to a well-defined flash drought that occurred during otherwise near-average climatic conditions—a condition that has not been explicitly identified in most prior research. We hypothesized that trees occupying hillslopes would experience more severe declines in sap flow than trees occupying the valley bottom. This hypothesis is based on the expectation that soil dehydration and water-table subsidence will be exacerbated at hillslope positions during flash drought in comparison with the valley bottom. We expected groundwater to comprise a greater portion of tree transpiration as soil moisture was depleted, potentially revealing thresholds in rooting depth and water table accessibility. To further test our assertion that riparian groundwater supports transpiration over this intense drought period and can prevent drought induced stress, we compare a remotely sensed vegetation index at the watershed scale to examine the spatial patterns that could indicate where in the watershed a stress response to the drought was apparent.

4.3   Materials and Methods

4.3.1   Study Site

This study was conducted at the Panola Mountain Research Watershed (PMRW), a forested 41-hectare (ha), 2nd-order catchment in the Piedmont physiographic province in the Southeastern U.S. (Figure 4.1). Our main focus is on the approximately 3-ha riparian zone adjacent to the main perennial stream. The riparian zone has a tree assemblage similar to many southeastern piedmont floodplains, dominated by *Liriodendron tulipifera*, *Nyssa sylvatica*, *Quercus alba*, *Acer rubrum*, and *Liquidambar styraciflua*. Soils in the riparian zone are loamy to sandy loam and are classified as Cartecay and Chewacla series (Natural Resources Conservation

Service, 2017). The water table is relatively shallow, ranging from locally ponded during wet periods to 3 meters below land surface. Mean annual precipitation (1986 - 2015) is 1240-mm and is spread evenly over the year and average-annual temperature is 15.2 C (Aulenbach and Peters, 2018). Greater details on the study site can be found in (Riley, 2022, ch.2).

4.3.2 *Meteorological Variables and Soil Moisture*

We collected air temperature, relative humidity, and precipitation data in a clearing just outside the watershed (Riley, 2021). From these data we estimated potential evapotranspiration (PET) using the Priestly-Taylor method (Priestley & Taylor, 1972). Tree growth at the edge of the clearing had biased the solar radiation data; therefore, we used a 1-kilometer gridded product
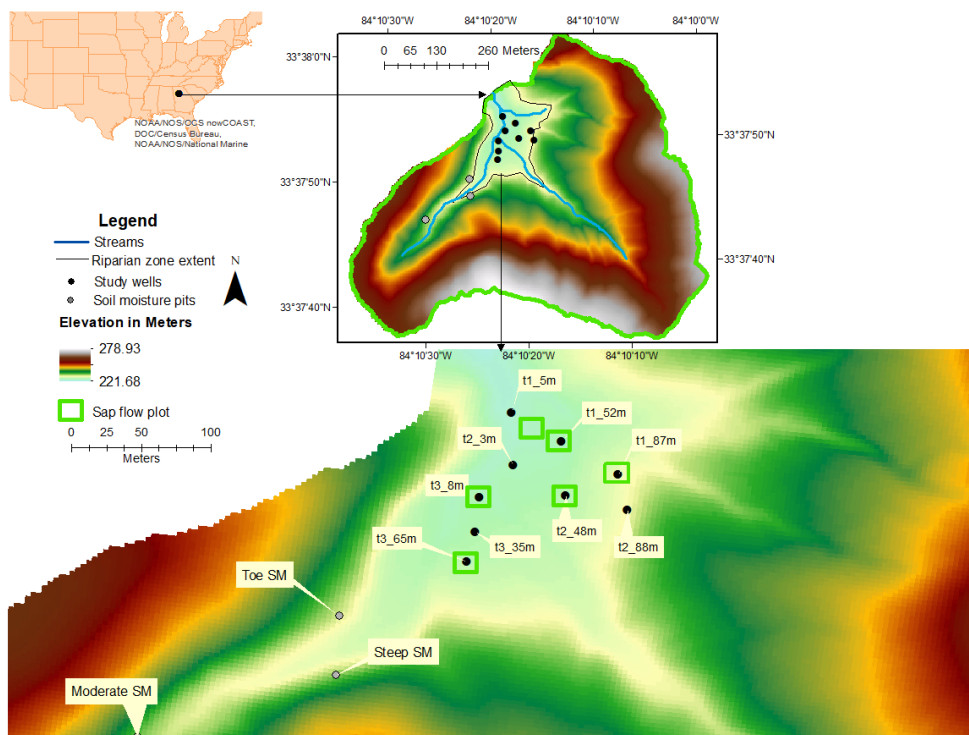
Figure 4.1 Location of study site and layout of monitoring equipment in the riparian zone.

derived from the Geostationary Operational Environmental Satellite (SolarAnywhere, 2019). Soil moisture was monitored at three locations that represented different hillslope positions: upper, middle, and toe slope positions. At each monitoring location we installed sensors

(Campbell CS 616 or Campbell CS 650) at 15, 40, and 70 cm below the land surface in the face of a soil pit and then back filled the pit after installation.

4.3.3   Tree Water Use

To examine water use patterns in individual trees, we installed heat pulse velocity sensors in 4 *Liriodendron tulipifera* (LITU), 3 *Liquidambar styraciflua* (LIST), 3 *Pinus taeda* (PITA)*, and 2 Nyssa sylvatica* (NYSY) (East30 sensors, Pullman, WA or Implexx Sap Flow Sensor, Implexx Sense, Melbourne, Australia). The sensors were comprised of three needles: two outer needles with three thermistors each, distributed along the length, and a central needle that was an inline heater. The central needle delivered a heat pulse, and the heat-pulse was detected by the downstream and upstream thermistors. The time taken for the heat pulse to the reach the sensor, along with physical characteristics and thermal properties of the wood and sap matrix, were used to estimate sap velocity (Barrett et al., 1995; Forster, 2019; Marshall, 1958). The velocity was then be multiplied by the sapwood area of the tree to estimate a volumetric flow rate. More details on the sap flow data collection and processing can be found in Riley (2022, ch.3). In our past study (Riley, 2022, ch3) we used correlations with sap flow and meteorological variables to gap fill missing data. However, in this study we are specifically interested in drought response from individual trees, so we only included measured data and only from trees that had at least two individuals of a given species.

To investigate possible changes in tree water use in response to the flash drought event we compared sapflow over 8-day periods that varied in their mean antecedent wetness conditions, which was based on soil moisture storage in the top 1-m of the soil profile (Figure 4.2). This approach was necessary due to only a single monitoring season, thus no prior years to

compare to. It is also important to note the time frames in which the periods occurred and the

relative energy available to drive transpiration (Figure 4.3). To that end, we also evaluated

normalized fluxes to account for the changing energy conditions over the periods.
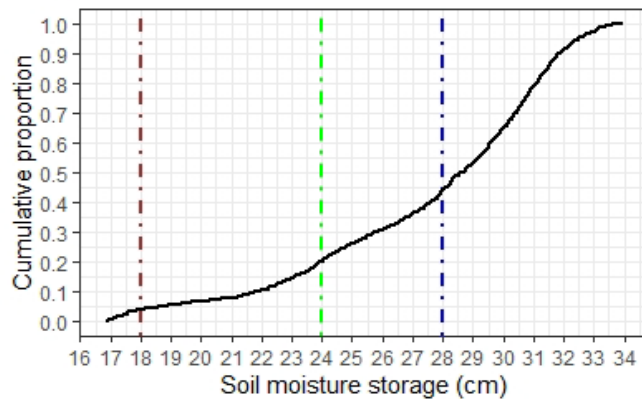
Figure 4.2 *Cumulative probability function of soil moisture storage at the toe slope monitoring stations. The three vertical lines illustrate the mean soil moisture storage for each eight-day period based on soil moisture storage. These periods corresponded to exceedance probabilities of 0.05, 0.20, and 0.45 and are referred to as the drought, dry, and wet periods, respectively.*
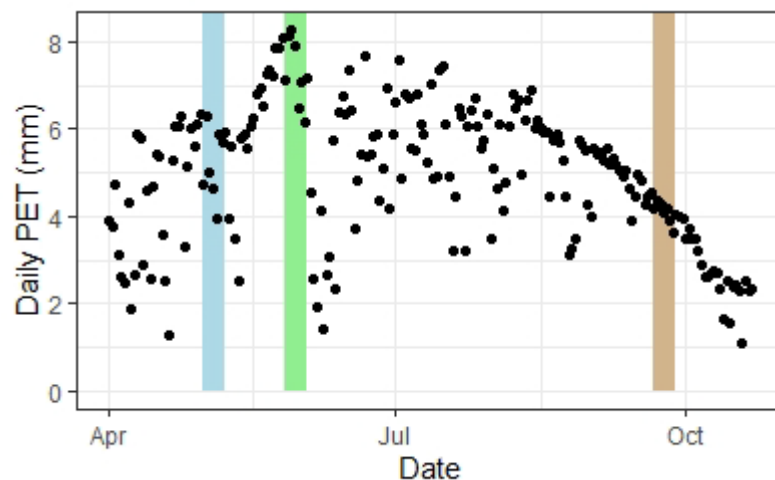
Figure 4.3 *Daily potential evapotranspiration (PET) for the 2019 growing season (Apr – Oct.). The colored vertical bars correspond to the periods selected for comparative analysis described above. The first period (blue) is from May 1 – May 8, the second per period (green) is from May 27 – Jun 3, and the third period (brown) is from Sept. 21 – Sept. 28*

4.3.4   Water-table fluctuations

We instrumented nine monitoring wells, screened across the water table, with total pressure sensors (HOBO U-20) to monitor water-levels across the riparian zone. These wells were arranged in three transects to specifically target different topographic positions within the riparian zone and represented a relatively narrow gradient of depth to the water table (WTD). An additional "dry well" (i.e., not screened) was installed into the water table and vented to the atmosphere to monitor atmospheric pressure for correcting the total pressure sensors for water level (McLaughlin & Cohen, 2011).

We estimated transpiration derived from the saturated zone using water table fluctuations and the empirical approach of Gribovszki et al. (2008). A previous investigation at the site called into the question the absolute values of transpiration derived from the saturated zone (Riley, 2022, ch.2). We suspected the uncertainty was attributable to the unknown area of vegetation that is responsible for generating the signal. However, the signals can still be used to infer relative changes in the amount of groundwater utilized at the different plots and in response to different antecedent wetness conditions and WTD. Therefore, we relied on the ratio of T_G to PET to infer changes in the relative amount of groundwater used by vegetation.

4.3.5   Remotely sensed indices of drought response

To explore watershed scale impacts from the flash drought event and place the perceived buffering effect of the riparian aquifer in a broader context, we calculated the normalized difference water index (NDWI, Gao, 1996) using Sentinel 2 surface reflectance data. The calculated NDWI had a spatial resolution of 20 m and was focused on 6 cloud-free days over the 2019 growing season. Numerous studies have demonstrated the use of remotely sensed vegetation indices for evaluating drought impacts (Assal et al., 2016; Schwartz et al., 2019; Xulu

et al., 2019). We chose to use NDWI because it has been shown to be effective at detecting drought impacts in forest and it is less sensitive to atmospheric effects than the normalized vegetation index (Gao, 1996). The NDWI is as follows:

$$NDWI = \frac{(NIR-SWIR)}{(NIR+SWIR)}$$
Equation 4.1

Where NIR is the near infrared radiation band (band 8A in Sentinel 2) and SWIR is short wave infrared radiation band (band 11 in Sentinel 2). This ratio is relevant to plant water status based on the relatively higher absorption of SWIR by water and greater reflectivity in the NIR range by water (Schwartz et al., 2019). We evaluated the change in mean NDWI values over periods of high antecedent moisture prior to the drought, during the drought, and into senescence over the entire watershed and just the riparian zone to infer possible buffering effects of the riparian aquifer.

4.4. Results

4.4.1 Flash drought characterization

From August, 28th to October, 8th the watershed received less than 3 mm of precipitation (Figure 4.4a). Over that period, maximum daily temperatures rose above 32°C for 25 days (Figure 4.4b). For comparison, over the same sequence of days, 32°C was equaled or exceeded only 33 times in total across the preceding 20 years of 1998 to 2018. Maximum daily vapor pressure deficits exceeded 2.5 kPa on 21 days (Figure 4.4c). In the prior two years (2017 & 2018), over the same period, a VPD of 2.5 kPa was only exceeded 4 times; underscoring the relatively high atmospheric moisture demand during this drought. During the drought period day-to-day variability in solar radiation decreased (compared to before the drought, figure 4.4d) due to low cloud cover.
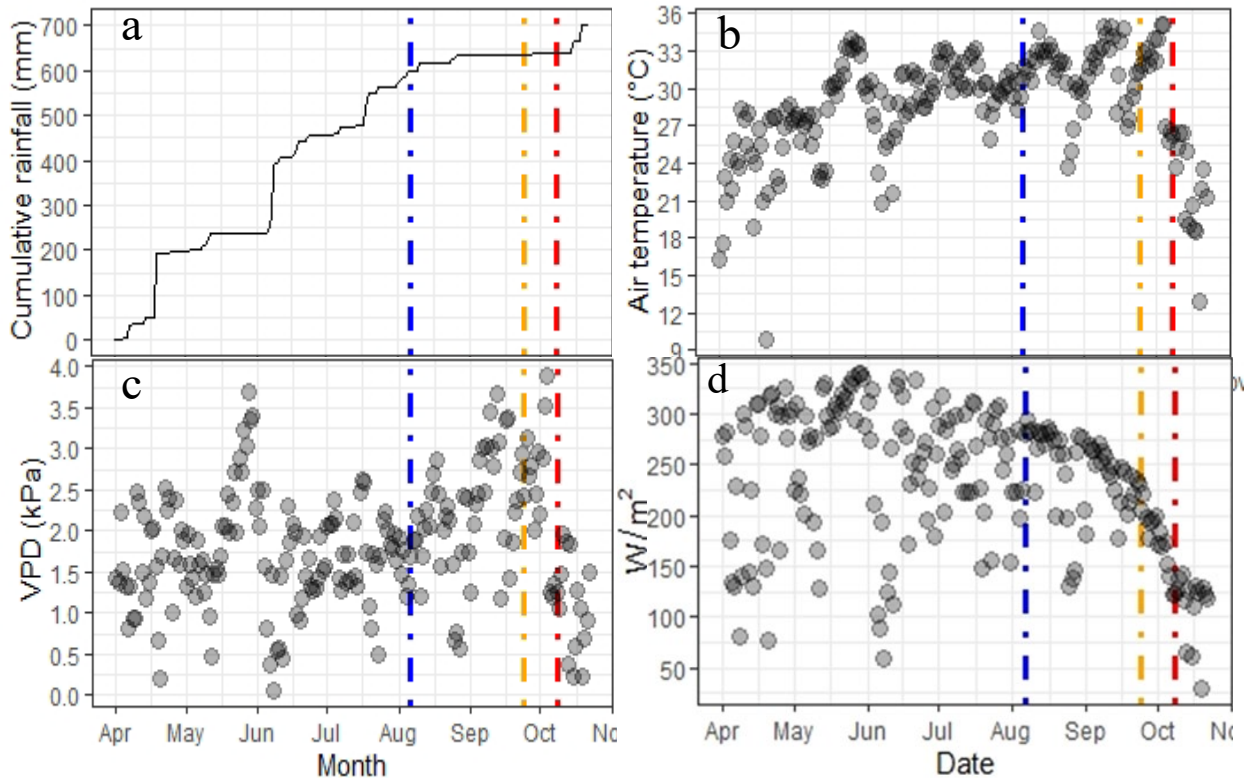
Figure 4.4 Meteorological Conditions over the 2019 growing season (April - October). Panel a: cumulative rainfall, b: maximum daily air temperature, c: maximum daily vapor pressure deficit, d: daily mean insolation. Dashed lines refer to drought status from U.S. Drought Monitor, where blue = last day of no drought, yellow = severe drought, and red = extreme drought.

Soil moisture content at the toe slope position reached its lowest average volumetric water content (~17 %, Figure 4.5) during the flash drought, which was the lowest observed since monitoring began (2016-2019). Two other monitoring locations, higher up hillslopes, dried out more rapidly and appeared to approach the wilting point based on the near flat-lined response in September – October; however, we focus attention on the toe slope location because it is closer to, and more representative of the riparian zone.
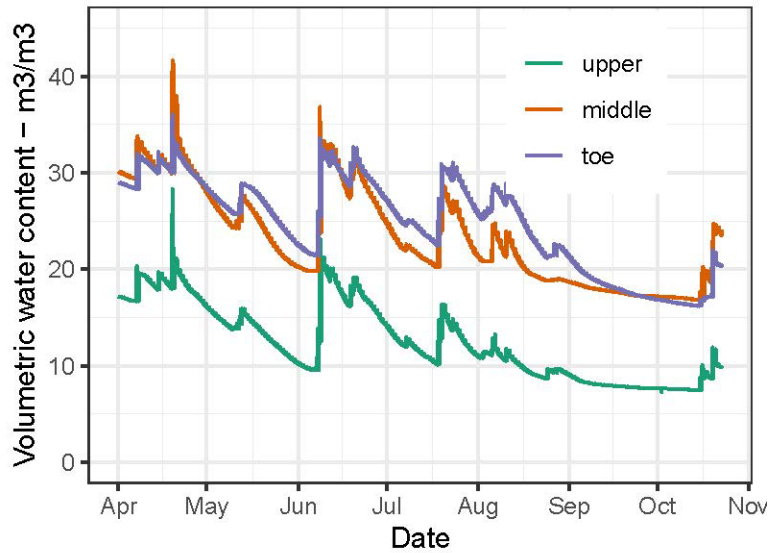
Figure 4.5 Average volumetric water content at three soil monitoring locations. Data cover the 2019 growing season. Note, the VWC is the average from 3-sensors installed at 15, 40, and 70 cm below the land surface.

Streamflow was near normal or slightly above the median for every month until August

when rainfall started to diminish (Figure 4.6). Beyond August, streamflow demonstrated a
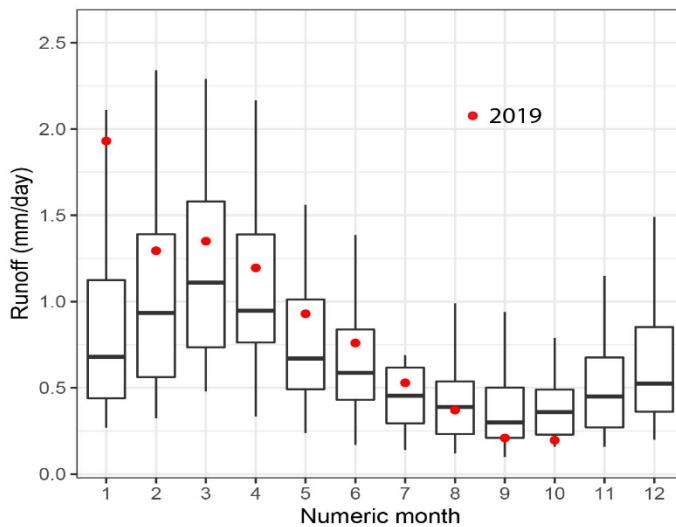
Figure 4.6 Boxplots of monthly median stream runoff for June1985 – October 2019. Red filled dots indicate the monthly value for that month in 2019 (the focal year). X-axis is calendar months, 1 = January to 12 = December.

strong response to the flash drought. When compared to the historical record (36 years), September 2019 had the 10th lowest median daily runoff for any September and October 2019 had the 6th lowest median daily runoff for the month of October (Figure 4.6).

4.4.2 Response of Tree Water Use to Drought

At the species level, we observed similar patterns in the distribution of daily sap flow over the three periods amongst the hardwoods (LIST, LITU, NYSY), which all differed from pine (PITA, Figure 4.7). The general pattern among hardwood species was that the greatest sap flow occurred during the dry period but in pines the greatest occurred during the wet period. We attempted to minimize this confounding influence of different energy conditions among periods by normalizing sap flux density (*Js*) by PET—what we refer to here as relative water use. When evaluating relative water use (J_S/PET), the pattern was not as consistent among species and indicated the differences that did exists were small (table 4.1, Figure 4.7b).

Table 4.1 Results of Games-Howell multiple comparison test (α = 0.05) of difference in Js/PET across the three periods. Rows in bold indicate comparison where p < α.

Species	Period Comparison	Mean difference	Lower 95% CI	Upper 95% CI	p-value
LITU	**drought-dry**	**-0.06**	**-0.12**	**-0.01**	**0.02**
LITU	drought-wet	-0.01	-0.08	0.05	0.84
LITU	**dry-wet**	**0.05**	**0.00**	**0.09**	**0.03**
PITA	**drought-dry**	**-0.05**	**-0.07**	**-0.03**	**0.00**
PITA	drought-wet	0.00	-0.03	0.04	0.96
PITA	**dry-wet**	**0.05**	**0.02**	**0.08**	**0.00**
NYSY	**drought-dry**	**-0.10**	**-0.14**	**-0.05**	**0.00**
NYSY	**drought-wet**	**-0.12**	**-0.16**	**-0.08**	**0.00**
NYSY	dry-wet	-0.02	-0.04	0.01	0.15
LIST	drought-dry	0.09	-0.08	0.26	0.41
LIST	drought-wet	0.08	-0.05	0.22	0.29
LIST	dry-wet	0.00	-0.17	0.17	1.00

However, J_S/PET during the dry period was lower than either the drought or the wet period in LITU and PITA (Figure 4.7b). This difference was supported using a non-parametric Games-Howell test (table 4.1). Similar patterns were not present in LIST or NYSY, and these two

species demonstrated opposite patterns among the periods (Figure 4.7b), likely reflecting

different localized wetness conditions. Reverse sap flow was most pronounced during the

drought (Figure 4.7c) and had an overall greater magnitude in the hardwoods. It is worth
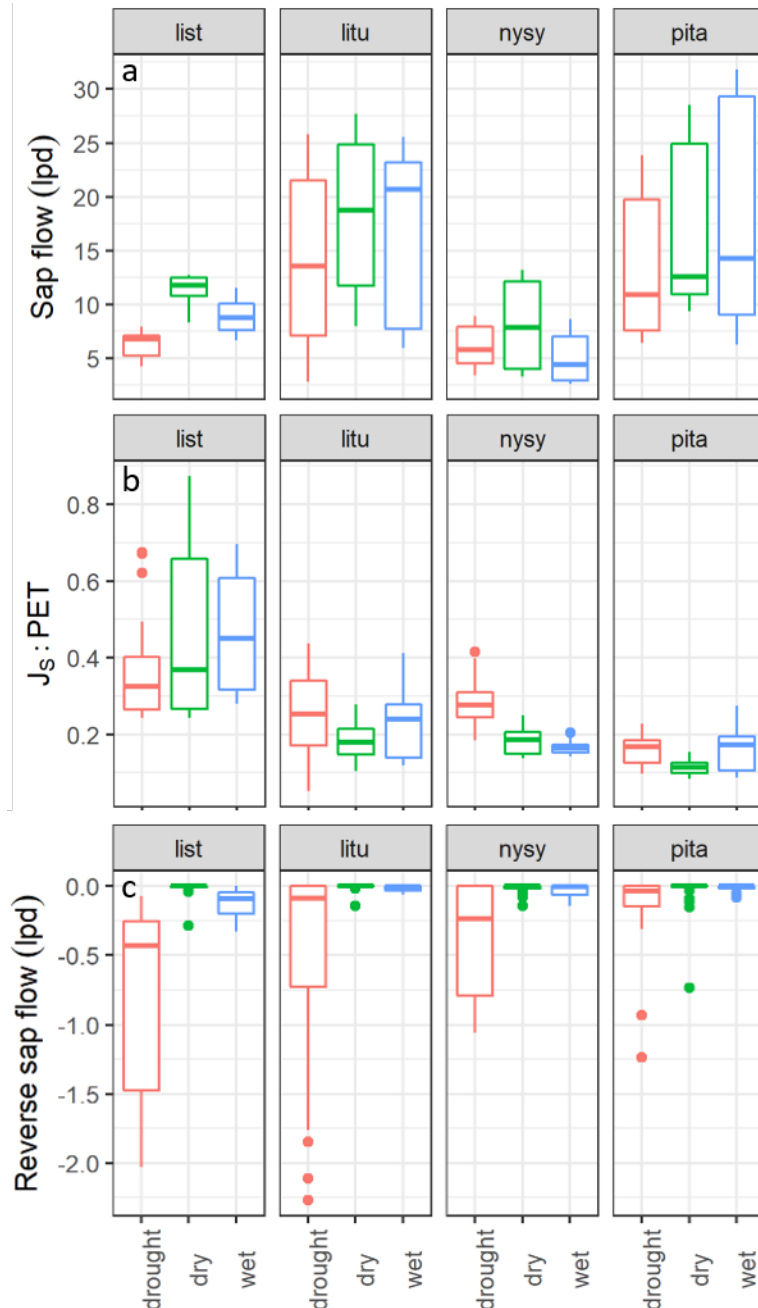
Figure 4.7 Species level response of water use metrics across three periods. Top panel (a) is daily sap flow in liters per day, (b) daily sap flux normalized by PET, and (c) is reverse sap flow. Box contains data from the 25th to 75th percentile (IQR), horizontal line in the box indicates the median, vertical lines extend to ± 1.5 times the IQR, and dots are data beyond that

pointing out that the species level patterns were driven largely by a single individual of each species (Figure 4.8c).

Considering monitored trees individually, most demonstrated enhanced sap flow during the dry period in comparison with the wet period (Figure 4.8a). Eight of the 11 monitored trees exhibited this response, with total transpiration increasing by 9-73 %, with an average of 30%. (Figure 4.8a). The only trees that did not show this increase were the two largest pine trees, which had the greatest sap flow during the wet period and decreased 11% during the dry period and a single NYSY that exhibited marginally higher sap flow during the drought period.

Every monitored tree except a single NYSY had lower sap flow during the flash drought than during the preceding dry period, with an average decline of 25% (Figure 4.8a). This is likely partially attributable to reduced solar radiation during the former period compared to the latter. Compared to the dry period, nine of the eleven trees had greater relative water use during the drought, with an average increase of 46%. Six of these trees had the greatest relative water use during the drought period (Figure 4.8b). However, of these six trees only two were located at an upslope position, where the water table was deeper below the surface, suggesting groundwater access may have decreased for some hillslope trees.

An additional line of evidence that suggest trees had a pronounced response to drought is the change in negative, or reverse, flow over the periods (Figure 4.8c). The mean reverse flow for the wet period was 0.32L. During the dry period this decreased slightly to 0.18 L, likely due to the high atmospheric demand over that period. The drought period saw a large increase, with the average reverse flow for the period increasing to 2.93L, and one tree (LITU14) having a reverse flow of ~ 13 liters, which was just under 50% of the total flow for the period. While our study was not specifically designed to track hydraulic redistribution, and no roots were

monitored, this data does suggest hydraulic redistribution may have been a common occurrence during this drought period.
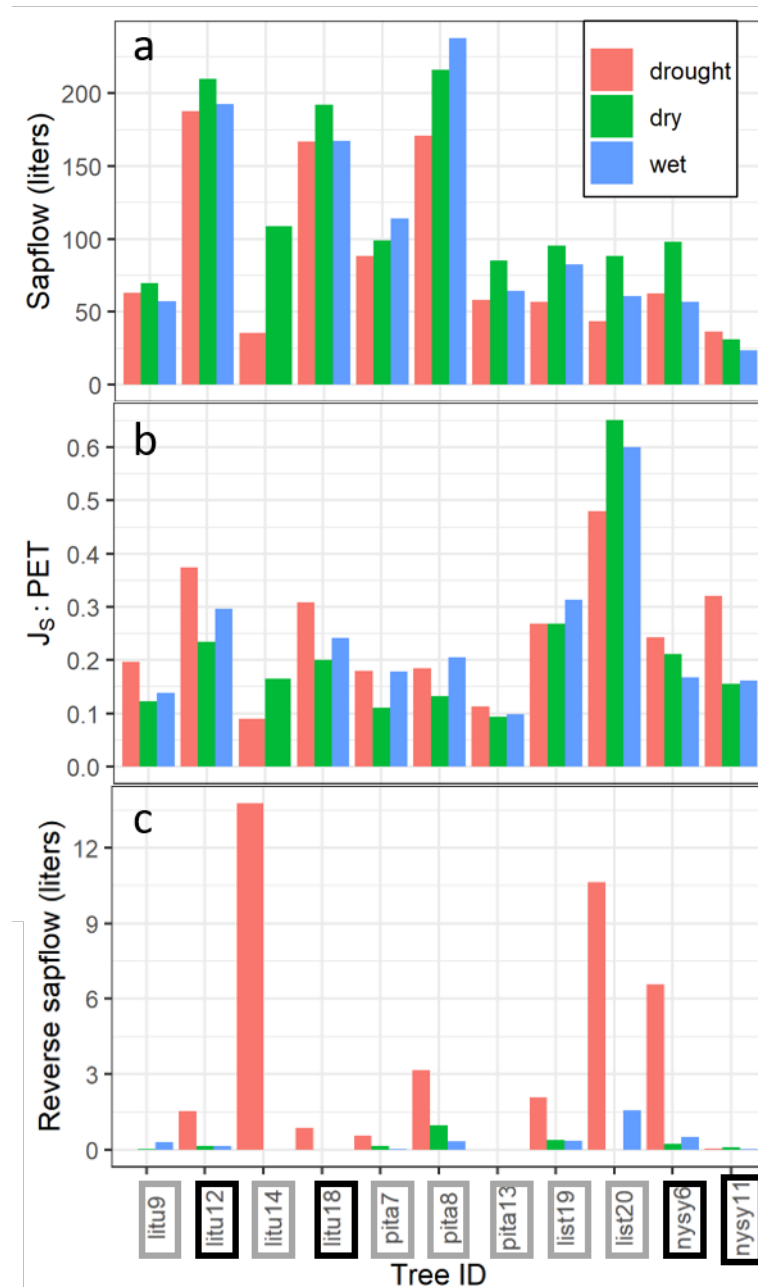
Figure 4.8 Water use metrics over each 8-day period. Total sap flow for each study tree (a), ratio of mean sap flux density to PET (b), and total negative (reverse) flow (c). Tree ID surrounded with grey boxes are hillslope trees and black boxes are mid

4.4.3   Water Table Response to Drought

To allow for direct comparison with tree water use we focus our assessment of water

table response on the same periods evaluated for tree water use. We observe a high degree of

variability over the different periods related to landscape position (Figure 4.9). Considering the

differences just among these periods, WTD at near stream wells dropped 7 – 22 cm. The middle
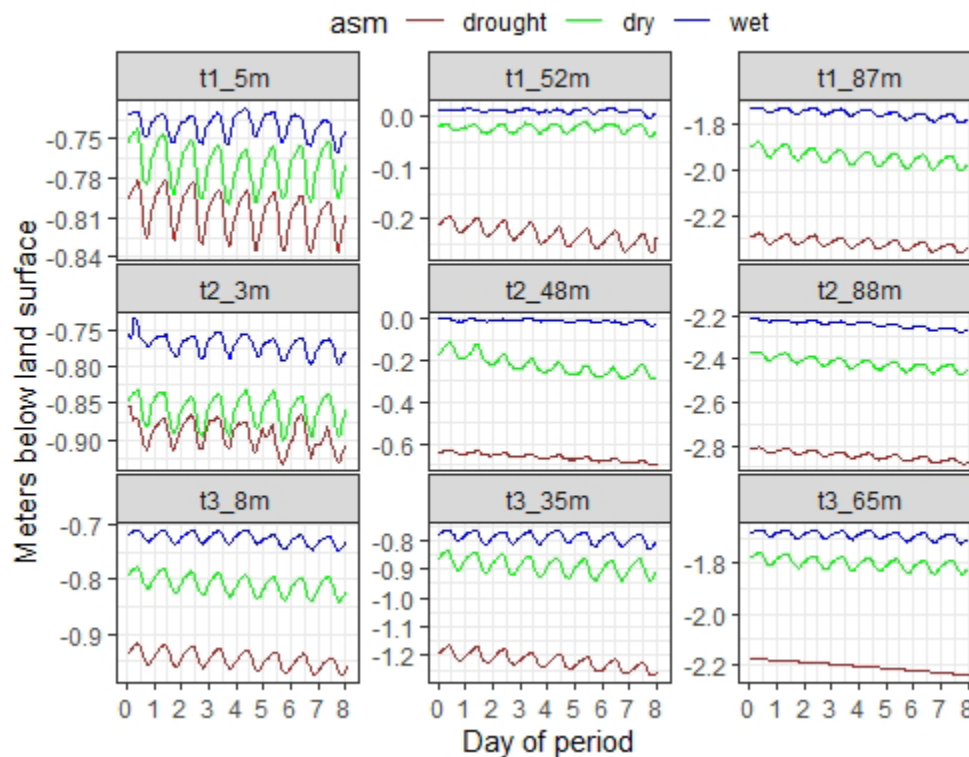
Figure 4.9 Water table hydrographs for all 9 monitoring plots. Colors reflect the antecedent soil moisture (asm) periods associated with figures 4.4 & 4.5. Panels are arranged so that rows represent transects (down valley - up valley) top to bottom and landscape position (near stream to hillslope) left to right. Note, y-axes are not equal and represent the range of water table depths observed at each plot

riparian zone wells were saturated (t2_48m) or slightly ponded in the case of well t1_52m (wet

period) but did exhibit substantial drop across the periods ranging from 24 – 65 cm. At the

hillslope position we observed the greatest consistent decline across the periods with all wells

dropping 52 – 60 cm. These changes in water table position over the periods are directly related

to the accessibility by tree roots and the potential for the saturated zone to act as a subsidy to stave off drought impacts.

Diurnal water table fluctuations (DWTF, an indication of groundwater use by plants) over these periods showed an increasing pattern going from the wet to the dry period followed by a subsequent decrease in magnitude heading into the drought period, which is consistent with the patterns of sap flow (figures 4.7a & 4.8a) and PET (Figure 4.3). The daily magnitude was consistent across all landscape positions, with a max around 0.06 m and min about 0.01 m. When the fluctuations were converted to groundwater transpiration (T_G) the patterns were similar. However, when the T_G was normalized by PET the picture is slightly different (Figure 4.10).
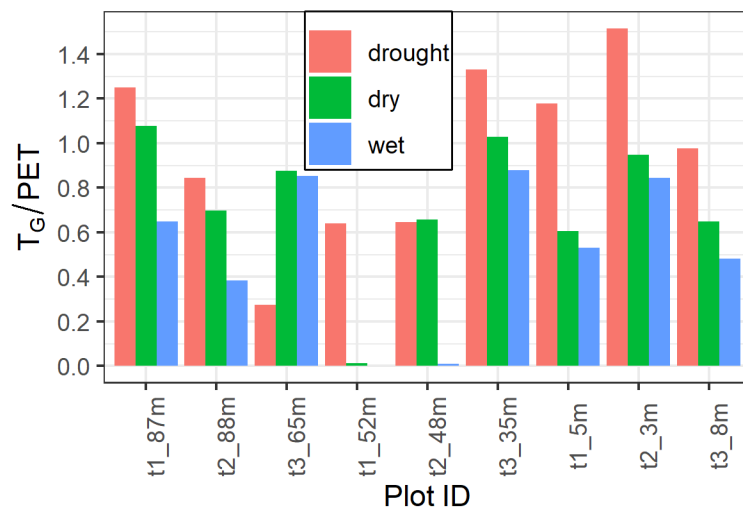
Figure 4.10 Ratio of transpiration derived from groundwater to PET. Ratios over one may be expected due to nocturnal water uptake by plants that is not captured in PET estimates.

Figure 4.10 shows that even though overall transpiration was decreasing the relative amount derived from groundwater was increasing. Thus, highlighting the role of groundwater as a subsidy during drought periods. There was only one plot in this study where trees appeared to lose access the saturate zone. Around plot t3_65m DWTF ceased, driving down T_G approximately 68% compared to the other periods.

4.4.4   *Watershed Scale Assessment of Drought Response*

We found that the average NDWI was within a relatively small range across all growing

season scenes evaluated (n=5). Variation within a scene was slightly greater at the watershed

scale than the riparian zone (table 4.2), which was not surprising, given the greater diversity of

the landscape positions and species present. Figure 4.11 presents scenes that represent different

soil moisture conditions and span most of the growing season. While the mean NDWI values for
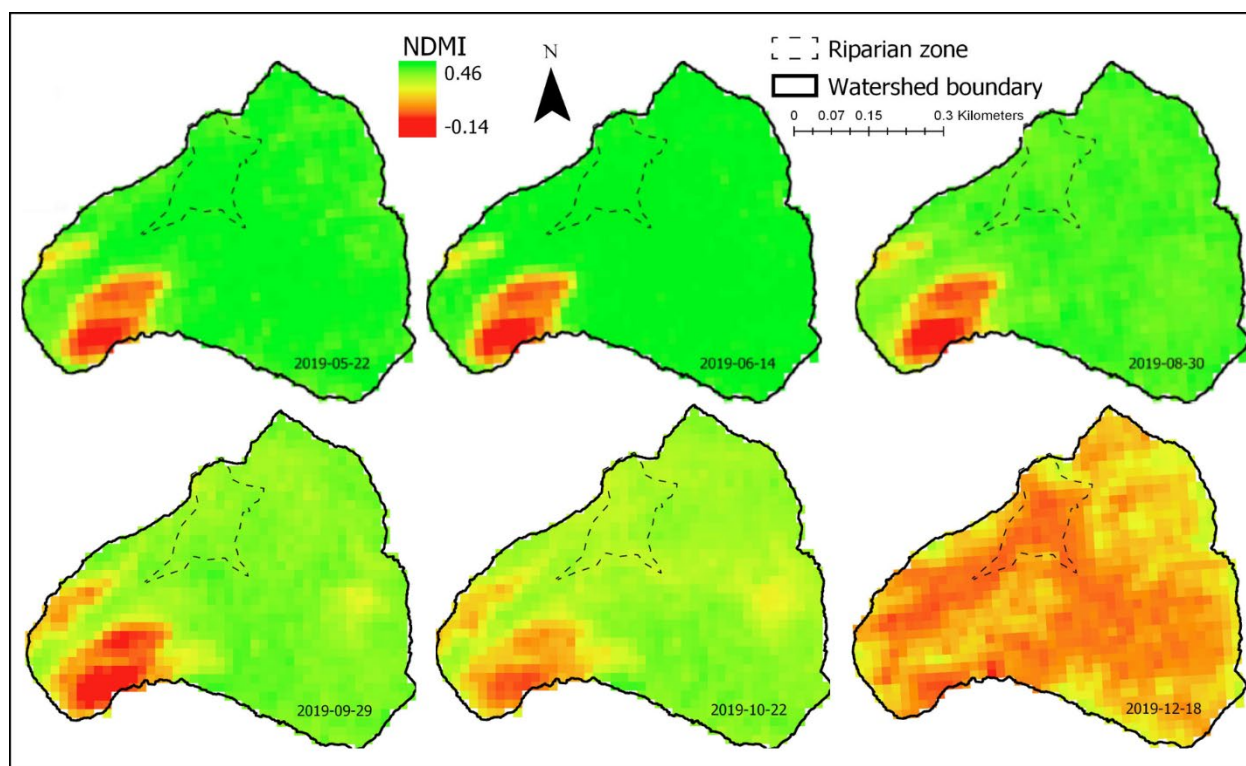
Figure 4.11 Normalized difference water index (NDWI) derived from Sentinel 2 surface reflectance data. The selected dates represent progression through the growing season with the 2019-09-29 scene representing peak drought conditions. The scene from 2019-12-18 is for reference to what the NDWI signature looks like during near complete dormancy. The consistently low (negative) NDWI values in the southwest corner are over a sparsely vegetated bedrock outcrops.

a given scene were generally higher in the riparian zone than for the entire watershed, the

changes between scenes, which would be more indicative of a drought onset or impact, were

very similar at both scales (table 4.2). This suggests that changes in canopy moisture content

during the drought were not extensive and if drought induced changes were occurring, they were

not of substantial magnitude. In general, the patterns of change in NDWI are in-line with seasonal changes in energy and tree growing conditions. The 2019-12-18 scene is after leaf senescence and indicative of near leaf off conditions for most of the catchment and may be similar to what a canopy scale response to the flash drought would look like, had it occurred.

Table 4.2 Change in the normalized difference water index (NDWI) between successive scenes in just the riparian zone and at the watershed scales. Note, the watershed scale excludes the riparian zone and bedrock outcrops to compare only areas with forest cover.

Date	Scale	Standard Deviation	Mean	Change in mean
5/22/2019	riparian	0.02	0.42	0.00
6/14/2019	riparian	0.02	0.45	0.03
8/30/2019	riparian	0.02	0.37	-0.08
9/29/2019	riparian	0.02	0.30	-0.07
10/22/2019	riparian	0.02	0.26	-0.04
12/18/2019	riparian	0.07	0.00	-0.26
5/22/2019	watershed	0.05	0.40	0.00
6/14/2019	watershed	0.06	0.43	0.03
8/30/2019	watershed	0.05	0.36	-0.07
9/29/2019	watershed	0.07	0.30	-0.06
10/22/2019	watershed	0.06	0.27	-0.03
12/18/2019	watershed	0.07	0.05	-0.22

4.5. Discussion

4.5.1 *Species Level Water Use Response to Flash Drought Conditions*

Species level water use response to droughts have been demonstrated in numerous studies with similar species composition (e.g., Denham et al., 2021; Oishi et al., 2010; Pataki & Oren, 2003). In these studies, *Liriodendron tulipifera* (LITU) has been noted as being particularly sensitive to drought, typically showing reduced sap flow. We focus our discussion on the relative water use (J_S/PET) as it attempts to control for the changing energy conditions between the periods- that alone could lead to changing water use- and facilitates more direct comparisons between periods. Interestingly, in this study we observed a greater decrease in relative water use

during the dry period rather than during the flash drought (Figure 4.7b) when soil moisture was more depleted (Figure 4.3). This pattern was also demonstrated by *Pinus taeda* (PITA). Both species are considered to be isohydric (Choat et al., 2012; Roman et al., 2015 supplemental material T1*)*, maintaining a leaf water potential under reduced soil moisture thereby reducing transpiration. This result may reflect an interaction between VPD and soil moisture. While soil moisture was lower during the drought, so too was VPD, therefore, the actual difference in water potentials between soil and leaves may have been greater during the dry period resulting in greater stomatal regulation by LITU and PITA, and lower relative water use. Another possible explanation could be related to the normalization approach (Js/PET) and the presence of high VPD during the dry period. Oishi et al (2010) demonstrated that LITU sap flux can reach a saturation (i.e., Js increases asymptotically and levels off with no further increase in Js with increasing VPD) at a VPD well below what we observed. Therefore, our normalization by PET, which incorporates VPD could be leading to a low bias during the dry period.

Water use response to drought in the other two species (LIST and NYSY) have not been reported as consistently. For example, Oishi et al. (2010) observed LIST to increase water use during a drought, even more so than oaks, which are generally considered to lie toward the anisohydric end of the spectrum and be relatively drought tolerant. In contrast, Pataki and Oren (2003) reported that LIST presented a modest decline in sap flux in response to a short duration drought. Our observations tend to agree with the later, as we observed modest decreases in relative water use as soils progressively became drier (Figure 4.7b). While NYSY is a widely distributed species that can occupy virtually any site type (Abrams, 2007), it is rarely dominant, and it seems few studies have characterized the species water use characteristics in relation to drought conditions. Based on estimates of water potential in Choate et al (2012, supplemental

table 1) and conclusions presented by Abrams (2007), NYSY tends to be a drought avoider and tightly regulates stomata in response to drying soils. However, our results demonstrate an opposite pattern, one where water use increased during the drought. We think this can be explained by the environmental setting. The NYSY in this study were at the edge of a seepage bog that stayed saturated until the flash drought event. Therefore, stress from waterlogging and anoxia may have limited water use during the wet and dry periods, and only during the drought did the soils dry out enough to be re-oxygenated and facilitate greater water use. A final consideration regarding species level response is our small within species samples (2- 4), potentially limiting the ability to widely extrapolate our findings. However, we purposefully focused on a narrow gradient within a riparian forest and the results may represent the typical response in these environments.

4.5.2   Absence of Consistent Landscape Position Effects on Tree Water Use

Previous studies have found landscape position to influence patterns of tree water use (Mitchell et al., 2012; Tromp-van Meerveld & McDonnell, 2006) or canopy water storage (Swartz et al., 2019) in response to drought. In some cases, the influence of landscape position was also species dependent (Hawthorne & Miniat, 2018; Schwartz et al., 2020). The general pattern observed in these studies is that trees of a given species further upslope tended to demonstrate a more pronounced drought response compared to those in lower landscape positions. This makes sense considering there is greater recharge potential on lower slopes simply by the down gradient flow of saturated and unsaturated zone moisture.

In contrast to some previous studies, we did not observe a consistent pattern in the response of sap flow, or relative water use, to drought associated with landscape position. We think this is partly attributable to the relief and landscape positions encompassed by our study

design which were not sufficiently different to induce systematic differences in the trees' sap flow in response to drought. We anticipated that the landscape transition from valley bottom to hillslope would also correspond to a hydrological transition—a transition defined by continuous access to groundwater in the valley bottom and seasonal, transient access to groundwater on hillslopes. Yet even during the flash drought, the water table was sufficiently close to the land surface at two of three hillslope positions for trees to access groundwater for transpiration (Figure 4.9). Furthermore, our "hillslope" plots were located along the toe-slope position, so compared to the overall watershed relief, they were in a topographically low landscape position but higher than the rest of the riparian zone. Dymond et al. (2017) pointed out that in their low-relief study area, topography was not great enough to generate significant differences in plant available water and that community composition, soil texture and depth exerted a greater influence. This could also be true in our study area. Had we focused on a ridge top site and the riparian zone we may have observed substantial differences consistent with other studies (e.g., Mitchell et al., 2012; Tromp-van Meerveld & McDonnell, 2006).

4.5.2.1 Discrete location of drought response in transitional landscape

As mentioned above, there was a single plot where drought impacts appeared evident. This plot was located at a hillslope position and was on the most up-valley transect (plot t3_65m, Figure 4.1). There were several lines of evidence here that suggested trees were responding to the drought, and the effects were most evident in hardwoods (litu14, list19, & list20 – no patterns observed in the one pine tree, pita13). These three trees contrasted the general patterns observed in figure 4.8b & c. They were the only trees to demonstrate the lowest J_S/PET during the drought period and they had among the highest reverse (negative) sap flow of all trees during the drought period (Figure 4.8c). The low J_S/PET during the drought suggest these trees likely experienced

water limiting conditions, since no other individuals of either species displayed a similar pattern, nor did any other species (Figure 4.8b).

Water table fluctuations ceased around this plot during the drought (Figure 4.9). This indicates that few trees in this area could access the water-table or at least not in a manner that resulted in the substantial drawdown that was present at higher water table elevations or across other plots. The loss, or reduction, of groundwater access could be driving the large increase in reverse sap flow (HR) observed at these three trees (Figure 4.8c). We also observed the greatest relative amount of groundwater consumption during the flash drought at all plots except this one (t3_65m, Figure 4.10). This finding, of a single location containing evidence of drought response indicates that landscape position alone may not differentiate whether drought induced changes to tree water use will occur along relatively narrow gradients of water availability (i.e., water table depth). Tree water use response likely reflects the interaction of rooting depths and critical zone structure that controls the movement and storage of subsurface moisture; something that our results suggest may be difficult to predict by landscape position alone.

4.5.2.2. Hydraulic redistribution as a drought response

The occurrence of hydraulic redistribution (HR) during drought has been documented across a wide range of species and climates (e.g., Bleby et al., 2010; Dawson, 1993, 1996; Hafner et al., 2017; Oliveira et al., 2005) While our study was not designed to specifically investigate HR (i.e., no roots were instrumented) several aspects of the patterns of reverse sap flow during the drought (Figure 4.7c & 8c) suggest it is likely occurring (Nadezhdina et al., 2010; Oliveira et al., 2005). Specifically, the fact all negative sap flow occurred in the overnight hours is in line with numerous studies that have demonstrated this as the dominant time of hydraulic redistribution (e.g., Bleby et al., 2010; Nadezhdina et al., 2010). Furthermore,

examining how negative sap flow varied across the periods with different antecedent conditions also supports the flash drought induced HR (Figure 4.7c & 8c). Reverse sap flow was most prominent in hillslope trees, but surprisingly, was also observed in a few trees in a lower landscape position (Figure 4.8c), where the water table was relatively shallow. During the flash drought, soil moisture in the top 1m reached the lowest observed value over the 4-years of monitoring, suggesting root zone moisture was greatly reduced, leading to increased matric potential in surficial soils. During the drought, HR would represent an effective strategy to maintain water uptake and potentially access nutrients that are in greater supply in shallow soils. However, since we only monitored the stem (trunk) we cannot make further assessment regarding lateral or other patterns of HR.

4.5.2.3 Groundwater as a buffer against drought stress

Groundwater has been identified in many studies as providing a water subsidy during times of decreased soil moisture and can act to ameliorate drought effects (Dawson, 1993, 1996; Vincke & Thiry, 2008). Groundwater uptake is evident in Figure 4.9 that shows the consistent diurnal water table fluctuations (DWTF) across all the periods evaluated at all landscape positions. We observed that groundwater use varied by soil moisture status, atmospheric demand, and the assumed relationship between water table depth and rooting depth, since a single plot seemed to lose access to the water table (plot t3_65m). Had our monitoring plots extended further up the hillslopes or had the flash drought started earlier in the growing season, we may have observed a more general response among trees at hillslope positions where water-tables are relatively deep (2 – 3 meters) even in non-drought conditions. This was the pattern we hypothesized observing. Across the periods evaluated, it was during the flash drought period that

groundwater made up the greatest proportion of PET (Figure 4.10); highlighting the buffering role groundwater played across all landscape positions during the flash drought.

4.5.3 Drought Timing and Forest Structure may Drive Lack of Observed Response to Flash Drought

We did not observe any patterns indicative of a broadscale response to the flash drought event (figure 11). Our results suggest a single plot (t3_65m) was a transition location, which we hypothesized that all hillslope plots would be. If a similar species composition persisted further upslope from t3_65m we would expect the NDWI (Figure 4.11 & table 4.2) to look very different and show indications of canopy level effects to the flash drought. However, the lack of watershed scale response to the flash drought could have resulted from the timing of the event. The peak intensity occurred toward the end of the growing season when plant vigor was already beginning to decline prior to winter senescence. Zhang et al. (2020) explored broad scale flash drought impacts across all of China and found that the decreases in gross (and net) primary production was more rapid in semiarid regions (primarily grasslands) compared with more humid regions (primarily forested). Possibly indicating a resilience of forests to short term water deficits even if the onset is very intense and rapid.

Another factor that may have limited the degree of observed response to the flash drought could reflect forest demographics and spatial segregation of species. The distribution of species across the watershed reflects the relative drought tolerance and likelihood of drought exposure (Silvertown et al. 2015). In the present study, hillslopes above the riparian zone are dominated by hickories (*Carya sp.*) and red and chestnut oak (*Quercus rubra and Q. montana*). These species have been shown to be more resilient to drought, at least in relation to the species found in our riparian zone, which have been shown to have pronounced drought responses (Denham et al.,

2021; Hawthorne & Miniat, 2018; Pataki & Oren, 2003; Roman et al., 2015). Their location in the riparian zone ensures a source of water under all but the most extreme circumstances, effectively staving off drought induce stress or injury. Thus, the shallow water table is likely an important buffer in the riparian zone but outside of that, trees are adapted to living in more water limited environments and have evolved strategies to survive. Thus, not observing a drought response could be due to the combination of drought timing and duration, the relative resilience of forest over other plant forms, and species spatial distributions and their adaptation strategies for coping with short term moisture deficits.

A final point worth highlighting, is the dichotomous response of the forest canopy versus streamflow to the flash drought. Figure 4.11 indicates that there were not wholesale changes in canopy water storage linked to the flash drought event. In contrast, Figure 4.6 highlights a progressive decline in runoff over the flash drought, with runoffs falling outside of the interquartile range during September and October. This raises many questions regarding the manifestation of drought impacts and the role of catchment storage and the connection between pools of water sustaining streamflow and transpiration.

4.6. Conclusions

In this study we evaluated the water use response of 11 riparian trees to a rapid onset flash drought event. This flash drought was relatively short lived but demonstrated a very rapid intensification that led to some of the lowest daily soil moisture observed at the study site. Trees did not display a consistent response to the drought when evaluated by species or landscape position. Only three trees at a single plot showed multiple lines of evidence that suggested moisture stress by reducing the ratio of J_S/PET during the drought and increasing reverse sap

flow. Along with the tree water use responses we also observed the cessation of diel water table fluctuations around this plot. This indicated that the water table dropped below the root zone and was no longer acting as a readily accessible subsidy. This one location that did seem to have a drought response was at a hillslope location. Had the drought started earlier in the growing season it is more likely that we may have observed a more consistent response. Furthermore, when viewing drought response at the watershed scale using the NDWI, we did not observe any indication of substantial drought impacts in any landscape position.

While our findings don't necessarily point to broad scale impacts of the flash drought, they do highlight strategies used by trees to avoid or cope with drought and are similar to those observed in other drought studies. Based on these findings, in areas with accessible water tables or deep vadose zones accessible to tree roots, it appears flash droughts of limited duration may not have a significant impact on forests water use or survivability. However, Berdanier & Clark (2016) showed that mortality from drought was often a slow process, with reduced growth for multiple years before mortality. Flash droughts can occur in tandem with hydrologic or ecological drought and if soil moisture is already low, more substantial drought stress or even tree mortality could occur in similar well-watered humid environments. This study provided insight into possible response to the rapid onset drought event, but a more complete picture will emerge with more studies that capture a greater range of flash drought conditions and durations.

5   CONCLUSION AND FUTURE STUDIES

This dissertation explored several knowledge gaps associated with groundwater and forest water use. I specifically focused on a humid riparian forest and the importance of groundwater use therein. Although transpiration in general has long been recognized as a dominant flux in the water balance of temperate-humid catchments, the specific role of *riparian forests* has not been investigated. This is perhaps due to the assumption that the riparian forest is not ecohydrologically distinctive from forest cover in the uplands. Yet, through direct uptake of groundwater for transpiration, riparian trees do exert a more direct control on streamflow than do upland trees whose roots do not reach the aquifer. Therefore, the goal was to understand how techniques used in other environments could be applied in these settings, and given the paucity of studies in similar environments, evaluate the spatial and temporal variability. Chapter two presented a new conceptual model which refutes many existing studies. It showed that T_G was not just a function of the root biomass interacting with the aquifer – rather, soil moisture depletion drives the reliance of vegetation on groundwater. This chapter also demonstrated that on a seasonal basis, riparian forest transpiration can be of substantial magnitude, averaging approximately 22% of growing season baseflow in the stream. However, results from individual groundwater wells were quite variable, calling into question the use of only one or two wells as have been used in other environments. Thus, a final contribution from this first investigation was the demonstration that to consistently fall within the 95% confidence interval of the true mean of groundwater transpiration, at least 6 wells were needed. This information can be used by other researchers to help guide study design when local scale information is lacking.

Another important concern following from the above investigation was adequately constraining estimates of groundwater transpiration using an independent estimate of tree water

use. This was explored in chapter three by estimating canopy transpiration from scaled sap flux estimates and comparing with the estimates of groundwater transpiration. Results were very surprising, I hypothesized that groundwater transpiration would be some fraction, less than one, of canopy transpiration. However, I observed groundwater transpiration was consistently greater than total canopy transpiration. This led me to rigorously validate raw data and processing steps. After this evaluation I turned back to the formula used for groundwater transpiration estimation and recognized that none of the published formulae specified an area of influence. Rather, this is an implied variable. Therefore, in this landscape it seems that assuming the groundwater transpiration flux can apply to the desired landscape area did not hold true. In fact, based on tree size and published relationships with rooting extent, the area of trees accessing the riparian aquifer is likely 2 – 3 times greater than just the riparian zone. This study brought to light an important methodological short coming that had not been explored in the current body of literature and presents a call to action for other researchers exploring this technique.

In chapter four of this dissertation, I investigated the response of individual riparian trees to a rapid onset flash drought event. Forest response to drought has been extensively studied; however, flash drought is relatively newly recognized class of drought that is characterized by a very rapid intensification and periods of high atmospheric moisture demand. Most of the literature investigating impacts of flash drought have focused on agricultural environments. This presented an opportunity for novel insights into water use response of trees to a short duration but intense drought event. While streamflow and soil moisture during the drought had some of the lowest observations on record indicating a strong drought response, there was not a broad scale impact on canopy water storage based on remotely sensed indices (normalized difference water index – NDWI). However, at the individual tree level water use patterns were altered.

Reverse flow (toward the base of the tree instead of the canopy) at night increased substantially during the drought suggesting hydraulic redistribution was occurring. Over the drought period I also found the relative amount of groundwater used was greater than the rest of the growing season. Thus, while the flash drought didn't result in widespread leaf drop or tree mortality, there were intrinsic responses in water use strategies in the monitored trees, indicating that even if drought does not out-right lead to tree biomass response the increased groundwater uptake can have important bearing on other fluxes of water as well, such as streamflow that is also sourced from the riparian aquifer.

As is often the case in science, and especially field science in natural environments, many more questions than answers may arise. This dissertation was no exception. Of particular surprise were the result from chapter 3. I think there are a couple of ways forward to address the true area of vegetation that is responsible for the diurnal water table fluctuations. The first would be manipulative experiments. Forest harvest experiments could occur at larger and larger radii around a central well. The well response could be tracked until the fluctuation ceases. In an ideal situation this would be done with replication and directionally of harvest. Is it primarily vegetation in the upslope or downslope direction? This could shed light and allow for additional formula to be developed that contain an area of influence which may be based on surface slope, tree species, density, age, size, etc.

Another approach to constrain the area of influence could be through the use of chemical tracers. Specifically, introduction of water enriched with deuterium or another conservative solute that is readily taken up by tree roots. Active tracer additions could be added to groundwater wells at discrete points in the landscape. Tissue from nearby trees could then be sampled on a routine basis and analyzed for the introduced constituent(s). This could be a less

invasive means to examine the area of influence where manipulations may not be possible. This approach has the added benefit that proportional water source analyses could be conducted if other water source concentrations (soil water) were also known.

A final thought on follow-up studies that answers some of the remaining uncertainties relates to drought impacts. I purposefully focused on a rather narrow, riparian zone gradient. Assuming that the most upslope location would only have temporary access the water table and I could constrain, in space and time, the watershed area with consistent access to the riparian aquifer. However, the data suggested, with one exception, my wells and sample plots needed to extend further upslope to capture the threshold location where the water table was no longer accessible. However, this provided valuable information which can be used for future monitoring efforts. Specifically, in regard to drought, sample plots could be distributed based on distance from riparian zone, where we know the water table is accessible, or some other metric that similarly describes this, so that a location for time substitution design could be used to investigate drought impacts even when only minor drought is occurring. Setting up this gradient at the present study site is further aided by the present of rock outcrops which also provide a gradient of soil depth which can limit soil moisture storage. The one challenge I see in this approach would be sampling a consistent forest community across the gradient of the aforementioned variables. I think these additional studies would push the science advances presented in this dissertation even further; providing more tools and progressing our ability to account for all fluxes in the water balance and manage water resources for future generations under uncertain climate trajectories.

REFERENCES

Alexander, R. B., Boyer, E. W., Smith, R. A., Schwarz, G. E., & Moore, R. B. (2007). The Role of Headwater Streams in Downstream Water Quality1. *JAWRA Journal of the American Water Resources Association*, *43*(1), 41–59. https://doi.org/10.1111/j.1752-1688.2007.00005.x

Allen, R. G., Pereira, L. S., Raes, D., & Smith, M. (1998). Crop evapotranspiration—Guidelines for computing crop water requirements (Food and Agriculture Organization of the United Nations Irrigation and Drainage Paper 56, 174 pp.).

Anderson, L. O., Malhi, Y., Aragão, L. E. O. C., Ladle, R., Arai, E., Barbier, N., & Phillips, O. (2010). Remote sensing detection of droughts in Amazonian forest canopies. New Phytologist, 187(3), 733–750. https://doi.org/10.1111/j.1469-8137.2010.03355.x

Assal, T. J., Anderson, P. J., & Sibold, J. (2016). Spatial and temporal trends of drought effects in a heterogeneous semi-arid forest ecosystem. Forest Ecology and Management, 365, 137–151. https://doi.org/10.1016/j.foreco.2016.01.017

Aulenbach, B. T., & Peters, N. E. (2018). Quantifying Climate-Related Interactions in Shallow and Deep Storage and Evapotranspiration in a Forested, Seasonally Water-Limited Watershed in the Southeastern United States. *Water Resources Research*, *54*(4), 3037–3061. https://doi.org/10.1002/2017WR020964

Barbeta, A., & Peñuelas, J. (2017). Relative contribution of groundwater to plant transpiration estimated with stable isotopes. *Scientific Reports*, *7*(1), 10580. https://doi.org/10.1038/s41598-017-09643-x

Barbeta, A., & Peñuelas, J. (2017). Relative contribution of groundwater to plant transpiration estimated with stable isotopes. Scientific Reports, 7(1), 10580. https://doi.org/10.1038/s41598-017-09643-x

BARRETT, D. J., HATTON, T. J., ASH, J. E., & BALL, M. C. (1995). Evaluation of the heat pulse velocity technique for measurement of sap flow in rainforest and eucalypt forest species of south-eastern Australia. *Plant, Cell & Environment*, *18*(4), 463–469. https://doi.org/10.1111/j.1365-3040.1995.tb00381.x

Batelaan, O., F. De Smedt, and L. Triest (2003), Regional groundwater discharge: phreatophyte mapping, groundwater modelling and impact analysis of land-use change, J. Hydrol., 275(1-2), 86-108, doi:10.1016/s0022-1694(03)00018-0.

Beven, K. J., & Kirkby, M. J. (1979). A physically based, variable contributing area model of basin hydrology / Un modèle à base physique de zone d'appel variable de l'hydrologie du bassin versant. *Hydrological Sciences Bulletin*, *24*(1), 43–69. https://doi.org/10.1080/02626667909491834

BLEBY, T. M., MCELRONE, A. J., & JACKSON, R. B. (2010). Water uptake and hydraulic redistribution across large woody root systems to 20 m depth. Plant, Cell & Environment, 33(12), 2132–2148. https://doi.org/10.1111/j.1365-3040.2010.02212.x

Bond, B. J., Jones, J. A., Moore, G., Phillips, N., Post, D., & McDonnell, J. J. (2002). The zone of vegetation influence on baseflow revealed by diel patterns of streamflow and vegetation water use in a headwater basin. *Hydrological Processes*, *16*(8), 1671–1677. https://doi.org/10.1002/hyp.5022

Bosch, J. M., & Hewlett, J. D. (1982). A review of catchment experiments to determine the

effect of vegetation changes on water yield and evapotranspiration. *Journal of Hydrology*,

55(1), 3–23. https://doi.org/10.1016/0022-1694(82)90117-2

Brantley, S. T., Schulte, M. L., Bolstad, P. V., & Miniat, C. F. (2016). *Equations for Estimating*

Biomass, Foliage Area, and Sapwood of Small Trees in the Southern Appalachians. *62*(4),

414–421. https://doi.org/doi:10.5849/forsci.15-041

Bren, L. J. (1997). Effects of slope vegetation removal on the diurnal variations of a small

mountain stream. *Water Resources Research*, *33*(2), 321–331.

https://doi.org/10.1029/96WR02648

Brum, M., Vadeboncoeur, M. A., Ivanov, V., Asbjornsen, H., Saleska, S., Alves, L. F., et al.

(2019). Hydrological niche segregation defines forest structure and drought tolerance

strategies in a seasonal Amazon forest. Journal of Ecology, 107(1), 318–333.

https://doi.org/10.1111/1365-2745.13022

Brunner, I., Herzog, C., Dawes, M. A., Arend, M., & Sperisen, C. (2015). How tree roots

respond to drought. *Frontiers in Plant Science*, *6*, 547.

https://doi.org/10.3389/fpls.2015.00547

Burgess, S. S. O., Adams, M. A., Turner, N. C., Beverly, C. R., Ong, C. K., Khan, A. A. H., &

Bleby, T. M. (2001). An improved heat pulse method to measure low and reverse rates of

sap flow in woody plants†. *Tree Physiology*, *21*(9), 589–598.

https://doi.org/10.1093/treephys/21.9.589

Butler, J. J., Kluitenberg, G. J., Whittemore, D. O., Loheide, S. P., Jin, W., Billinger, M. A., & Zhan, X. (2007). A field investigation of phreatophyte-induced fluctuations in the water table. *Water Resources Research*, *43*(2), n/a-n/a. https://doi.org/10.1029/2005WR004627

Cappellato, R., & E. Peters, N. (1995). Dry deposition and canopy leaching rates in deciduous and coniferous forests of the Georgia Piedmont: an assessment of a regression model. *Journal of Hydrology*, *169*(1), 131–150. https://doi.org/10.1016/0022-1694(94)02653-S

Carter, L., Terando, A., Dow, K., Hiers, K., Kunkel, K., Lascurain, A., et al. (2018). Chapter 19 : Southeast. Impacts, Risks, and Adaptation in the United States: The Fourth National Climate Assessment, Volume II.

Čermák, J., Kučera, J., & Nadezhdina, N. (2004). Sap flow measurements with some thermodynamic methods, flow integration within trees and scaling up from sample trees to entire forest stands. *Trees*, *18*(5), 529–546. https://doi.org/10.1007/s00468-004-0339-6

Chang, H., & Bonnette, M. R. (2016). Climate change and water-related ecosystem services: impacts of drought in California, USA. Ecosystem Health and Sustainability, 2(12), e01254.

Chen, L. G., Gottschalck, J., Hartman, A., Miskus, D., Tinker, R., & Artusa, A. (2019). Flash Drought Characteristics Based on U.S. Drought Monitor. Atmosphere, 10(9). https://doi.org/10.3390/atmos10090498

Chiu, C.-W., Komatsu, H., Katayama, A., & Otsuki, K. (2016). Scaling-up from tree to stand transpiration for a warm-temperate multi-specific broadleaved forest with a wide variation in stem diameter. *Journal of Forest Research*, *21*(4), 161–169. https://doi.org/10.1007/s10310-016-0532-7

Christian, J. I., Basara, J. B., Otkin, J. A., Hunt, E. D., Wakefield, R. A., Flanagan, P. X., & Xiao, X. (2019). A Methodology for Flash Drought Identification: Application of Flash Drought Frequency across the United States. Journal of Hydrometeorology, 20(5), 833–846. https://doi.org/10.1175/JHM-D-18-0198.1

Ciruzzi, D. M., & Loheide II, S. P. (2021). Groundwater subsidizes tree growth and transpiration in sandy humid forests. Ecohydrology, 14(5), e2294. https://doi.org/10.1002/eco.2294

COHEN, Y., FUCHS, M., & GREEN, G. C. (1981). Improvement of the heat pulse method for determining sap flow in trees. *Plant, Cell & Environment*, *4*(5), 391–397. https://doi.org/10.1111/j.1365-3040.1981.tb02117.x

Cooper, D. J., Sanderson, J. S., Stannard, D. I., & Groeneveld, D. P. (2006). Effects of long-term water table drawdown on evapotranspiration and vegetation in an arid region phreatophyte community. *Journal of Hydrology*, *325*(1), 21–34. https://doi.org/10.1016/j.jhydrol.2005.09.035

Crosbie, R. S., Binning, P., & Kalma, J. D. (2005). A time series approach to inferring groundwater recharge using the water table fluctuation method. *Water Resources Research*, *41*(1). https://doi.org/10.1029/2004WR003077

Csáfordi, P., Szabó, A., Balog, K., Gribovszki, Z., Bidló, A., & Tóth, T. (2017). Factors controlling the daily change in groundwater level during the growing season on the Great Hungarian Plain: a statistical approach. *Environmental Earth Sciences*, *76*(20), 675. https://doi.org/10.1007/s12665-017-7002-1

Czikowsky, M. J., & Fitzjarrald, D. R. (2004). Evidence of Seasonal Changes in Evapotranspiration in Eastern U.S. Hydrological Records. *Journal of Hydrometeorology*, *5*(5), 974–988. https://doi.org/10.1175/1525-7541(2004)005<0974:EOSCIE>2.0.CO;2

Dawson, T. E. (1993). Hydraulic lift and water use by plants: implications for water balance, performance and plant-plant interactions. Oecologia, 95(4), 565–574. https://doi.org/10.1007/BF00317442

Dawson, T. E. (1996). Determining water use by trees and forests from isotopic, energy balance and transpiration analyses: The roles of tree size and hydraulic lift. *Tree Physiology*, *16*(1–2), 263–272. https://doi.org/10.1093/treephys/16.1-2.263

Dawson, T. E., & Ehleringer, J. R. (1991). Streamside trees that do not use stream water. *Nature*, *350*, 335. Retrieved from https://doi.org/10.1038/350335a0

Denham, S. O., Oishi, A. C., Miniat, C. F., Wood, J. D., Yi, K., Benson, M. C., & Novick, K. A. (2021). Eastern US deciduous tree species respond dissimilarly to declining soil moisture but similarly to rising evaporative demand. Tree Physiology, 41(6), 944–959. https://doi.org/10.1093/treephys/tpaa153

Di Liberto, T. (n.d.). Flash drought engulfs the U.S. Southeast in September 2019 | NOAA Climate.gov. Retrieved May 11, 2020, from https://www.climate.gov/news-features/event-tracker/flash-drought-engulfs-us-southeast-september-2019

Domec, J.-C., Sun, G., Noormets, A., Gavazzi, M. J., Treasure, E. A., Cohen, E., Swenson, J. J., McNulty, S. G., & King, J. S. (2012). A Comparison of Three Methods to Estimate Evapotranspiration in Two Contrasting Loblolly Pine Plantations: Age-Related Changes in Water Use and Drought Sensitivity of Evapotranspiration Components. *Forest Science*, *58*(5), 497–512. https://doi.org/10.5849/forsci.11-051

Duke, H. R. (1972). Capillary Properties of Soils - Influence Upon Specific Yield. *Transactions of the ASAE*, *15*(4), 688–691. https://doi.org/10.13031/2013.37986

Dunford, E. G., & Fletcher, P. W. (1947). Effect of removal of stream-bank vegetation upon

    water yield. *Eos, Transactions American Geophysical Union*, *28*(1), 105–110.

    https://doi.org/10.1029/TR028i001p00105

Dymond, S. F., Bradford, J. B., Bolstad, P. V., Kolka, R. K., Sebestyen, S. D., & DeSutter, T. M.

    (2017). Topographic, edaphic, and vegetative controls on plant-available water.

    Ecohydrology, 10(8), e1897. https://doi.org/10.1002/eco.1897

Ehleringer, J. R., & Dawson, T. E. (1992). Water uptake by plants: perspectives from stable

    isotope composition. *Plant, Cell & Environment*, *15*(9), 1073–1082.

    https://doi.org/10.1111/j.1365-3040.1992.tb01657.x

Engel, V., Jobbágy, E. G., Stieglitz, M., Williams, M., & Jackson, R. B. (2005). Hydrological

    consequences of Eucalyptus afforestation in the Argentine Pampas. *Water Resources*

    Research, *41*(10). https://doi.org/10.1029/2004WR003761

Fahle, M., & Dietrich, O. (2014). Estimation of evapotranspiration using diurnal groundwater

    level fluctuations: Comparison of different approaches with groundwater lysimeter data.

    Water Resources Research, *50*(1), 273–286. https://doi.org/10.1002/2013WR014472

Fan, J., Oestergaard, K. T., Guyot, A., & Lockington, D. A. (2014). Estimating groundwater

    recharge and evapotranspiration from water table fluctuations under three vegetation

    covers in a coastal sandy aquifer of subtropical Australia. *Journal of Hydrology*, *519*,

    1120–1129. https://doi.org/10.1016/j.jhydrol.2014.08.039

Fan, Y., Li, H., & Miguez-Macho, G. (2013). Global Patterns of Groundwater Table Depth.

    Science, *339*(6122), 940. https://doi.org/10.1126/science.1229881

Ford, C. R., Goranson, C. E., Mitchell, R. J., Will, R. E., & Teskey, R. O. (2005). Modeling

    canopy transpiration using time series analysis: A case study illustrating the effect of soil

moisture deficit on Pinus taeda. *Agricultural and Forest Meteorology*, *130*(3), 163–175.

https://doi.org/10.1016/j.agrformet.2005.03.004

Ford, C. R., Laseter, S. H., Swank, W. T., & Vose, J. M. (2011). Can forest management be used

to sustain water-based ecosystem services in the face of climate change? *Ecological*

Applications, *21*(6), 2049–2067. https://doi.org/10.1890/10-2246.1

Ford, T. W., & Labosier, C. F. (2017). Meteorological conditions associated with the onset of

flash drought in the eastern United States. Agricultural and Forest Meteorology, 247, 414–

423.

Forster, M. A. (2017). How Reliable Are Heat Pulse Velocity Methods for Estimating Tree

Transpiration? *Forests*, *8*(9). https://doi.org/10.3390/f8090350

Forster, M. A. (2019). The Dual Method Approach (DMA) Resolves Measurement Range

Limitations of Heat Pulse Velocity Sap Flow Sensors. *Forests*, *10*(1).

https://doi.org/10.3390/f10010046

Gao, B. (1996). NDWI—A normalized difference water index for remote sensing of vegetation

liquid water from space. Remote Sensing of Environment, 58(3), 257–266.

https://doi.org/10.1016/S0034-4257(96)00067-3

Goodrich, D. C., et al. (2000), Seasonal estimates of riparian evapotranspiration using remote

and in situ measurements, Agricultural and Forest Meteorology, 105(1-3), 281-309,

doi:10.1016/s0168-1923(00)00197-0.

Gribovszki, Z. (2018). Comparison of specific-yield estimates for calculating evapotranspiration

from diurnal groundwater-level fluctuations (Z. Gribovszki, Trans.). *Hydrogeology*

Journal, *v. 26*(3), 869–880. PubAg. https://doi.org/10.1007/s10040-017-1687-9

Gribovszki, Z., Kalicz, P., Szilágyi, J., & Kucsara, M. (2008). Riparian zone evapotranspiration estimation from diurnal groundwater level fluctuations. *Journal of Hydrology*, *349*(1), 6–17. https://doi.org/10.1016/j.jhydrol.2007.10.049

Gribovszki, Z., Szilágyi, J., & Kalicz, P. (2010). Diurnal fluctuations in shallow groundwater levels and streamflow rates and their interpretation – A review. *Journal of Hydrology*, *385*(1–4), 371–383. https://doi.org/10.1016/j.jhydrol.2010.02.001

Guo, L., Sun, F., Liu, W., Zhang, Y., Wang, H., Cui, H., et al. (2019). Response of Ecosystem Water Use Efficiency to Drought over China during 1982–2015: Spatiotemporal Variability and Resilience. Forests, 10(7). https://doi.org/10.3390/f10070598

Hafner, B. D., Tomasella, M., Häberle, K.-H., Goebel, M., Matyssek, R., & Grams, T. E. E. (2017). Hydraulic redistribution under moderate drought among English oak, European beech and Norway spruce determined by deuterium isotope labeling in a split-root experiment. Tree Physiology, 37(7), 950–960. https://doi.org/10.1093/treephys/tpx050

Harmon, R., Barnard, H. R., & Singha, K. (2020). Water Table Depth and Bedrock Permeability Control Magnitude and Timing of Transpiration-Induced Diel Fluctuations in Groundwater. *Water Resources Research*, *56*(5), e2019WR025967. https://doi.org/10.1029/2019WR025967

Hatton, T. J., & Wu, H.-I. (1995). Scaling theory to extrapolate individual tree water use to stand water use. *Hydrological Processes*, *9*(5-6), 527–540. https://doi.org/10.1002/hyp.3360090505

Hawthorne, S., & Miniat, C. F. (2018). Topography may mitigate drought effects on vegetation along a hillslope gradient. *Ecohydrology*, *11*(1). https://doi.org/10.1002/eco.1825

Healy, R. W., & Cook, P. G. (2002). Using groundwater levels to estimate recharge. *Hydrogeology Journal*, *10*(1), 91–109. https://doi.org/10.1007/s10040-001-0178-0

Hogg, E. H. (1997). Temporal scaling of moisture and the forest-grassland boundary in western Canada. *Research on Forest Environmental Influences in a Changing World*, *84*(1), 115–122. https://doi.org/10.1016/S0168-1923(96)02380-5

Jackson, R. B., Canadell, J., Ehleringer, J. R., Mooney, H. A., Sala, O. E., & Schulze, E. D. (1996). A Global Analysis of Root Distributions for Terrestrial Biomes. Oecologia, 108(3), 389–411.

Jia, W., Yin, L., Zhang, M., Yu, K., Wang, L., & Hu, F. (2021). Estimation of Groundwater Evapotranspiration of Different Dominant Phreatophytes in the Mu Us Sandy Region. *Water*, *13*(4). https://doi.org/10.3390/w13040440

Kozlowski, T. T. (1984). Plant Responses to Flooding of Soil. *BioScience*, *34*(3), 162–167. https://doi.org/10.2307/1309751

Kuster, T. M., Arend, M., Günthardt-Goerg, M. S., & Schulin, R. (2013). Root growth of different oak provenances in two soils under drought stress and air warming conditions. *Plant and Soil*, *369*(1), 61–71. https://doi.org/10.1007/s11104-012-1541-8

Lautz, L. K. (2008). Estimating groundwater evapotranspiration rates using diurnal water-table fluctuations in a semi-arid riparian zone. *Hydrogeology Journal*, *16*(3), 483–497. https://doi.org/10.1007/s10040-007-0239-0

Lisonbee, J., Woloszyn, M., & Skumanich, M. (2021). Making sense of flash drought: definitions, indicators, and where we go from here. Journal of Applied and Service Climatology, 2021, 1–19. https://doi.org/10.46275/JOASC.2021.02.001

Loheide II, S. P. (2008). A method for estimating subdaily evapotranspiration of shallow groundwater using diurnal water table fluctuations. *Ecohydrology*, *1*(1), 59–66. https://doi.org/10.1002/eco.7

Loheide, S. P., Butler, J. J., & Gorelick, S. M. (2005). Estimation of groundwater consumption by phreatophytes using diurnal water table fluctuations: A saturated-unsaturated flow assessment. *Water Resources Research*, *41*(7), n/a-n/a. https://doi.org/10.1029/2005WR003942

Lowry, C. S., & Loheide II, S. P. (2010). Groundwater-dependent vegetation: Quantifying the groundwater subsidy. *Water Resources Research*, *46*(6). https://doi.org/10.1029/2009WR008874

Lu, J., Sun, G., McNulty, S. G., & Amatya, D. M. (2005). A comparison of six potential evapotranspiration methods for regional use in the southeastern united states1. *JAWRA Journal of the American Water Resources Association*, *41*(3), 621–633. https://doi.org/10.1111/j.1752-1688.2005.tb03759.x

Lubczynski, M. W. (2008). The hydrogeological role of trees in water-limited environments. *Hydrogeology Journal*, *17*(1), 247. https://doi.org/10.1007/s10040-008-0357-3

Lundquist, J. D., & Cayan, D. R. (2002). Seasonal and Spatial Patterns in Diurnal Cycles in Streamflow in the Western United States. *Journal of Hydrometeorology*, *3*(5), 591–603. https://doi.org/10.1175/1525-7541(2002)003<0591:SASPID>2.0.CO;2

Mac Nish, R. D., C. L. Unkrich, E. Smythe, D. C. Goodrich, and T. Maddock (2000), Comparison of riparian evapotranspiration estimates based on a water balance approach and sap flow measurements, Agricultural and Forest Meteorology, 105(1-3), 271-279, doi:10.1016/s0168-1923(00)00196-9.

Marshall, D. C. (1958). Measurement of Sap Flow in Conifers by Heat Transport. 1. *Plant Physiology*, *33*(6), 385–396. https://doi.org/10.1104/pp.33.6.385

Martinet, M. C., Vivoni, E. R., Cleverly, J. R., Thibault, J. R., Schuetz, J. F., & Dahm, C. N. (2009). On groundwater fluctuations, evapotranspiration, and understory removal in riparian corridors. *Water Resources Research*, *45*(5). https://doi.org/10.1029/2008WR007152

Marusig, D., Petruzzellis, F., Tomasella, M., Napolitano, R., Altobelli, A., & Nardini, A. (2020). Correlation of Field-Measured and Remotely Sensed Plant Water Status as a Tool to Monitor the Risk of Drought-Induced Forest Decline. Forests, 11(1). https://doi.org/10.3390/f11010077

McDowell, N., Pockman, W. T., Allen, C. D., Breshears, D. D., Cobb, N., Kolb, T., et al. (2008). Mechanisms of plant survival and mortality during drought: why do some plants survive while others succumb to drought? New Phytologist, 178(4), 719–739. https://doi.org/10.1111/j.1469-8137.2008.02436.x

McLaughlin, D. L., & Cohen, M. J. (2011). Thermal artifacts in measurements of fine-scale water level variation. Water Resources Research, 47(9). https://doi.org/10.1029/2010WR010288

McLaughlin, D. L., & Cohen, M. J. (2012). Ecosystem specific yield for estimating evapotranspiration and groundwater exchange from diel surface water variation. *Hydrological Processes*, *28*(3), 1495–1506. https://doi.org/10.1002/hyp.9672

McLendon, T., Hubbard, P. J., & Martin, D. W. (2008). Partitioning the use of precipitation- and groundwater-derived moisture by vegetation in an arid ecosystem in California. *Journal of Arid Environments*, *72*(6), 986–1001. https://doi.org/10.1016/j.jaridenv.2007.11.019

Meyboom, P. (1965). Three observations on streamflow depletion by phreatophytes. *Journal of Hydrology*, *2*(3), 248–261. https://doi.org/10.1016/0022-1694(65)90040-5

Miller, G. R., Chen, X., Rubin, Y., Ma, S., & Baldocchi, D. D. (2010). Groundwater uptake by woody vegetation in a semiarid oak savanna. *Water Resources Research*, *46*(10). https://doi.org/10.1029/2009WR008902

Mitchell, P. J., Benyon, R. G., & Lane, P. N. J. (2012). Responses of evapotranspiration at different topographic positions and catchment water balance following a pronounced drought in a mixed species eucalypt forest, Australia. *Journal of Hydrology*, *440–441*, 62–74. https://doi.org/10.1016/j.jhydrol.2012.03.026

Mo, K. C., & Lettenmaier, D. P. (2015). Heat wave flash droughts in decline. Geophysical Research Letters, 42(8), 2823–2829. https://doi.org/10.1002/2015GL064018

Mo, K. C., & Lettenmaier, D. P. (2016). Precipitation Deficit Flash Droughts over the United States. Journal of Hydrometeorology, 17(4), 1169–1184. https://doi.org/10.1175/JHM-D-15-0158.1

Nachabe, M. H. (2002). Analytical expressions for transient specific yield and shallow water table drainage. *Water Resources Research*, *38*(10), 11–1. https://doi.org/10.1029/2001WR001071

Nachabe, M., Shah, N., Ross, M., & Vomacka, J. (2005). Evapotranspiration of Two Vegetation Covers in a Shallow Water Table Environment. *Soil Science Society of America Journal*, *69*(2), 492–499. https://doi.org/10.2136/sssaj2005.0492

Nadezhdina, N., David, T. S., David, J. S., Ferreira, M. I., Dohnal, M., Tesař, M., et al. (2010). Trees never rest: the multiple facets of hydraulic redistribution. Ecohydrology, 3(4), 431–444. https://doi.org/10.1002/eco.148

Natural Resources Conservation Service. (2017). Web soil survey for Newton and Rockdale

    Counties, Georgia. U.S. Department of Agriculture. Retrieved from:

    https://websoilsurvey.nrcs.usda.gov/app/

Naumburg, E., R. Mata-Gonzalez, R. G. Hunter, T. McLendon, and D. W. Martin (2005),

    Phreatophytic vegetation and groundwater fluctuations: A review of current research and

    application of ecosystem response modeling with an emphasis on Great Basin vegetation,

    Environmental Management, 35(6), 726-740, doi:10.1007/s00267-004-0194-7.

Nosetto, M. D., E. G. Jobbagy, and J. M. Paruelo (2005), Land-use change and water losses: the

    case of grassland afforestation across a soil textural gradient in central Argentina, Glob.

    Change Biol., 11(7), 1101-1117, doi:10.1111/j.1365-2486.2005.00975.x.

Nosetto, M. D., E. G. Jobbagy, T. Toth, and C. M. Di Bella (2007), The effects of tree

    establishment on water and salt dynamics in naturally salt-affected grasslands, Oecologia,

    152(4), 695-705, doi:10.1007/s00442-007-0694-2.

Oishi, A. C., Oren, R., & Stoy, P. C. (2008). Estimating components of forest evapotranspiration:

    A footprint approach for scaling sap flux measurements. *Agricultural and Forest

    Meteorology*, *148*(11), 1719–1732. https://doi.org/10.1016/j.agrformet.2008.06.013

Oishi, A. C., Oren, R., Novick, K. A., Palmroth, S., & Katul, G. G. (2010). Interannual

    Invariability of Forest Evapotranspiration and Its Consequence to Water Flow

    Downstream. *Ecosystems*, *13*(3), 421–436. https://doi.org/10.1007/s10021-010-9328-3

Oliveira, R. S., Dawson, T. E., Burgess, S. S. O., & Nepstad, D. C. (2005). Hydraulic

    redistribution in three Amazonian trees. Oecologia, 145(3), 354–363.

    https://doi.org/10.1007/s00442-005-0108-2

Orth, R., Destouni, G., Jung, M., & Reichstein, M. (2020). Large-scale biospheric drought

    response intensifies linearly with drought duration in arid regions. Biogeosciences, 17(9),

    2647–2656. https://doi.org/10.5194/bg-17-2647-2020

Osman, M., Zaitchik, B. F., Badr, H. S., Christian, J. I., Tadesse, T., Otkin, J. A., & Anderson,

    M. C. (2021). Flash drought onset over the contiguous United States: sensitivity of

    inventories and trends to quantitative definitions. Hydrology and Earth System Sciences,

    25(2), 565–581. https://doi.org/10.5194/hess-25-565-2021

Otkin, J. A., Anderson, M. C., Hain, C., Mladenova, I. E., Basara, J. B., & Svoboda, M. (2013).

    Examining Rapid Onset Drought Development Using the Thermal Infrared–Based

    Evaporative Stress Index. Journal of Hydrometeorology, 14(4), 1057–1074.

    https://doi.org/10.1175/JHM-D-12-0144.1

Otkin, J. A., Anderson, M. C., Hain, C., Svoboda, M., Johnson, D., Mueller, R., et al. (2016).

    Assessing the evolution of soil moisture and vegetation conditions during the 2012 United

    States flash drought. Agricultural and Forest Meteorology, 218–219, 230–242.

    https://doi.org/10.1016/j.agrformet.2015.12.065

Otkin, J. A., Svoboda, M., Hunt, E. D., Ford, T. W., Anderson, M. C., Hain, C., & Basara, J. B.

    (2017). Flash Droughts: A Review and Assessment of the Challenges Imposed by Rapid-

    Onset Droughts in the United States. Bulletin of the American Meteorological Society,

    99(5), 911–919. https://doi.org/10.1175/BAMS-D-17-0149.1

Park Williams, A., Cook, B. I., Smerdon, J. E., Bishop, D. A., Seager, R., & Mankin, J. S.

    (2017). The 2016 Southeastern U.S. Drought: An Extreme Departure From Centennial

    Wetting and Cooling. Journal of Geophysical Research: Atmospheres, 122(20), 10,888-

    10,905. https://doi.org/10.1002/2017JD027523

Pataki, D. E., & Oren, R. (2003). Species differences in stomatal control of water loss at the canopy scale in a mature bottomland deciduous forest. *Advances in Water Resources*, *26*(12), 1267–1278. https://doi.org/10.1016/j.advwatres.2003.08.001

Pausch, R. C., Grote, E. E., & Dawson, T. E. (2000). Estimating water use by sugar maple trees: Considerations when using heat-pulse methods in trees with deep functional sapwood. *Tree Physiology*, *20*(4), 217–227. https://doi.org/10.1093/treephys/20.4.217

Perry, T. (1982). The Ecology of Tree Roots and the Practical Significance Thereof. *Journal of Arboriculture*, *8*(8), 197–211.

Poorter, H., Niklas, K. J., Reich, P. B., Oleksyn, J., Poot, P., & Mommer, L. (2012). Biomass allocation to leaves, stems and roots: meta-analyses of interspecific variation and environmental control. *New Phytologist*, *193*(1), 30–50. https://doi.org/10.1111/j.1469-8137.2011.03952.x

Priestley, C. H. B., & Taylor, R. J. (1972). On the Assessment of Surface Heat Flux and Evaporation Using Large-Scale Parameters. *Monthly Weather Review*, *100*(2), 81–92. https://doi.org/10.1175/1520-0493(1972)100<0081:OTAOSH>2.3.CO;2

R Core Team (2020). R: A language and environment for statistical computing. R Foundation for Statistical Computing, Vienna, Austria. URL https://www.R-project.org/.

Riley, J. W., 2021, Water table depth, soil moisture, and meteorological data from Panola Mountain Research Watershed, 2017 - 2020: U.S. Geological Survey data release, https://doi.org/10.5066/P9QZ0RCN

Rosenberry, D. O., & Winter, T. C. (1997). Dynamics of water-table fluctuations in an upland between two prairie-pothole wetlands in North Dakota. *Journal of Hydrology*, *191*(1), 266–289. https://doi.org/10.1016/S0022-1694(96)03050-8

Sanderson, J. S., & Cooper, D. J. (2008). Ground water discharge by evapotranspiration in

    wetlands of an arid intermountain basin. *Journal of Hydrology*, *351*(3), 344–359.

    https://doi.org/10.1016/j.jhydrol.2007.12.023

Satchithanantham, S., Wilson, H. F., & Glenn, A. J. (2017). Contrasting patterns of groundwater

    evapotranspiration in grass and tree dominated riparian zones of a temperate agricultural

    catchment. *Journal of Hydrology*, *549*, 654–666.

    https://doi.org/10.1016/j.jhydrol.2017.04.016

Schaap, M. G., Leij, F. J., & van Genuchten, M. Th. (2001). rosetta: a computer program for

    estimating soil hydraulic parameters with hierarchical pedotransfer functions. *Journal of

    Hydrology*, *251*(3), 163–176. https://doi.org/10.1016/S0022-1694(01)00466-8

Schenk, H. J., & Jackson, R. B. (2002). The Global Biogeography of Roots. *Ecological

    Monographs*, *72*(3), 311–328. JSTOR. https://doi.org/10.2307/3100092

Schenk, H. J., & Jackson, R. B. (2005). Mapping the global distribution of deep roots in relation

    to climate and soil characteristics. Deep Regolith: Exploring the Lower Reaches of Soil,

    126(1), 129–140. https://doi.org/10.1016/j.geoderma.2004.11.018

Schilling, K. E. (2007). Water table fluctuations under three riparian land covers, Iowa (USA).

    Hydrological Processes, *21*(18), 2415–2424. https://doi.org/10.1002/hyp.6393

Schlesinger, W. H., & Jasechko, S. (2014). Transpiration in the global water cycle. *Agricultural

    and Forest Meteorology*, *189–190*, 115–117.

    https://doi.org/10.1016/j.agrformet.2014.01.011

Schwartz, N. B., Budsock, A. M., & Uriarte, M. (2019). Fragmentation, forest structure, and

    topography modulate impacts of drought in a tropical forest landscape. Ecology, 100(6),

    e02677. https://doi.org/10.1002/ecy.2677

Schwartz, N. B., Feng, X., Muscarella, R., Swenson, N. G., Umaña, M. N., Zimmerman, J. K., & Uriarte, M. (2020). Topography and Traits Modulate Tree Performance and Drought Response in a Tropical Forest. Frontiers in Forests and Global Change, 3, 136. https://doi.org/10.3389/ffgc.2020.596256

Scott, R. L., Cable, W. L., Huxman, T. E., Nagler, P. L., Hernandez, M., & Goodrich, D. C. (2008). Multiyear riparian evapotranspiration and groundwater use for a semiarid watershed. *Journal of Arid Environments*, *72*(7), 1232–1246. https://doi.org/10.1016/j.jaridenv.2008.01.001

Scott, R. L., W. J. Shuttleworth, D. C. Goodrich, and T. Maddock (2000), The water use of two dominant vegetation communities in a semiarid riparian ecosystem, Agricultural and Forest Meteorology, 105(1-3), 241-256, doi:10.1016/s0168-1923(00)00181-7.

Seager, R., Tzanova, A., & Nakamura, J. (2009). Drought in the Southeastern United States: Causes, Variability over the Last Millennium, and the Potential for Future Hydroclimate Change. *Journal of Climate*, *22*(19), 5021–5045. https://doi.org/10.1175/2009JCLI2683.1

Shafroth, P. B., Stromberg, J. C., & Patten, D. T. (2000). Woody riparian vegetation response to different alluvial water table regimes. *Western North American Naturalist*, *60*(1), 66–76. Retrieved from www.jstor.org/stable/41717015

Shah Nirjhar, & Ross Mark. (2009). Variability in Specific Yield under Shallow Water Table Conditions. *Journal of Hydrologic Engineering*, *14*(12), 1290–1298. https://doi.org/10.1061/(ASCE)HE.1943-5584.0000121

Shah Nirjhar, Nachabe Mahmood, & Ross Mark. (2007). Extinction Depth and Evapotranspiration from Ground Water under Selected Land Covers. *Groundwater*, *45*(3), 329–338. https://doi.org/10.1111/j.1745-6584.2007.00302.x

Silvertown, J., Araya, Y., & Gowing, D. (2015). Hydrological niches in terrestrial plant communities: a review. Journal of Ecology, 103(1), 93–108. https://doi.org/10.1111/1365-2745.12332

Šimůnek, J., Šejna, M., Saito, H., Sakai, M., & van Genuchten, M. Th., The HYDRUS-1D Software Package for Simulating the Movement of Water, Heat, and Multiple Solutes in Variably Saturated Media, Version 4.17, HYDRUS Software Series 3, Department of Environmental Sciences, University of California Riverside, Riverside, California, USA, pp. 343, 2013.

Smith, S. D., D. A. Devitt, A. Sala, J. R. Cleverly, and D. E. Busch (1998), Water relations of riparian plants from warm desert regions, Wetlands, 18(4), 687-696, doi:10.1007/bf03161683.

Smith, S. D., Wellington, A. B., Nachlinger, J. L., & Fox, C. A. (1991). Functional Responses of Riparian Vegetation to Streamflow Diversion in the Eastern Sierra Nevada. *Ecological Applications*, *1*(1), 89–97. https://doi.org/10.2307/1941850

Soylu, M. E., Lenters, J. D., Istanbulluoglu, E., & Loheide, S. P. (2012). On evapotranspiration and shallow groundwater fluctuations: A Fourier-based improvement to the White method. *Water Resources Research*, *48*(6), n/a-n/a. https://doi.org/10.1029/2011WR010964

Steinwand, A. L., R. F. Harrington, and D. Or (2006), Water balance for Great Basin phreatophytes derived from eddy covariance, soil water, and water table measurements, J. Hydrol., 329(3-4), 595-605, doi:10.1016/j.jhydrol.2006.03.013.

Steppe, K., De Pauw, D. J. W., Doody, T. M., & Teskey, R. O. (2010). A comparison of sap flux density using thermal dissipation, heat pulse velocity and heat field deformation methods.

Agricultural and Forest Meteorology, *150*(7), 1046–1056.

https://doi.org/10.1016/j.agrformet.2010.04.004

Sueki, S., Acharya, K., Huntington, J., Liebert, R., Healey, J., Jasoni, R., & Young, M. (2015).

Defoliation effects of Diorhabda carinulata on tamarisk evapotranspiration and

groundwater levels. *Ecohydrology*, *8*(8), 1560–1571. https://doi.org/10.1002/eco.1604

Thompson, S. E., Harman, C. J., Konings, A. G., Sivapalan, M., Neal, A., & Troch, P. A. (2011).

Comparative hydrology across AmeriFlux sites: The variable roles of climate, vegetation,

and groundwater. *Water Resources Research*, *47*(10).

https://doi.org/10.1029/2010WR009797

Tromp-van Meerveld, H. J., & McDonnell, J. J. (2006). On the interrelations between

topography, soil depth, soil moisture, transpiration rates and species distribution at the

hillslope scale. *Experimental Hydrology: A Bright Future*, *29*(2), 293–310.

https://doi.org/10.1016/j.advwatres.2005.02.016

Tromp-van Meerveld, H. J., Peters, N. E., & McDonnell, J. J. (2007). Effect of bedrock

permeability on subsurface stormflow and the water balance of a trenched hillslope at the

Panola Mountain Research Watershed, Georgia, USA. *Hydrological Processes*, *21*(6),

750–769. https://doi.org/10.1002/hyp.6265

Troxell, H. C. (1936). The diurnal fluctuation in the ground-water and flow of the santa ana river

and its meaning. *Eos, Transactions American Geophysical Union*, *17*(2), 496–504.

https://doi.org/10.1029/TR017i002p00496

Tucker, C. J. (1979). Red and photographic infrared linear combinations for monitoring

vegetation. Remote Sensing of Environment, 8(2), 127–150. https://doi.org/10.1016/0034-

4257(79)90013-0

USBR (1984) Drainage manual: a water resources technical publication, 2nd printing. US

    Bureau of Reclamation, Denver, CO, 286 pp

Van Beers, W.F.J. 1983. The auger-hole method; a field measurement of the hydraulic

    conductivity of soil below the watertable. 6th edition. ILRI Bulletin 1. Wageningen, The

    Netherlands, ILRI.

van der Molen, W. H., Beltrán, J. M., Ochs, W. J. (2007). Guidelines and computer programs for

    the planning and design of land drainage systems.FAO Irrigation and Drainage Paper 62,

    FAO, Rome, 228 pp

Vertessy, R. A., Benyon, R. G., O'Sullivan, S. K., & Gribben, P. R. (1995). Relationships

    between stem diameter, sapwood area, leaf area and transpiration in a young mountain ash

    forest. *Tree Physiology*, *15*(9), 559–567. https://doi.org/10.1093/treephys/15.9.559

Vertessy, R. A., Hatton, T. J., Reece, P., O'Sullivan, S. K., & Benyon, R. G. (1997). Estimating

    stand water use of large mountain ash trees and validation of the sap flow measurement

    technique. *Tree Physiology*, *17*(12), 747–756. https://doi.org/10.1093/treephys/17.12.747

Vincke, C., & Thiry, Y. (2008). Water table is a relevant source for water uptake by a Scots pine

    (Pinus sylvestris L.) stand: Evidences from continuous evapotranspiration and water table

    monitoring. *Agricultural and Forest Meteorology*, *148*(10), 1419–1432.

    https://doi.org/10.1016/j.agrformet.2008.04.009

von Arx, G., Dobbertin, M., & Rebetez, M. (2012). Spatio-temporal effects of forest canopy on

    understory microclimate in a long-term experiment in Switzerland. *Agricultural and

    Forest Meteorology*, *166–167*, 144–155. https://doi.org/10.1016/j.agrformet.2012.07.018

Wang, H., Schubert, S. D., Koster, R. D., & Chang, Y. (2019). Attribution of the 2017 Northern High Plains Drought. Bulletin of the American Meteorological Society, 100(1), S25–S29. https://doi.org/10.1175/BAMS-D-18-0115.1

White, W. N. (1932). *A method of estimating ground-water supplies based on discharge by plants and evaporation from soil: Results of investigations in Escalante Valley, Utah* (Report No. 659A; Water Supply Paper, p. 115). USGS Publications Warehouse. https://doi.org/10.3133/wsp659A

Wickham, H., François, R., Henry, L., and Müller, K. (2019). dplyr: A Grammar of Data Manipulation. R package version 0.8.0.1. https://CRAN.R-project.org/package=dplyr

Wilson, K. B., Hanson, P. J., Mulholland, P. J., Baldocchi, D. D., & Wullschleger, S. D. (2001). A comparison of methods for determining forest evapotranspiration and its components: Sap-flow, soil water budget, eddy covariance and catchment water balance. *Agricultural and Forest Meteorology*, *106*(2), 153–168. https://doi.org/10.1016/S0168-1923(00)00199-4

WULLSCHLEGER, S. D., & HANSON, P. J. (2006). Sensitivity of canopy transpiration to altered precipitation in an upland oak forest: Evidence from a long-term field manipulation study. *Global Change Biology*, *12*(1), 97–109. https://doi.org/10.1111/j.1365-2486.2005.001082.x

Wullschleger, S. D., Hanson, P. J., & Todd, D. E. (2001). Transpiration from a multi-species deciduous forest as estimated by xylem sap flow techniques. *Special Issue: THE SCIENCE OF MANAGING FORESTS TO SUSTAIN*, *143*(1), 205–213. https://doi.org/10.1016/S0378-1127(00)00518-1

Xulu, S., Peerbhay, K., Gebreslasie, M., & Ismail, R. (2019). Unsupervised Clustering of Forest Response to Drought Stress in Zululand Region, South Africa. Forests, 10(7). https://doi.org/10.3390/f10070531

Y. Rao, L., Sun, G., R. Ford, C., & M. Vose, J. (2011). Modeling Potential Evapotranspiration of Two Forested Watersheds in the Southern Appalachians. *Transactions of the ASABE*, *54*(6), 2067–2078. https://doi.org/10.13031/2013.40666

Yuan, X., Wang, L., Wu, P., Ji, P., Sheffield, J., & Zhang, M. (2019). Anthropogenic shift towards higher risk of flash drought over China. Nature Communications, 10(1), 4661. https://doi.org/10.1038/s41467-019-12692-7

Yue, W., Wang, T., Franz, T. E., & Chen, X. (2016). Spatiotemporal patterns of water table fluctuations and evapotranspiration induced by riparian vegetation in a semiarid area. *Water Resources Research*, *52*(3), 1948–1960. https://doi.org/10.1002/2015WR017546

Zhang, M., Yuan, X., & Otkin, J. A. (2020). Remote sensing of the impact of flash drought events on terrestrial carbon dynamics over China. Carbon Balance and Management, 15(1), 20. https://doi.org/10.1186/s13021-020-00156-1

Zhang, Y., You, Q., Mao, G., Chen, C., Li, X., & Yu, J. (2021). Flash Drought Characteristics by Different Severities in Humid Subtropical Basins: A Case Study in the Gan River Basin, China. Journal of Climate, 34(18), 7337–7357. https://doi.org/10.1175/JCLI-D-20-0596.1

APPENDICES

Appendix A. Supplemental Material for Chapter 3

Text S1.

Several of the monitor trees had missing records due to sensor failure. This led to large gaps that needed to be filled to allow for broader scale analyses. Following approaches used by Domec et al. (2011) and Ford et al. (2005) we regressed daily tree water use (in liters per day) against average daily meteorological drivers (air temperature, relative humidity, and solar radiation) and average volumetric water content to fill in the missing records. To assess how well our regression equations would predict unseen data we used k-fold cross validation. The results for each tree where records were gap filled are presented in the table S1. We relied on R^2 values for selecting the best fitting model for each tree. Our cross-validation analysis focused on R^2 and the mean absolute error (MAE). MAE is similar to RMSE but is more robust to outliers or extreme values. The observed and modeled daily sapflow are presented in figure S1. Trees with substantial portions gap filled demonstrate the same patterns as the trees that did not have sensor failures. For example, tree3 and tree4 highlight that the gap-filling models capture the period of low atmospheric demand (in June) observed in all other trees.

Table S1. Gapfilling models and statistics

Tree ID	species	gap period	variables in best fit regression[1]	R^2	RMSE	MAE	Mean daily sapflow (lpd)	k-folds
tree1	QUNI	20190717 - 20191023	rh, atc, sr	0.66	4.15	2.97	19	10
tree4	QUAL	20190605 - 20191023	sr	0.58	2.06	1.62	7.6	5

tree17	QUAL	20190801 - 20191023	sr, atc	0.52	1.44	1.07	3.3	10
tree6	NYSY	20190630 - 20190906	sr, atc, vwc	0.7	2.58	1.94	6.8	10
tree3	LIST	20190404 - 20191023	sr, atc, vwc,rh	0.9	1.54	1.23	10.4	5

[1.] Variables in regression: daily mean air temperature in degrees Celsius (atc), daily mean relative humidity (rh), daily mean solar radiation (sr), daily mean volumetric water content averaged over three depths (vwc)
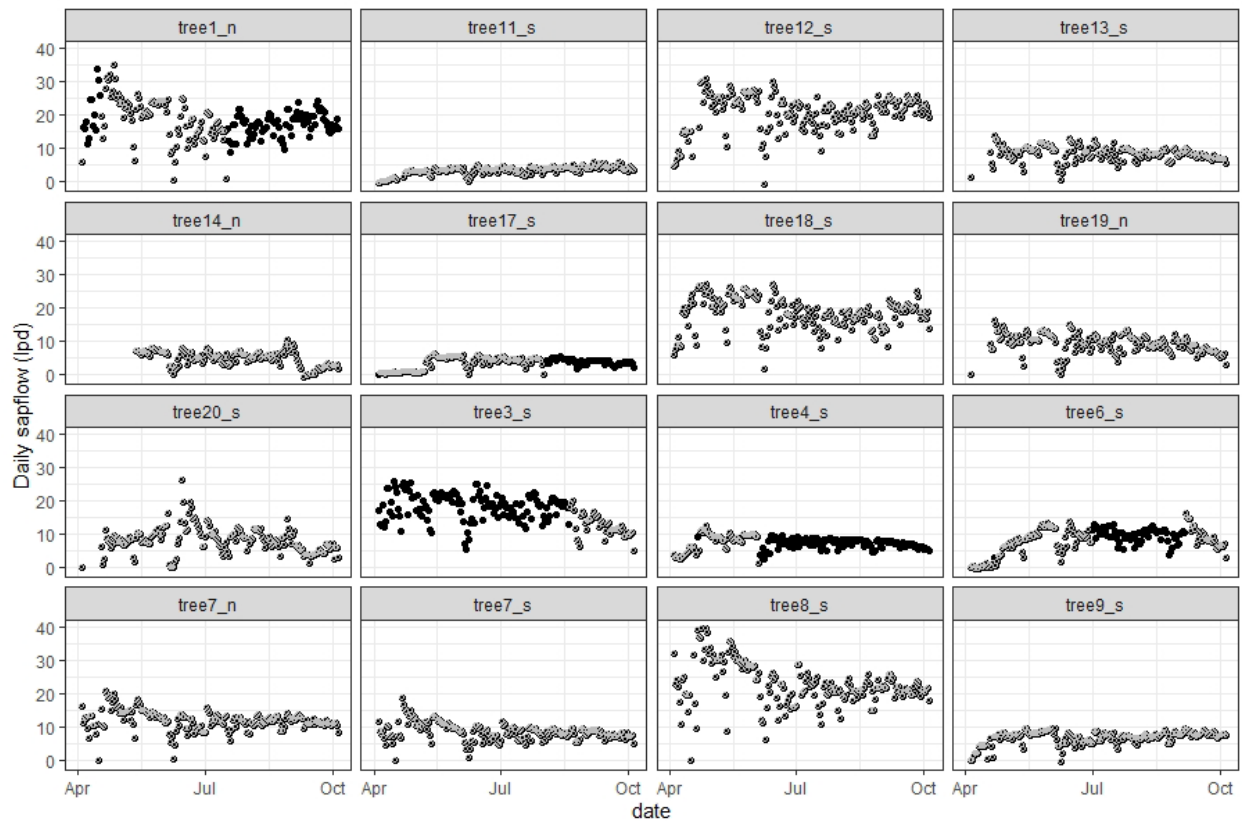

Figure S1. Comparison of measured and gap-filled data. Open grey points represent measured data and solid black points are gap filled data modeled from meteorological variables presented in table S1.
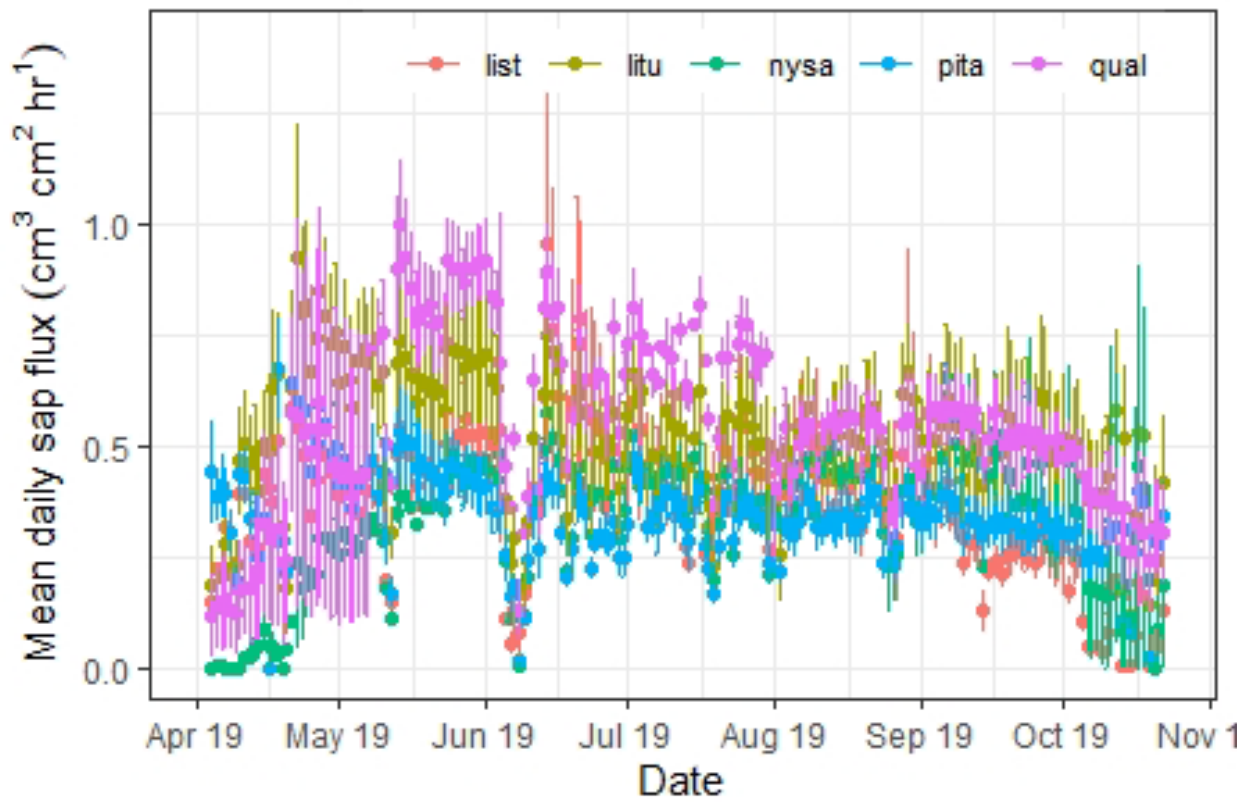
Figure S2. Mean daily sap flux density (± SE) by species. Note, "qual" also includes the one monitored quni.

Table S2. Crosswalk between figure names and source publications.

Study id_data year	Citation	DOI	Comments
boggs_2010_1, 2011_1, 2012_1, 2013_1, 2010, 2011, 2012, 2013	boggs et al., 2015	10.1002/hyp.10474	Boggs monitored 2 watersheds, "_1" indicates study watershed otherwise control watershed
bosch_2008	bosch et al., 2014	10.1016/j.agrformet.2013.12.002	
chiu_2014	chiu et al., 2016	10.1007/s10310-016-0532-7	
domec_2007,2008, 2009	domec et al., 2011	10.5849/forsci.11-051	17 yo pine plantation
ford_2004, 2005	ford et al., 2007	10.1016/j.agrformet.2007.04.010	
hawthorne_2004, 2006	hawthorne&miniat, 2016	10.1002/eco.1825	
meerveld_2002	tromp van meerveld&mcdonnell, 2006	10.1016/j.advwatres.2005.02.016	panola - trenched hillslope site

oishi_2002, 2003, 2004, 2005	oishi et al., 2010	10.1007/s10021-010-9328-3	
pataki_1997	pataki&oren, 2003	10.1016/j.advwatres.2003.08.001	
oren_1993	oren&pataki, 2001	10.1007/s004420000622	
vincke_2004	vincke&thiry, 2005	10.1016/j.agrformet.2008.04.009	
wilson_1998, 1999	wilson et al.,2001	10.1016/S0168-1923(00)00199-4	
wullschleger_1997	wullschleger et al.,2001	10.1016/S0378-1127(00)00518-1	
w_h_2000, 2001, 2002, 2003	wullschleger&hanson, 2006	10.1111/j.1365-2486.2005.01082.x	
this_study_2019, 2018	This study	unpublished	
nach_2002	nachabe et al., 2005	10.2136/sssaj2005.0492	
butler_2002	butler et al., 2007	10.1029/2005WR004627	
engel_2003	engel et al., 2005	10.1029/2004WR003761	E. camaldulensis plantation
sach_2014_acer, 2015_acer, 2014_grass, 2015_grass	satchithanantham et al., 2017	10.1016/j.jhydrol.2017.04.016	compared TG in grass and acer negundo

fan_total_pine, total_banksia	fan et al., 2014	10.1016/j.jhydrol.2014.08.039	fan compared TG in pine and banksia
grib_2006	gribovski et al., 2008	10.1016/j.jhydrol.2007.10.049	
miller_2005, 2006, 2007, 2008	miller et al., 2010	10.1029/2009WR008902	groundwater depth was ~7 - 12 m in fractured rock - vastly different from all other studies
schil_2004	shilling et al., 2007	10.1002/hyp.6393	compared corn, grass, and forest - graphs contain data from forest only